U.S. DEPARTMENT OF COMMERCE
National Technical Information Service
PB80-108574

Development of Droplet Sizing for the Evaluation of Scrubbing Systems

KLD Associates, Inc, Huntington, NY

Prepared for

Industrial Environmental Research Lab, Research Triangle Park, NC

Jul 79

United States
Environmental Protection
Agency

Industrial Environmental Research
Laboratory
Research Triangle Park NC 27711

EPA-600/7-79-166
July 1979

PB80-108574

EPA

Development of Droplet Sizing for the Evaluation of Scrubbing Systems

Interagency Energy/Environment R&D Program Report

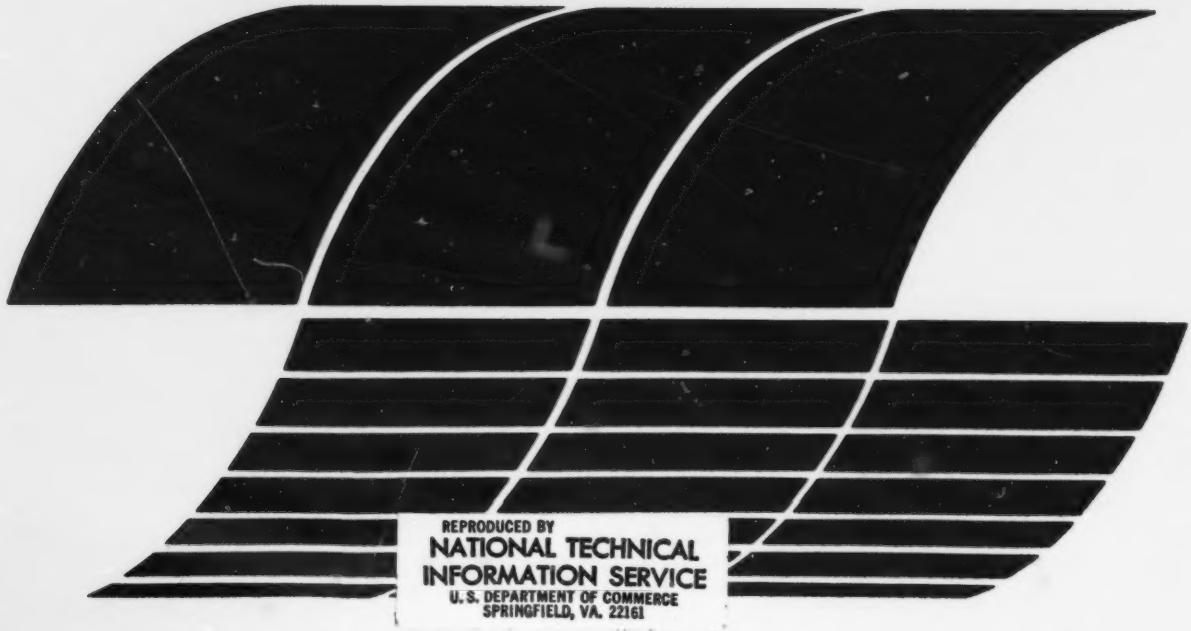

REPRODUCED BY
NATIONAL TECHNICAL
INFORMATION SERVICE
U.S. DEPARTMENT OF COMMERCE
SPRINGFIELD, VA. 22161

RESEARCH REPORTING SERIES

Research reports of the Office of Research and Development, U.S. Environmental Protection Agency, have been grouped into nine series. These nine broad categories were established to facilitate further development and application of environmental technology. Elimination of traditional grouping was consciously planned to foster technology transfer and a maximum interface in related fields. The nine series are:

1. Environmental Health Effects Research
2. Environmental Protection Technology
3. Ecological Research
4. Environmental Monitoring
5. Socioeconomic Environmental Studies
6. Scientific and Technical Assessment Reports (STAR)
7. Interagency Energy-Environment Research and Development
8. "Special" Reports
9. Miscellaneous Reports

This report has been assigned to the INTERAGENCY ENERGY-ENVIRONMENT RESEARCH AND DEVELOPMENT series. Reports in this series result from the effort funded under the 17-agency Federal Energy/Environment Research and Development Program. These studies relate to EPA's mission to protect the public health and welfare from adverse effects of pollutants associated with energy systems. The goal of the Program is to assure the rapid development of domestic energy supplies in an environmentally-compatible manner by providing the necessary environmental data and control technology. Investigations include analyses of the transport of energy-related pollutants and their health and ecological effects; assessments of, and development of, control technologies for energy systems; and integrated assessments of a wide range of energy-related environmental issues.

EPA REVIEW NOTICE

This report has been reviewed by the participating Federal Agencies, and approved for publication. Approval does not signify that the contents necessarily reflect the views and policies of the Government, nor does mention of trade names or commercial products constitute endorsement or recommendation for use.

This document is available to the public through the National Technical Information Service, Springfield, Virginia 22161.

TECHNICAL REPORT DATA (Please read Instructions on the reverse before completing)		
1. REPORT NO. EPA-600/7-79-166	2.	3. RECIPIENT'S ACCESSION NO. PB 80 108574
4. TITLE AND SUBTITLE Development of Droplet Sizing for the Evaluation of Scrubbing Systems		5. REPORT DATE July 1979 6. PERFORMING ORGANIZATION CODE
7. AUTHOR(S) Hector Medecki, K.C. Wu, and D.E. Magnus		8. PERFORMING ORGANIZATION REPORT NO.
9. PERFORMING ORGANIZATION NAME AND ADDRESS KLD Associates, Inc. 300 Broadway Huntington Station, New York 11746		10. PROGRAM ELEMENT NO. EHE624 11. CONTRACT/GRANT NO. 68-02-2111
12. SPONSORING AGENCY NAME AND ADDRESS EPA, Office of Research and Development Industrial Environmental Research Laboratory Research Triangle Park, NC 27711		13. TYPE OF REPORT AND PERIOD COVERED Final; 6/75 - 3/77 14. SPONSORING AGENCY CODE EPA/600/13

15. SUPPLEMENTARY NOTES IERL-RTP project officer is D. Bruce Harris, Mail Drop 62, 919/541-2557.

16. ABSTRACT The report describes the development and characteristics of the DC-2 Droplet Counter as used to evaluate scrubbing systems. The measurement of entrained droplets and their concentrations in gas streams is important in pollution control technology. The use of a hot-wire sensor can successfully measured the desired parameters for droplets in the size range from 1 to 600 micrometers. The report describes extensive testing in the laboratory and gives a comparison with results from the Brink impactor. A correlation of results for these two measurement techniques was achieved. The report also describes field tests at four different sites.

17. KEY WORDS AND DOCUMENT ANALYSIS

a. DESCRIPTORS	b. IDENTIFIERS/OPEN ENDED TERMS	c. COSATI Field/Group
Pollution Drops (Liquids) Measurement Testing Evaluation Gas Scrubbing Counters	Pollution Control Stationary Sources DC-2 Droplet Counter	13B 07D 14B 07A, 13H

18. DISTRIBUTION STATEMENT	19. SECURITY CLASS (This Report)	21. NO. OF PAGES
Release to Public	Unclassified	124
	20. SECURITY CLASS (This page) Unclassified	22. PRICE A06A01

EPA Form 2220-1 (9-73)

EPA-600/7-79-166

July 1979

Development of Droplet Sizing for the Evaluation of Scrubbing Systems

by

Hector Medecki, K.C. Wu, and D.E. Magnus

KLD Associates, Inc.
300 Broadway
Huntington Station, New York 11746

Contract No. 68-02-2111
Program Element No. EHE624

EPA Project Officer: D. Bruce Harris

Industrial Environmental Research Laboratory
Office of Energy, Minerals, and Industry
Research Triangle Park, NC 27711

Prepared for

U.S. ENVIRONMENTAL PROTECTION AGENCY
Office of Research and Development
Washington, DC 20460

DISCLAIMER

This report has been reviewed by the Office of Research and Development, U.S. Environmental Protection Agency, and approved for publication. Approval does not signify that the contents necessarily reflect the views and policies of the U.S. Environmental Protection Agency, nor does mention of trade names or commercial products constitute endorsement or recommendation for use.

ABSTRACT

The measurement of entrained droplets and their concentrations in gas streams is an important requirement in pollution control technology. The use of a hot-wire sensor can successfully measure the desired parameters for droplets in the size range from 1 μm to 600 μm.

The development and characteristics of the DC-2 Droplet Counter is reported herein. Extensive testing in the laboratory are described and the comparison with results from the Brink impactor is presented. A correlation of results for these two measurement techniques is achieved. Field tests at four different sites are also described.

CONTENTS

Abstract		iii
Figures		v
Tables		vii
Acknowledgments		viii
1.	GENERAL BACKGROUND	1
	Principle of Operation	2
	Program Plan for Improved Performance	6
2.	CONCLUSIONS AND RECOMMENDATIONS	9
3.	DEVELOPMENT OF THE PROBE	10
	General Background	12
4.	THE DC-2	23
	General Description	23
	Implementation of Temperature Measurement	26
	Implementation of Velocity Measurement	26
	Droplet Counting	31
	Physical Characteristics and Use of the DC-2	31
	Data Analysis	35
5.	PRINTER/CONTROLLER	41
	General Description	41
	Functions of Front Panel Switches	41
	Interfacing with Two DC-2's	46
	Probe Multiplexer System	46
6.	LABORATORY INVESTIGATIONS	49
	Calibration Tests	49
	Laboratory Tests with the Impactor	54
7.	FIELD TESTING	76
	Colbert Pilot Plant	76
	Water Treatment Plant in New York	78
	Shippingport Power Plane	78
	Cooling Tower of the High Flux Beam Reactor at Brookhaven National Laboratory	84
References		91
Appendix		
A.	Tabulation of Laboratory Tests	92

FIGURES

No.		Page
1	Principle of Operation of the Sensor	3
2	Electrical Signal from Sensor	4
3	Mechanical Model of Sensor	13
4	Aspirating Probe	16
5	Protected Probe	18
6	Disposable Sensor Probe	22
7	Temperature Conversion Block Diagram	27
8	Sensor Temperature Characteristics	28
9	DC-2 Velocity Measurement Network	30
10	View of the DC-2 Front Panel	33
11	Printout Illustration	42
12	Printer Panel Layout	43
13	Schematic of the DC-2 Interface with Printer/Controller	47
14	Schematic of DC-2 Interface with Multiplexer System	48
15	Droplet Calibration Apparatus	51
16	Capture Size vs. D_i/d	55
17	Laboratory Setup	56
18	Average Number Concentration for Impactor and the DC-2 Data (Test No. 216)	62
19	Average Number Concentration for Impactor and the DC-2 (Test No. 212)	63
20	Cumulative Entrainment Volume for Impactor and the DC-2 Data (Test No. 212)	64
21	Cumulative Entrainment Volume for Impactor and the DC-2 Data (Test No. 216)	65
22	Salt Collected on Stage 1	66
23	Salt Collected on Stage 3	67
24	Pressure Drop along the Impactor	71
25	Temperature Drop along the Impactor	72
26	Schematic of the Demister Scrubber at the Colbert Facility	77
27	Distribution at the Prescrubber Demister Inlet at the Colbert Facility	79
28	Distribution at the Prescrubber Demister Outlet at the Colbert Facility	80

FIGURES (Continued)

No.		Page
29	Distribution at the Exit Demister Inlet at the Colbert Facility	81
30	Distribution at the Demister Outlet at the Colbert Facility	82
31	Demister Cross Section at the Treatment Plant in Wantagh, New York	83
32	Test Section of a Duct at Shippingport, Pa.	85
33	Average Number Concentration for the Demister Sections at Shippingport, Pa.	86
34	Average Cumulative Entrainment Volume as a Function of Diameter for the Demister Sections at Shippingport, Pa.	87
35	Average Cumulative Entrainment Volume as a Function of Droplet Size in the Exhaust of the Cooling Tower at Brookhaven National Laboratory	89
36	Droplet Number Concentration Measured in the Exhaust of the Cooling Tower at Brookhaven National Laboratory	90

TABLES

No.		Page
1	Internal Sizing Distribution for Module 1	37
2	Internal Sizing Distribution for Module 2	38
3	Internal Sizing Distribution for Module 3	39
4	Internal Sizing Distribution for Module 4	40
5	D_{50} for Brink Impactor	59
6	Cascade Impactor Stage Parameters	70
7	Rate of Change in Radius for Water Droplets at 293°K and $P_\infty - P_o$ = 0.1 mmHg	73
8	Supersaturation Ratio, P_r/P_∞, for Water Droplet at 293°K	74
9	Rate of Change in Radius for Water Droplet at 293°K	74

ACKNOWLEDGMENTS

The work reported herein was performed by KLD Associates, Inc. under Contract No. 68-02-2111 from the Environmental Protection Agency, Research Triangle Park, North Carolina. Mr. Bruce Harris was the Project Officer for the EPA and his support and suggestions are acknowledged.

The field testing of the instrumentation was performed at three sites--the Colbert Pilot Plant in Muscle Shoals, Alabama; the Shippingport Power Plant in Shippingport, Pennsylvania; and Brookhaven National Laboratory in Upton, New York. Mr. Robert Statnick of EPA made the necessary arrangements at the Colbert Facility, Mr. Dennis Martin of York Research was responsible for the arrangements at Shippingport, and Messrs. Seymour Protter, Michael Brooks and Daniel Oldham assisted us at Brookhaven. Their support is gratefully acknowledged. The cooperation of all individuals at the plants was outstanding and contributed greatly to the success of the field testing.

SECTION 1

GENERAL BACKGROUND

The measurement of size and concentration of liquid droplets in the gas stream of scrubbers and mist eliminators is a requirement in pollution control technology. The capability of making such measurements will lead to improved performance of such devices and to a better understanding of the processes involved. Several methods of measuring droplets in such devices can be suggested, but one measuring device, which uses the heat transfer principle, appears most advantageous because of its simplicity and capability for in-situ measurements without sample extraction.

The technique uses a hot wire exposed to the flow with entrained liquid droplets. As a droplet attaches to the wire, an electrical signal is generated. The analysis of this signal provides information on droplet size. By electronically processing the signal, the droplets can be sorted into diameter ranges and the droplet distribution function determined. Another parameter required for the computation of droplet concentration is the gas stream velocity which is obtained from the same sensor operating as a hot wire anenometer.

In 1974, KLD Associates, Inc. developed and successfully demonstrated an instrument using this hot wire principle. The device, which is designed as the DC-1 Droplet Counter, sorts the droplets into six size ranges. The laboratory and field studies provided extensive insight into the droplet distribution in demisters. Originally, the measurement range for such devices was thought to be 20 μm to 500 μm. However, the field studies with the DC-1 clearly showed the importance of measurements in the range from 1 μm to 100 μm. In addition, the field studies indicated several areas for improving the operation of the instrument; these improvements are summarized below:

- Allocation of more than six droplet diameter ranges for a better description of droplet size distribution.

- Reduction or elimination of adjustments to be performed by the operator.

- Elimination of calibration curves, providing the result of the measurements in digital form and engineering units (metric system).

- Improvement of the probe ruggedness, since this is the only element with limited life, subject to breakage and contamination.

In the present report, the work performed in the improvement of the DC-1 is presented. The result of this effort is a second-generation instrument designated the DC-2 Droplet Counter.

PRINCIPLE OF OPERATION

The operation of the heat transfer droplet sensor is based on the cooling caused by a droplet attaching to a hot wire. The concept is schematically shown in Figure 1, where the hot wire sensor and its longitudinal temperature distribution are shown before (a) and after (b) a water droplet (cross-hatched circle) attaches. The electrical resistance of the wire is a function of the wire temperature which in (a) is high and substantially uniform along the wire. In situation (b) the portion of the wire covered by the droplet is cooled to approximately the droplet temperature. A constant electrical current, which flows along the wire to heat it, shows a measurable voltage drop at the wire support when a droplet is attached to the wire. The voltage encountered before droplet attachment (a) is reduced for condition (b) in direct proportion to the cooled length of wire; i.e., the droplet diameter. The electrical energy delivered to the wire evaporates the water, leaving the sensor dry and ready for further interaction.

The above description of the principle of operation of the instrument is an idealization, and in actual practice, the electrical signal is rather complex. A typical electrical signal obtained during a droplet-hot wire interaction is shown in Figure 2. Reduction of the voltage implies cooling of the wire. An initial fast decay of the signal is observed; it corresponds to the initial lateral contact of the droplet and wire with a basically radial cooling of the wire. The duration of this portion is of the order of a few microseconds. The less steep signal following the initial contact is caused by the droplet centering around the wire and by the longitudinal

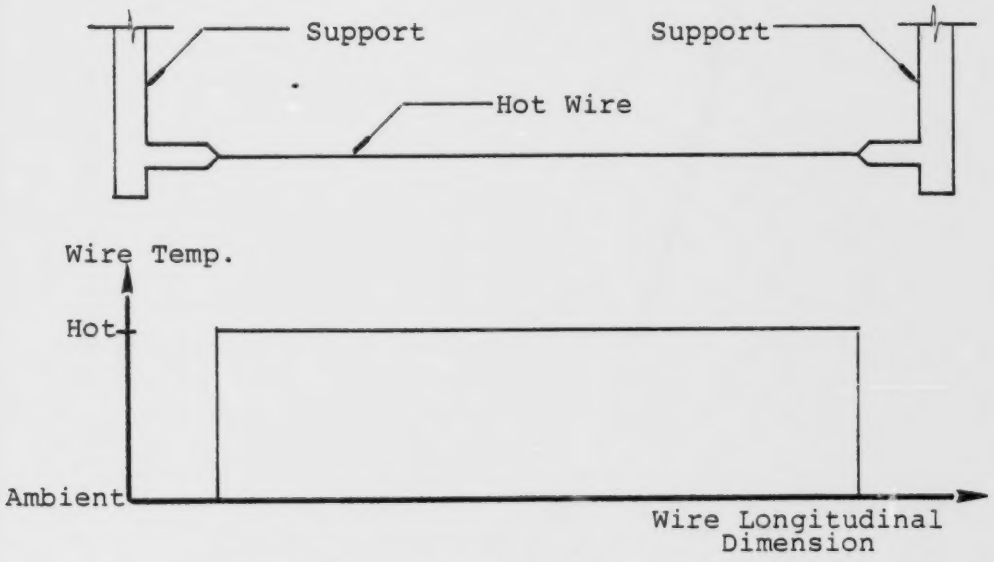

(a) Temperature before Attachment

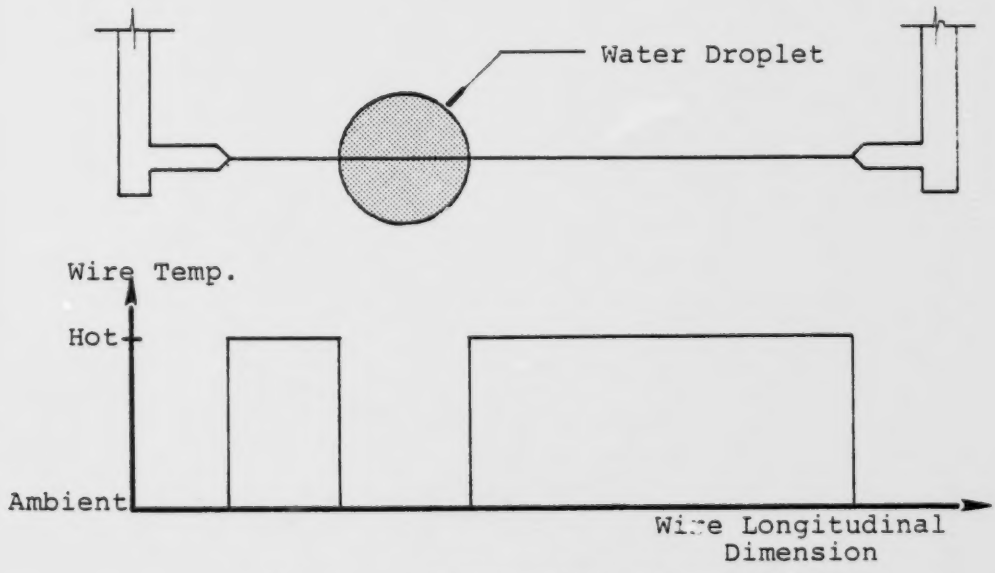

(b) Temperature after Attachment

Figure 1: Principle of Operation of the Sensor

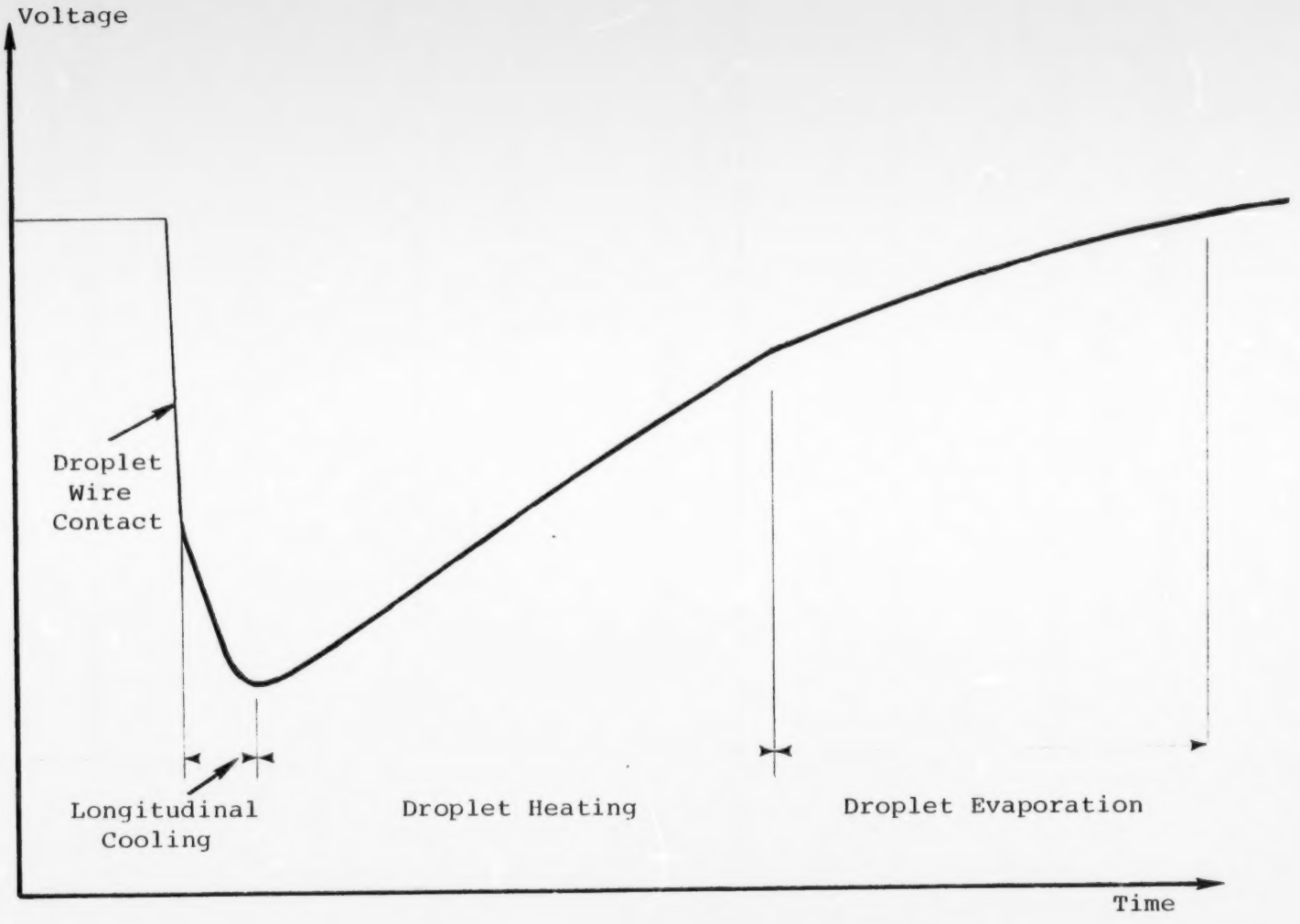

Figure 2: Electrical Signal from Sensor.

cooling of the wire beyond the area covered by the droplet. During this time, a warming of the droplet-wire takes place, raising the signal until the boiling temperature is reached; the droplet shrinks due to evaporation and disappears. The voltage in the wire then returns to the initial level prior to interaction of the droplet.

For the purpose of determining the droplet diameter, only the signal during the droplet contact is relevant and this portion is processed in both the DC-1 and DC-2 instruments. The processing is performed electronically, separating the front of the signal and frequency filtering it. After the analysis of a droplet is started, the processor does not accept a second droplet until the first droplet is fully evaporated and the hot wire sensor is restored to the proper operating temperature.

The calibration of the instrument (i.e., sensor output versus droplet diameter) is performed by simultaneously taking a microscopic picture of the droplet and measuring the corresponding electrical signal from the sensor (voltage drop). The apparatus for this purpose will be described later. Many calibrations may be obtained for different settings of operating conditions and signal processing; however, an optimum calibration was obtained as a compromise among many conflicting requirements, some of which are:

- One sensor and one operating temperature should cover the total droplet size range from 1 μm to 600 μm.
- The calibration curve should be monotonic.
- Air turbulence signals should not introduce false counting.
- The calibration curve should be independent of the droplet velocity relative to the sensor.

These requirements were achieved in the implementation of the DC-2 Droplet Counter, and its use in the field proved this approach to be sound.

PROGRAM PLAN FOR IMPROVED PERFORMANCE

A program to upgrade the characteristics of the droplet counter was undertaken. The major areas of work to improve its performance may be separated into five tasks as discussed below:

- Improve Probe Life and Reliability

  The objective was to improve the design of the probe by making it more durable in a field environment. Three probe configurations were investigated: the aspirating probe, the supported probe and the replaceable probe. The following improvements were implemented:

  a) The construction of the probe was modified to reduce damage during handling and installation. The configuration was modified to reduce the possibility of breakage due to large solid particles moving with the flow;

  b) Techniques of cleaning the sensor while operating in slurries and deposit-prone contaminants were developed;

  c) Effect of corrosive environment on the probe components was investigated in both laboratory and field tests;

  d) A replaceable probe was designed, built and tested in the laboratory.

- Improve the Functional Characteristics of the Instrument

  The objective was to provide increased capability of the droplet counter/measuring device. This objective was accomplished by:

  a) Increasing the storage capacity of each storage bin from 999 to 10,000 counts;

  b) Increasing the number of bins characterizing droplet size to fourteen (14);

c) Providing a buffered output for the measured data. Such output may be then interfaced with an external recording and display device:

d) Providing a display of flow velocity and temperature in engineering units;

e) Controlling the selection of the droplet size range of each bin by changing modules on the front panel;

f) Extending the capacity and control of the sample interval timer by providing several selectable time limits to a maximum of 1,000 seconds.

- Modification of the Physical Characteristics and Construction of the Instrument

The objective was to better adapt the droplet/counter/measuring device to field work by making it more transportable and convenient to use. The device was redesigned as a small package with space for cables and probes. Based upon the new design which incorporated all the electronic improvements discussed above, two (2) units were built for the EPA after receiving approval from the EPA Project Officer

- Develop a Printer/Controller

The objective of this phase of the effort was to provide the measured data in the form of printed hard copy. In addition, the controller was to automate the operation of the instrumentation and be able to simultaneously monitor two DC-2's. The device is also capable of controlling up to 12 hot-wire probes in a multiplex mode of operations. The Printer/Controller was used extensively in the laboratory and field tests of this project.

- Laboratory Test and Field Validation

The objective was to calibrate and validate the two droplet counter/measurement devices resulting from the modifications as discussed above in preparation for delivery to the EPA. The following work was performed in the laboratory in order to ascertain the performance of the improved instruments:

a) A calibration of the instruments was performed;

b) The instruments were made to operate with sprays simulating those encountered in typical facilities;

c) Design modifications were incorporated to improve the performance under the simulated conditions

d) An extensive test and measurement program was performed with a Brink impactor in the KLD laboratory. The primary purpose of these tests was to generate data for comparison with the measurements simultaneously recorded with the DC-2.

After the operation of the instruments was optimized in the laboratory, a program of field validation was undertaken. Four facilities were selected and approved for field measurement by the EPA Project Officer.

SECTION 2

CONCLUSIONS AND RECOMMENDATIONS

A prototype instrument had been previously built and successfully used in the field for measuring droplet size and concentration in gas flows. The device operated on the heat transfer principle described in Section 1. Under the program reported herein, a second generation of the instrument was implemented and demonstrated in the field. From the work on the improved version of the instrument, the following conclusions and results were reached:

- Water droplets from 1 to 600 microns in diameter, flow velocities up to 10 meters per second and gas temperatures between 0°C and 100°C can be readily measured by the improved instrument (DC-2). The distribution of droplet sizes is subdivided into 14 size ranges by the device.

- The involvement of the operator is reduced to a minimum and no auxiliary equipment is required to perform the measurement.

- The instrument is particularly suitable for field use because of its portability and the small size of the sampling probe.

- The probe is the only component which requires care during handling and use. Special effort was devoted to ruggedize this component. Furthermore, a replaceable sensor was designed and successfully tested in the laboratory.

- The Printer/Controller enhanced the operation of the DC-2 in the laboratory and in the field. The printed data facilitates the reduction and interpretation of results.

The results from the laboratory and field studies provided some specific conclusions with respect to the measurement of droplet distributions:

- The data obtained with the Brink impactor was higher than the data from the DC-2. This conclusion was reached after careful attention to minimize the data scatter in the impactor results.

- Measurements from the Brink impactor can be related to the DC-2 measurements using an equivalence factor, K, which is applied over the size range of 1 μm to 10 μm. The equivalence factor represents the aerodynamic influence on the capture area of the wire and other phenomena which characterize the difference in the two-measurement procedure. The aerodynamic influence was investigated and defined for the size ranges between 1 μm to 10 μm.

- Laboratory measurements with the impactor exhibited substantial scatter even with carefully controlled procedures. If the droplets were water without trace elements as a diagnostic, the scatter in the data was unacceptable and meaningful results could not be obtained. By using a 10% solution of NaCl, more reliable results were achieved.

- From a series of qualitative tests, it was concluded that the scatter in the impactor results is caused by evaporation/condensation within the impactor. Small changes in environmental conditions can significantly alter the measurements with the impactor.

- The DC-2 was used at four different field sites, and the device performed well. The Shippingsport Power Plant has a limestone scrubber, and the entrained liquid in the exhaust flow provided the most difficult test conditions. However, with the correct procedure, meaningful results were achieved with the DC-2.

As a result of this research project, several recommendations can be made with respect to future activities in droplet measurements:

- Further field testing should be performed with the DC-2 and Brink impactor. These measurements should be compared and the reliability of the two procedures established. The test sites should be selected to encompass many different test environments to establish a range of applications for both devices.

- Guidelines and procedures should be developed for the operation of the DC-2 and the impactor for droplet measurements at various types of facilities. These procedures should be documented in a handbook for use by a field team.

- The replaceable probe for the DC-2 provides many advantages for operating the equipment in the field. The development of this equipment should be completed and introduced as a field operating procedure.

SECTION 3

DEVELOPMENT OF THE PROBE

GENERAL BACKGROUND

The probe is the component which performs the droplet measurement when inserted into the flow under investigation. The probe has the shape of a thin cylinder and is connected to the electronic processor with a single coaxial cable. Attached to the probe is a sensor composed of a platinum wire, five microns in diameter and one millimeter long. The sensor detects droplets while the remaining part of the probe provides a means of mounting and protecting the sensor.

The diameter of the platinum wire was selected as a compromise between its mechanical strength, requiring a large wire diameter, and the minimum droplet diameter to be measured, requiring a small wire diameter. The sensor is the only component of the droplet counter subject to damage, contamination or destruction. The improvement of the probe, in particular the sensor, will result in a more useful and reliable instrument.

Sensor as a Mechanical Structure

The reliability of the sensor and its mount is directly related to the accuracy of its measuring capability as well as its structural soundness. Studies were conducted to test the sensor's reliability for measurement and handling.

The mechanical model of a typical sensor is shown in Figure 3. The main supporting structure is a rigid metal ring built around the sensor and at the end of the probe. The diameter of this ring is approximately one centimeter (.4 inches), which is large enough to prevent the accumulation of water which may eventually clog the sensor. The sensor is mounted across the ring on two prongs (b). The prongs, each 3 mm long, provide both mechanical support and electrical contact. The sensor, originally a silver plated platinum wire,

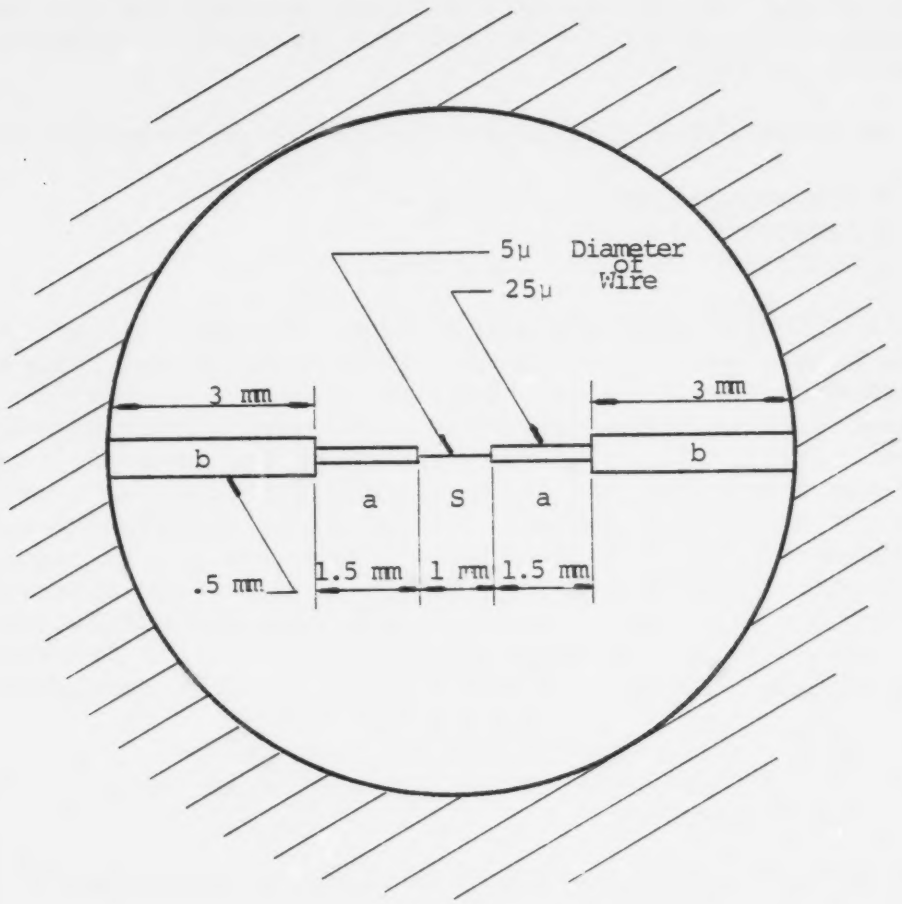

Figure 3: Mechanical Model of Sensor

is soldered at the two prongs. The silver coating is then removed from a section of the wire with nitric acid exposing one millimeter of sensor (S). It is this exposed section that is sensitive to and measures droplets. The remaining unexposed platinum wire (a) serves as additional support for the sensor. The dimensions of the sensor and its surrounding supports are presented in Figure 3.

This mechanical model was tested for its response to:

- Vibrations (acceleration),
- Aerodynamic flow,
- Collision of solid particles

In all practical situations, accelerations along the axis of the sensor and support cannot produce breakage. The sensor is much more sensitive to accelerations along directions perpendicular to the sensor axis. The sensitivity depends on the initial tension of the wire which is basically taut after the silver coating is dissolved, but acquires a certain amount of slack when heated. An additional limitation is introduced by the flexure of sensor supports (b) in Figure 3. The flexure increases the separation of the prong tips. The widening gap between the prongs eventually becomes larger than the length of the sensor, thus breaking it. The study indicates two separate solutions to the lateral acceleration:

- Very light supporting prongs so that the longitudinal strength of the sensor prevents its separation

- Strong prongs with large sections to minimize the deflection

For relative ease of construction and to minimize the electrical resistance of the connection, the second approach was taken. Also slack in the wire greatly improves the sensor integrity. Furthermore, it became apparent that the use of tapered prongs reduces deflection for a given value of lateral acceleration.

Extensive testing showed that a substantial gain in probe ruggedness may be achieved by mounting the supporting ring on a resilient structure. This substantially reduces the level of acceleration transmitted to the sensor. This feature was incorporated in the disposable sensor probe.

The effect of air flow and the turbulence normally associated with this flow may cause oscillation of the sensor. The amplitude of this oscillation increases with the slack in the wire. Other factors inducing sensor vibrations with associated flexure fatigue include the random attachment of water droplets on the sensor and the collision of solid particles with the sensor. The requirement of a taut sensor able to survive a strong gas flow contradicts the requirement of a slack sensor, necessary to withstand large lateral acceleration. A compromise between the conflicting requirements should allow a deflection of the sensor center point of the order of 50 microns. However, the technique used to build the sensor does not allow for such close control.

The collision of solid particles with the sensor requires it to be slack to withstand the impact without breaking. The maximum force which may be applied to the sensor before it breaks is approximately .5 gms. With the above mentioned 50 microns of slack, breakage occurs when a 100-micron diameter particle moving at 10 meters per second directly collides with the sensor. At a relative velocity of 1 meter per second, solid particles within the diameter range of a quarter of a millimeter may destroy the sensor. There are no obvious solutions to eliminate or reduce the risk of such collisions. The use of a deflecting rod located upstream of the sensor and mounted parallel to it was one of the approaches tested. This solution, however, had limited success. The function of this rod was to deviate the large solid particles or, at least, to reduce their velocity to a safe value prior to collision with the sensor. In practice, however, the excessive collection of water on the rod prevented the proper interaction of droplets with the sensor.

The Aspirating Probe

The aspirating probe shown in Figure 4 uses the same platinum wire sensor adopted for the open probe. This sensor is mounted across a small tube having a 1 mm to 6 mm inside diameter (.040 to .25 inch). A vacuum pump is used to create a gas flow along this tube.

Tests with the aspirating probe in the field and laboratory showed that the possibility of damaging the sensor during handling and operation is almost entirely eliminated. It was also shown that, with a proper design of the conduit entrance, the amount of noise due to air turbulence may be substantially reduced.

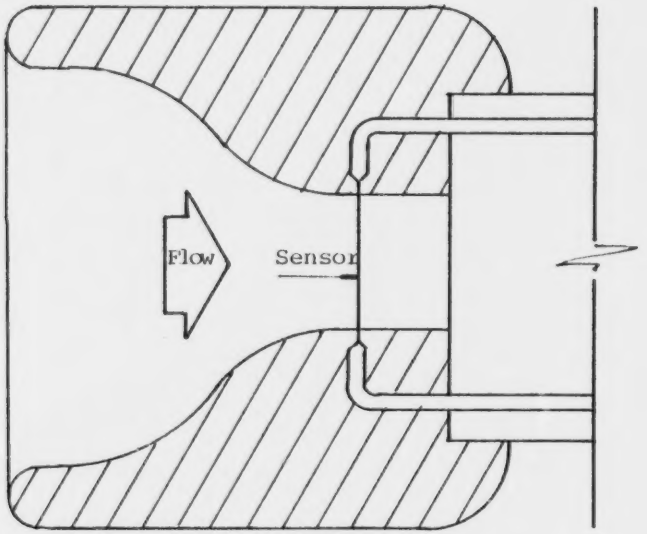

Enlarged Section of the Entrance

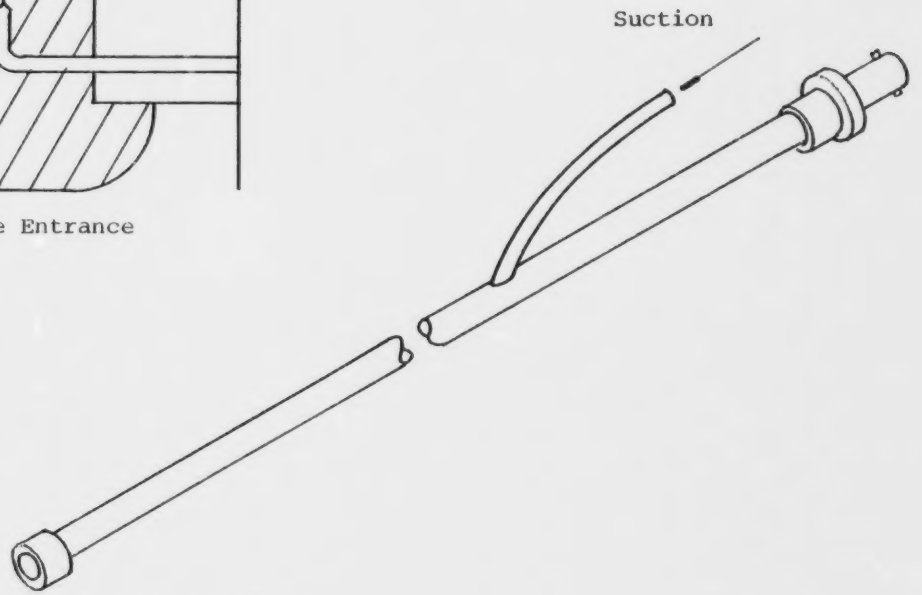

Figure 4: Aspirating Probe

Several problems are associated with the aspirating probe, a description of which follows.

To remove a droplet having a diameter of 600 microns from the sample flow and move it past the hot wire sensor requires an air flow velocity of approximately 30 meters/second (100 feet/second) around the sensor. However, this velocity is too high to assure proper interactions of droplets and sensor. Large droplets are shattered. Interaction time of the small droplets and sensor is too short, greatly reducing the signal output. The reduction of aspiration flow velocity below 30 meters/second prevents the detection of large droplets. As an example, a flow of 3 meters/second (10 feet/second) does not allow for detection of droplets 150 microns or larger.

Another problem associated with the operation of the aspirating probe at a high flow velocity is that the count rate may exceed the maximum counting rate of the instrument, which is 500 droplets per second. An attempt to solve this limitation was made by using a dilution stage. Such a stage mixes a measured droplet-carrying flow with a measured clean air flow, thus reducing the droplet concentration to a level which is compatible with the instrument count rate. The sensor is designed to operate on this diluted sample.

The implementation and operation of a dilution stage is a rather involved procedure. Measurements performed in the laboratory showed poor repeatability. Differences in the temperature of the mixing gases affected the measurements. Furthermore, in order to create a good sample dilution, strong mixing of the two flows is required. The turbulence necessary for this mixing affected the results of the measurement of small droplets. The results of this study were presented to the contract monitor and it was decided that further work with the aspirating probe should be discontinued.

Protected Probe

In order to increase the sensor life, a new probe configuration was implemented. The basic idea was to have a sturdy body with an enclosure to protect the sensor when not in use. Several configuratons were implemented and tested. The one finally selected is shown in Figure 5. It consists of tubing having a diameter of 10 mm (.39 inch) and a length of 30 cm (12 inches). A hole is bored in one end of the tube where the sensor is located. A BNC connector provides the electrical connection. A thin 12 mm (.5 inch) diameter tubing slides

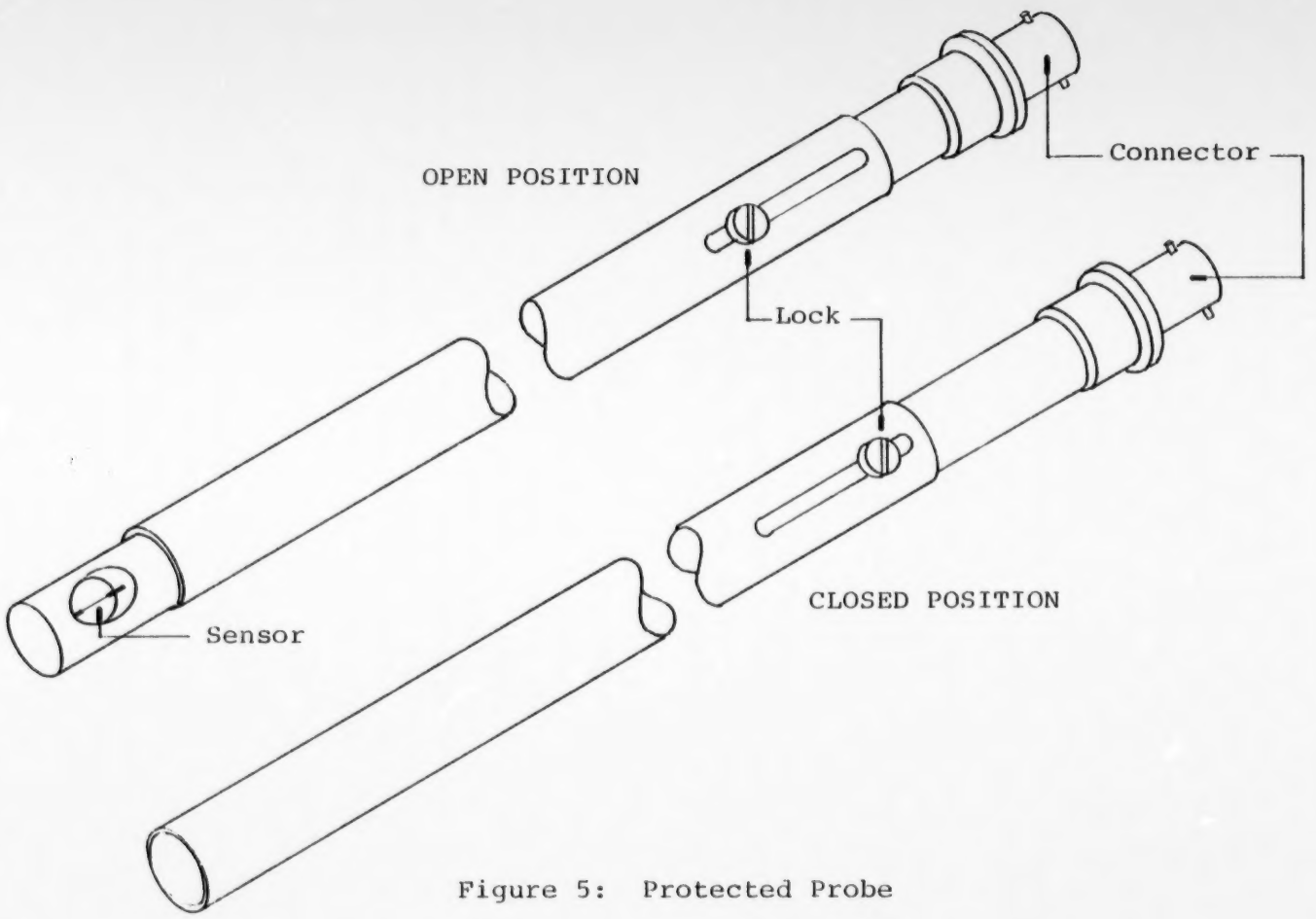

Figure 5: Protected Probe

along the probe closing the opening and protecting the sensor when not in use. The support for the sensor is short and strong to minimize the amplitude of vibration of the sensor when the probe is subject to impact during handling.

To use strong cleaning substances such as hydrochloric and other inorganic acids, the probe is constructed from corrosion-resistant materials. The body of the probe and support of the sensor is made with stainless steel and the insulating material is ceramic.

Techniques to Clean the Sensor

A study of techniques to clean the sensor after it has been operating in slurries and deposit-prone mists and sprays was undertaken. These techniques may be grouped into three approaches:

- Heating,
- Mechanical cleaning,
- Liquid cleaning.

Some of the contaminants which accumulate on the sensor may be removed by heating the probe above the contaminants' boiling or decomposition temperatures. Unfortunately, the contamination may include substances which become baked onto the sensor under the effect of heat. This results in a crust which is difficult to remove by other methods. Hence, it was concluded that heating the probe is not an acceptable cleaning technique.

The mechanical approaches included ultrasonic and sand cleaning techniques. The ultrasonic cleaning was performed by submerging the contaminated sensor in a cleaning fluid and subjecting it to an ultrasonic agitation. The enhancement of the fluid cleaning effect was negligible when low ultrasonic power was used. To be effective, the ultrasonic agitation technique required high power. The extent of this power, however, is capable of destroying the sensor due to mechanical vibration. An attempt to solve this problem was made by designing sensors with a smooth transition between the exposed platinum wire and the silver supporting wire. While sensors of this design did last longer than short transition sensors, they also tended to fail, probably due to flexural fatigue. All the ultrasonic cleaning was performed at a frequency of 30 KHz. If the assumption that sensors break due to flexural fatigue is valid, the use of higher frequencies, and thus substantially lower vibration amplitudes may achieve the

cleaning of the sensor without breaking it. Such an extension of the work was not pursued.

Sand cleaning techniques were performed by dropping sand on the contaminated sensor and also by sand blasting the sensor with a small air jet containing fine particles. The dripping technique was successful, but required relatively large particles and consumed excessive time. The sand blast approach consumed much less time, and was particularly effective for the removal of dry deposits. The sand blaster is mounted in a small jar with a rubber stopper one inch in diameter. The probe, air jet tube and ventilation tube are mounted on the stopper. The sensor must be rotated to expose all areas to the jet stream of sand. Sticky coatings on the sensor such as grease tended to collect the sand, stopping the cleaning action. The best results were achieved with alundum grade 400 which is used to grind optical glass. It was discovered that a slight increase of the sensor's resistance (~.04Ω) during the cleaning operation was a good indication that the bulk of the contaminants were removed. Care should be observed to keep the grinding sand dry.

Liquid cleaners are used either to dissolve the contaminants or to decompose them through chemical reactions.

A variety of organic grease and mineral oil type contaminants are easily removed with a sodium hydroxide solution, which is a good general-purpose cleaner. Greases and oils may also be removed with carbon tetrachloride. Carbon and soot may be removed with commercial liquids used to clean carburetors.

The operation of the probe exposed to tap water shows accumulation of white crystals, mostly sulfates. Solutions of hydrochloric acid 10% prove to be very effective to remove these crystals. As mentioned previously, to submerge the probe in such a corrosive medium, a corrosion proof probe was built using stainless steel for the body and sensor support. The sensor itself uses silver and platinum which are able to withstand the acid. As a dielectric insulator, a ceramic material was used.

Some of the contaminants encountered during the field test of the instrument are soluble in plain water or boiling water. Such is the case of the ammonia sulfate crystals typical of the pilot scrubber at the Colbert Steam Plant in Alabama. Water is also effective for the removal of sodium chloride crystals.

From the described work on sensor cleaning, it has been concluded that sand blasting as well as liquid cleaning may be used to deal with almost all contaminants. The selection of the most effective liquid cleaner requires some systematic search.

Work on Disposable Sensors

Work in the field showed that the cleaning of the contaminated sensor is a time consuming operation, especially when dealing with limestone solutions. In order to expedite the measurement procedure, direct replacement of the contaminated probe with a new one was adopted as a standard procedure. The convenience of having an inexpensive sensor which can be replaced in the field, saving most of the probe's supporting structure, is obvious and a study was undertaken.

The disposable sensor was built on a two-prong plug. The most important consideration was to have good mechanical supporting characteristics and low electrical resistance of the contacts. The corrosion resistance of the materials was not important, since it operates for a short time and it is disposable. Figure 6 shows the disposable sensor probe successfully tested in the laboratory.

Tests were performed with these probes in the laboratory without any problem or deterioration of performance as compared to other types of probes. A probe having the socket mounted on a resilient mount is presently being investigated by KLD. This will effectively reduce the acceleration of the sensor below the breaking point when the probe body or protective ring is impacted during handling or use. The cost of the disposable sensor material is negligible and only the cost of labor for its construction is relevant.

The laboratory work demonstrated the feasibility of the disposable probe, but only limited field experience was possible. KLD recommends that future activities include extensive field testing of the disposable probe.

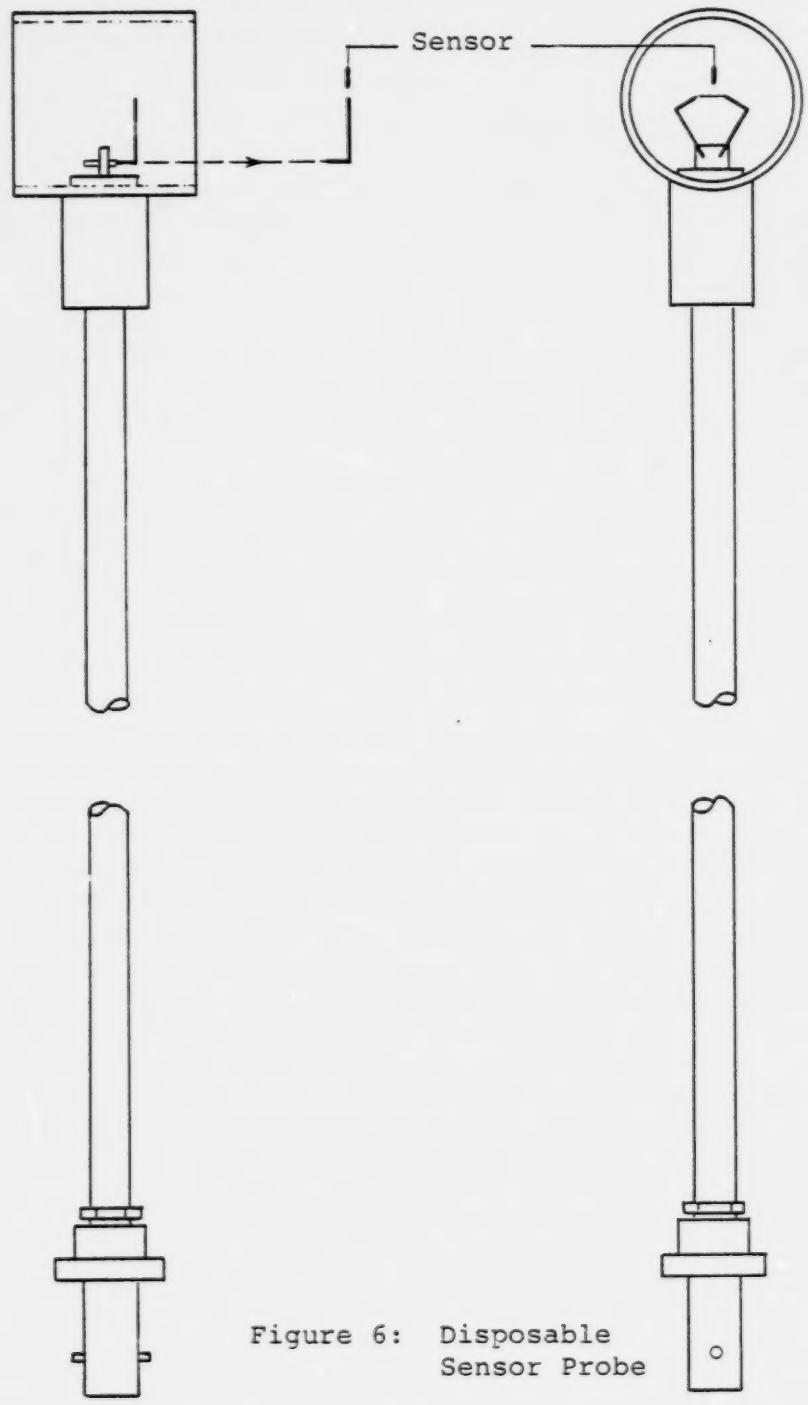

Figure 6: Disposable
Sensor Probe

SECTION 4

THE DC-2

GENERAL DESCRIPTION

The DC-2 is a modified and advanced version of the DC-1 model. The droplet counter/measuring device was extensively investigated in the following areas:

- Temperature flow measurement,
- Velocity flow measurement,
- Droplet counting,
- Modifications of the physical characteristics and construction of the instrument.

The use of the DC-1 droplet counter requires the operator to determine the precise measurement of the probe's resistance under various conditions of gas flow, velocity, temperature and instrument settings. A built-in meter (incorporating a Wheatstone bridge) is used to perform these measurements in the DC-1 as follows (see Ref. 1):

- Setting the DC-1 dial on "TEMPERATURE," the sensor resistance is measured as the temperature of the gas is obtained. This is accomplished by means of a calibration curve showing sensor resistance versus gas temperature.

- Setting the dial on "VELOCITY," the sensor resistance is first measured for a no-flow condition (zero velocity). This is achieved by enclosing the sensor within a shielded container. The sensor resistance is again measured by exposing the sensor to the flow under study. The gas flow velocity is obtained from a calibration curve, depicting gas flow velocity versus the ratio between shielded and exposed sensor resistance.

- After obtaining the sensor resistance for the gas temperature inside the stack, an overheat condition is set on the Wheatstone bridge at a resistance 1.75 times this resistance. The DC-1 is then set to count. The electronics automatically maintain the sensor temperature at 192°C above the gas temperature. At this time, the measurement of the droplet diameter occurs. The counting is allocated to six droplet diameter ranges determined by the particular plug-in distribution module selected.

The convenience of reducing the operator's involvement, as described above, to a minimum became evident after using the DC-1 Droplet Counter in the field. To achieve this, each one of the steps required to perform the measurements was investigated. Possible schemes for their automatic operation were devised and compared. The most suitable were then selected.

The success of automatic operation of the droplet counter depends on the following:

- To fabricate sensors so that a precise correlation between absolute temperature and sensor resistance is achieved. The fabrication of a calibrated sensor requires that a specific resistance be achieved at the ambient temperature at which the etching takes place.

- To replace operator handled calibration curves by automatic electronic processing. For this requirement, the highly non-linear relationship between gas flow velocity and electrical output is linearized by an appropriate circuit.

- To automatically balance the Wheatstone bridge during the measurement of the flow temperature. It should be emphasized that the measurement of the gas temperature itself has no relevance for the measurement of droplet size and concentration. However, this temperature is required to set the operating condition of the sensor at a specific and constant temperature above the stack temperature, thus achieving the proper cooling effect from the interacting droplets.

All the above aspects were successfully accomplished in the course of the project, resulting in an instrument which performs the entire measuring sequence automatically.

The operator of the DC-2 is only required to locate the probe on the facility and switch the power on. By pressing the START button, the following automatic sequence takes place:

- The sensor is cold. Its resistance, indicative of the gas temperature, is measured with an electronic circuit by balancing the Wheatstone bridge. The number of steps required to achieve this balance is a direct indication of the temperature. The temperature is displayed and stored in digital form. The entire measurement takes less than a second.

- At the completion of the temperature measuring cycle, the Wheatstone bridge becomes imbalanced. The electronic feedback circuit heats the sensor, increasing its temperature a prescribed amount above the measured gas temperature. The electric power required to keep the sensor temperature at this level is proportional to the cooling due to gas-to-sensor relative velocity. The electrical power is digitized, stored and displayed. This measurement requires less than a second.

- The pulses generated by the cooling of the sensor under the impaction of the droplets are analyzed for amplitude. Each is then categorized into one of 14 droplet size intervals, plus a total. The time required for this process depends on the number of droplets being counted or the time limit setting. During the counting period, a "C" appears on the display. On reaching a time or droplet count limit, an "H" (HOLD) appears on the display.

- If the "START" button is pressed while the instrument is measuring velocity or counting, a time delay assures that the sensor cools and reaches equilibrium with the surrounding gas prior to the measurement of the temperature.

- When the time or droplet count limit is reached, the power to the sensor is disconnected, extending its life and preventing the accumulation of deposits.

IMPLEMENTATION OF TEMPERATURE MEASUREMENT

The stack temperature is available directly at the DC-2 output display, via the front panel slide select switch. The operator simply sets the switch to "TEMPERATURE", presses the "START" pushbutton, and reads out the temperature directly. The readout is in units of degrees centigrade, with a range of 0°-100°C and a resolution of 1°C.

Figure 7 depicts a block diagram of the "Temperature Conversion Logic." In the DC-2 unit, a ladder network (not to be confused with the interval size module) controlled by a counter and comparator, replaces the potentiometer/null meter employed in the DC-1. When the "START" button is pressed, both the binary and decade counters are automatically incremented to the point where the ladder resistance equals the sensor resistance. The counters contain the available stored temperature information for display purposes. The etching of the platinum wire requires 4 ± .04Ω at 25°C to insure a match in thermal characteristics to the matched ladder network. Figure 8 depicts the sensor conductance versus temperature characteristics. The linear approximation curve resulting from the ladder network is also displayed. Sources of error in the temperature readout and their associated percentage of error are as follows:

- Linear approximation ±4%
- Resistance of ladder ±1%
- Resistance of probe ±1%
- DC drift in the comparator ±1%

These errors, of course, will not always cumulate in the same direction. An RMS average is more realistic, resulting in a full scale-percent error of ±4.35%.

IMPLEMENTATION OF VELOCITY MEASUREMENT

Several improvements for velocity measurement have been incorporated in the DC-2. First, the measurement was automated. In addition, the measurement range and accuracy were improved by three changes:

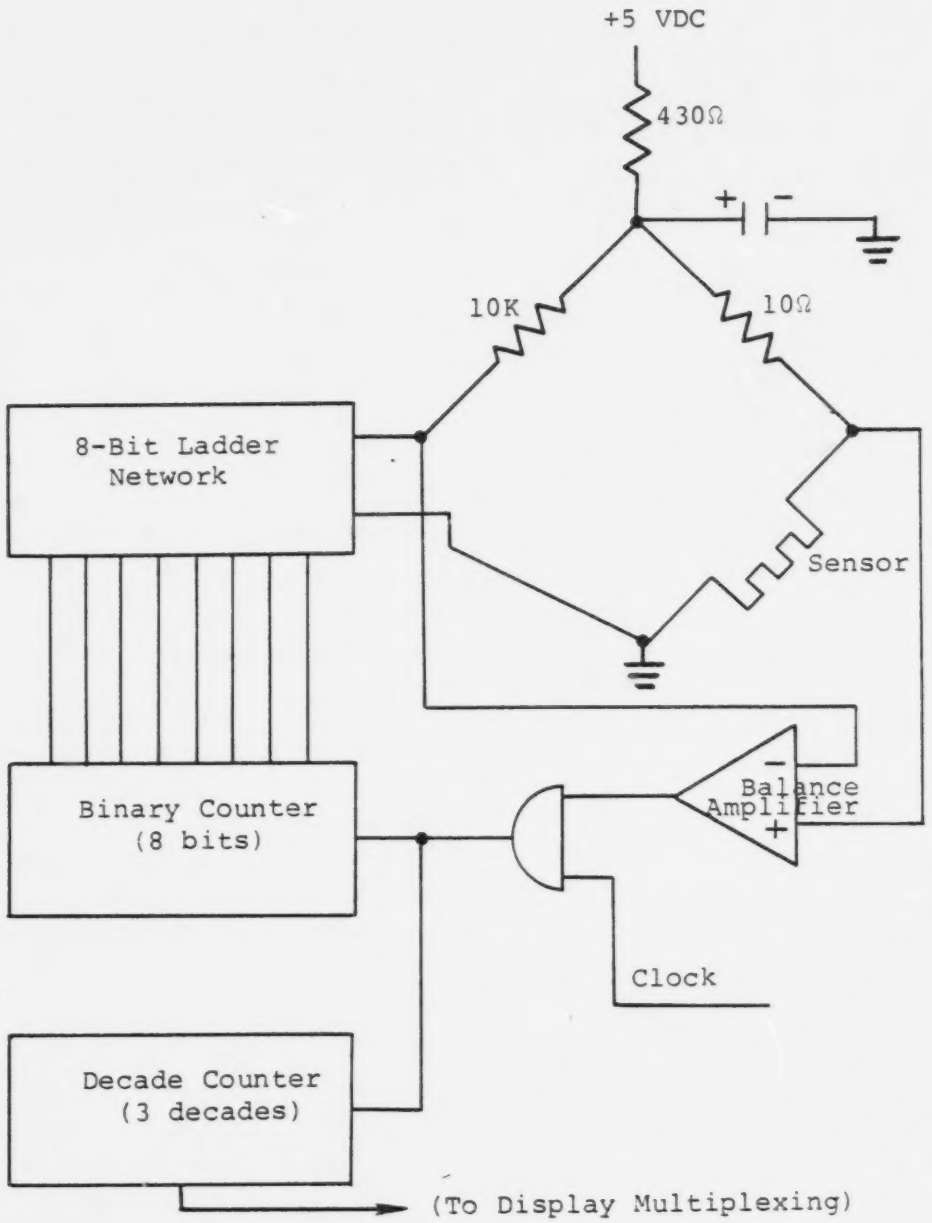

Figure 7: Temperature Conversion Block Diagram

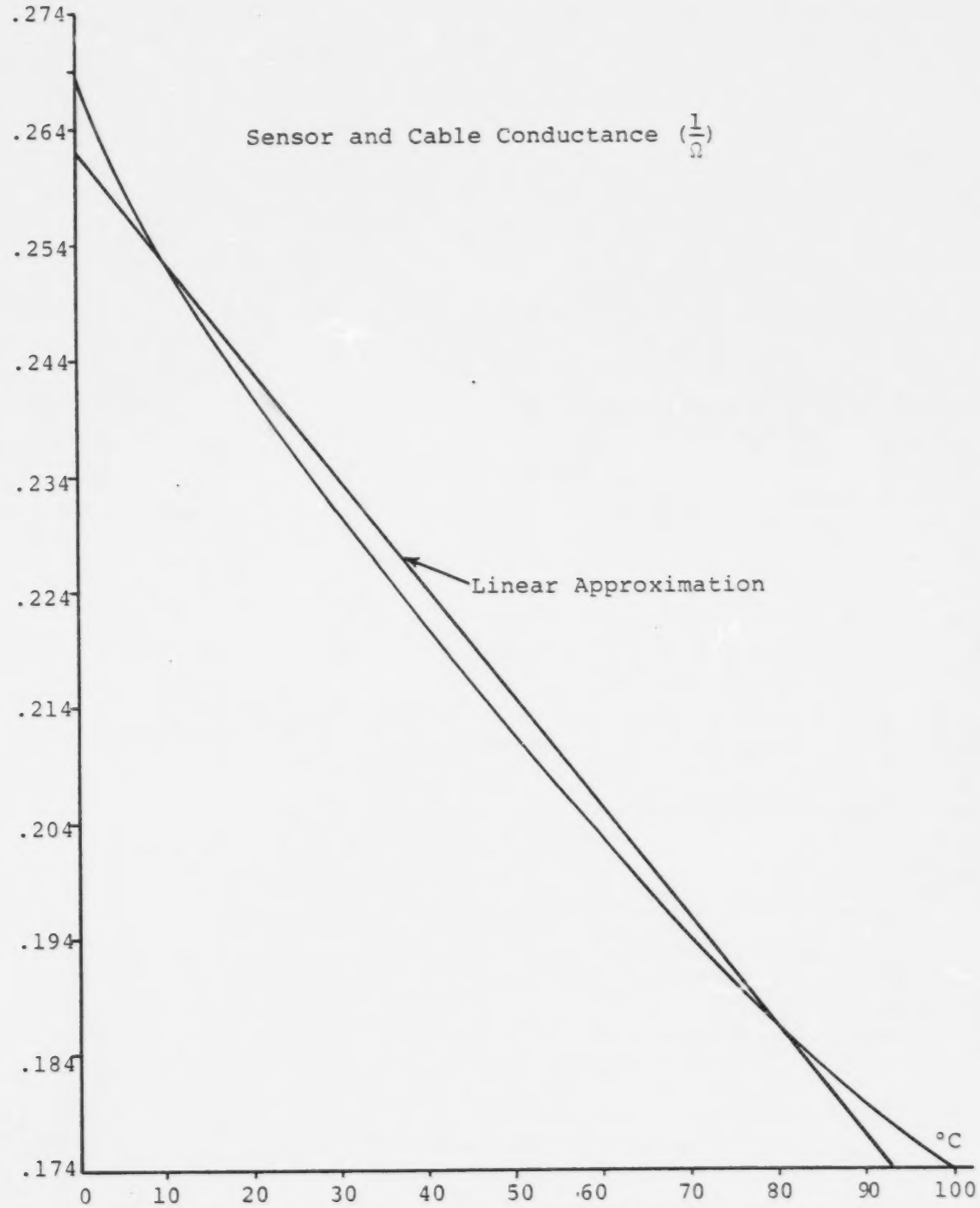

Figure 8: Sensor Temperature Characteristics

- The probe temperature was elevated (overheat mode).

- Constant probe temperature was employed instead of constant probe heating current.

- A precise linearizer circuit was used to compensate for the response of the sensor.

- A special circuit was incorporated to compensate for droplets which strike the probe and tend to cause velocity measurement errors.

The DC-2 Droplet Counter provides a direct indication of the flow velocity in digital form. It is displayed by setting the slide switch to "VELOCITY". The readout is in meters per second. The range is between 0 to 10 with a resolution of .1 meter per second.

In measuring velocity with the DC-1, a constant heating current is employed, whereas with the DC-2, the sensor is maintained at a constant temperature. A feedback power amplifier maintains a sensor temperature of approximately 250°C above the ambient temperature. This automatic setting is performed in two steps:

- The Wheatstone bridge is balanced, as described above, for the gas temperature measurement.

- The sensor is heated by short circuiting half of the bridge resistance, n, (see Figure 9) and connecting a power amplifier on the feedback loop. The sensor is heated until its increase in resistance restores the bridge balance.

From the principle associated with the operation of the hot wire anemometer, it is known that the cooling effect of a gas flow depends on the temperature difference of the sensor and gas and on the velocity of the gas. The voltage, V_B, is directly proportional to the energy released from the sensor because of the gas flow. This voltage ranges from .8 volts at zero velocity to 1.3 volts at a velocity of 10 meters per second. An amplifier is used to subtract the voltage at zero velocity. The amplifier also scales the electrical signal which is fed to a squaring network. This results in a relationship of linear voltage versus gas velocity.

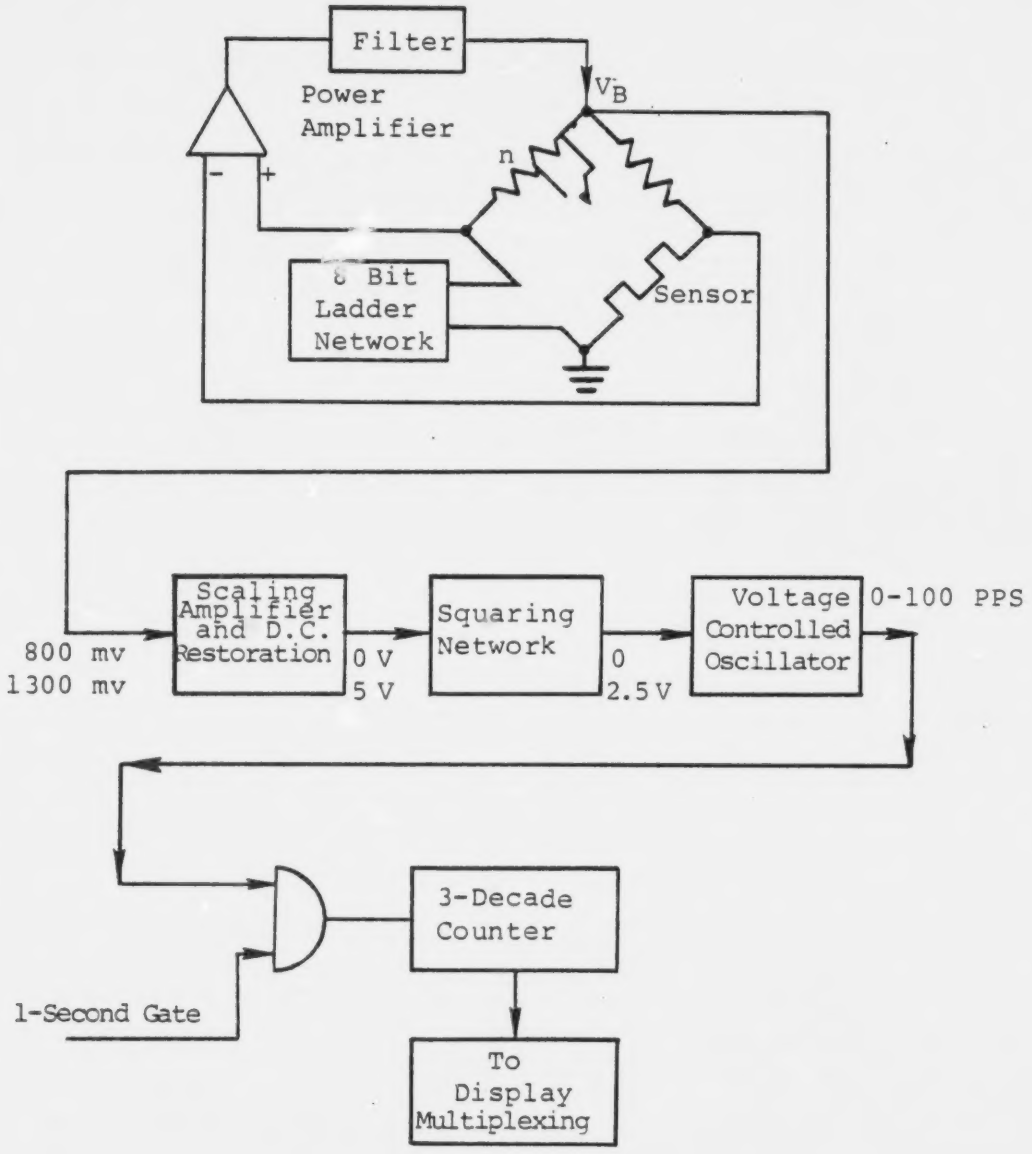

Figure 9 : DC-2 Velocity Measurement Network

To digitize the gas velocity information, the linearized signal acts on a voltage controlled oscillator whose frequency is zero for no flow and increases to 100 pulses per second for a flow of 10 meters per second. The output from the voltage controlled oscillator is accumulated during one second. The information is stored and displayed in meters per second. The presence of large numbers of droplets in the gas flow has a cooling effect which may be interpreted by the instrument as an apparent higher gas flow velocity. To compensate for this error, a special circuit was conceived and incorporated into the DC-2. The basic idea is the separation of droplet signals, with characteristic spikes, from the constant level electrical signal created by the gas flow. The droplet signals are integrated and the correction is subtracted from the total bridge voltage.

DROPLET COUNTING

The operation of the DC-2 in the count mode differs from the operation of the DC-1. The DC-2 is automated with three droplet TOTAL LIMITS and three TIME LIMITS. Furthermore, the number of droplet size intervals was increased from six to 14.

The operator of the DC-2 does not have to make any potentiometer/null meter measurements as is necessary with the DC-1. When the operator presses the "START" button, the temperature ladder network is automatically set to the probe resistance as previously described. At the end of the temperature conversion cycle, lasting for less than one second, the DC-2 automatically goes into the count mode. This starts with the overheat mode, which is described in the velocity flow section. The overheat is held throughout the entire count cycle and is released when the preset limit is reached. Overheating of the probe only occurs during the count mode, thus augmenting the life of the probe. The storage capacity of each of the size intervals for droplet diameter was increased to 10,000.

PHYSICAL CHARACTERISTICS AND USE OF THE DC-2

Particular attention was devoted to better adapt the Droplet Counter to field work by making it more transportable and convenient to use. The DC-2 consists of the device itself, five probes, four modules for different droplet size ranges and a coaxial cable approximately 15 feet long. All components are neatly contained in a portable case. The dimensions of the case are:

Length: 36.5 cm (14 1/2 inches)
Width: 15.1 cm (6 inches)
Height: 15.3 cm (5 27/32 inches)
Weight: 4 kgm (10 lbs.)

The case and card bucket are made of drawn aluminum. The circuit cards are wire-wrapped and made of glass epoxy. The instrument is powered from 125 VAC (±15%), 60 Hz line, requiring 2.5 watts of power. The electronics were designed with low power CMOS logic. The digital display is a liquid crystal type, chosen for its superior performance in bright ambient light.

A view of the instrument panel is presented in Figure 10.

Use of the Instrument

In order to collect data on droplet size and concentration, the instrument must be powered from a 110-volt, 60-Hz line. The coaxial cable and probe are connected with the instrument OFF. A toggle switch is used to activate the instrument; no warm-up period is required. The probe is inserted into the flow under study. It is important to realize that the DC-2 monitors the flow conditions and droplet population practically on a single stream line. Whenever average conditions over the facility cross section are desired, an appropriate set of sampling points must be adopted.

It is important to position the sensor axis perpendicular to the gas flow to obtain valid gas flow velocity and droplet population data. In certain facilities, the flow direction is not known; e.g., flow rotation generated by spinners, blowers or flow barriers. A proper sensor positioning is achieved by observing the velocity reading while reorienting the sensor direction. The maximum measured gas velocity corresponds to a sensor perpendicular to the flow direction.

The probe should be handled with care to avoid damage or destruction of the sensor due to impacts. Droplets and gas flow do not damage the sensor.

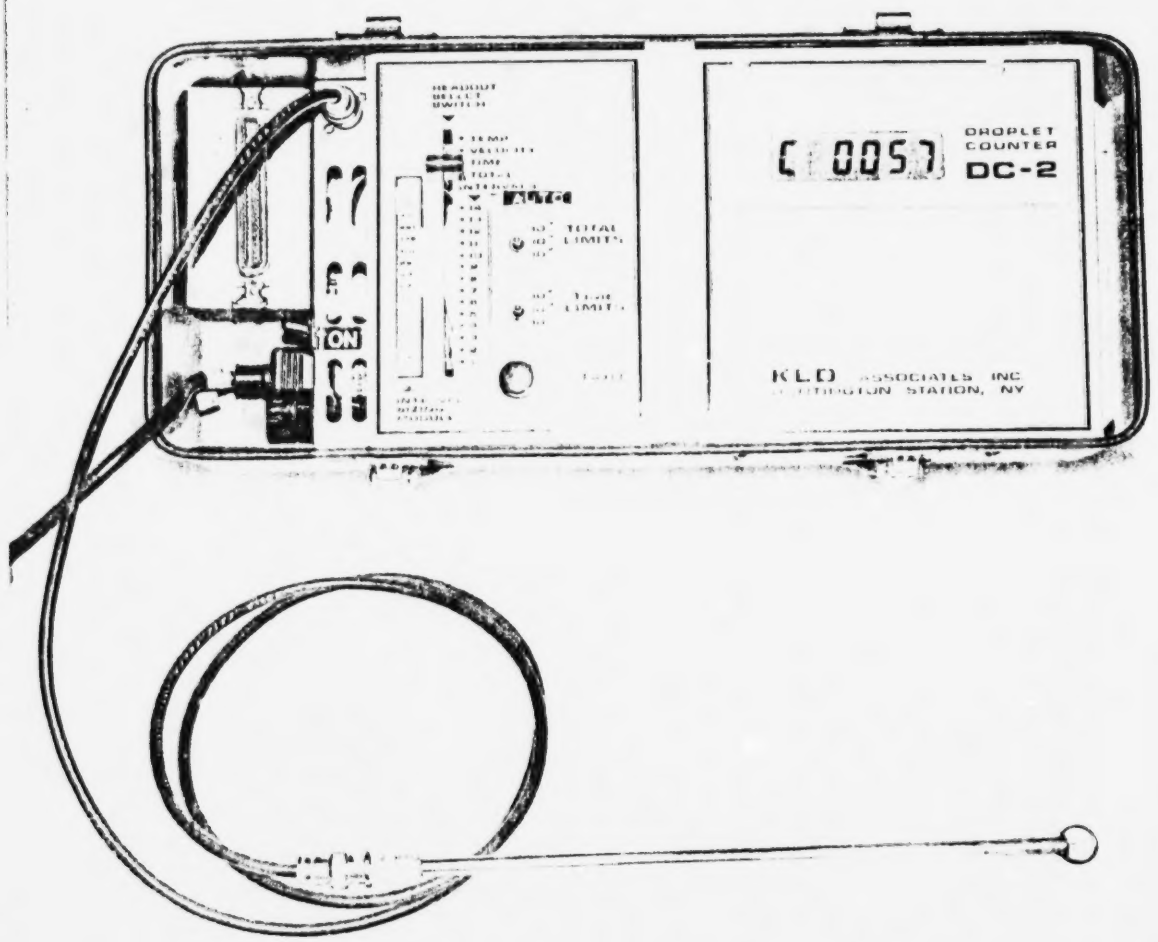

Figure 10: View of the DC-2 Front Panel

Selection of the Droplet Distribution

Four sizing modules are made available to the operator as shown in Tables 1, 2, 3 and 4. Two of them cover the entire droplet diameter range of the instrument, while the other two emphasize detection of smaller droplets. The operator selects the module which best describes the facility conditions and inserts it in the holder at the left side of the front panel. The removal of the module is performed by pushing upwards through a slot at the side of the module holder. A series of numbers are printed at the exposed side of each network. These numbers represent the droplet diameter in microns. The readout select switch points to the interval number on the right and the corresponding droplet diameters on the left. The interval size represents the smallest droplet diameter for each interval. The electronics also keeps a count of the total number of droplets.

The total number of droplets to be counted is selected by a toggle switch which allows for the selection of 100, 1,000 or 10,000 total number of droplets.

If so desired, the instrument can be operated on a time-limit basis by selecting, with another toggle switch, 10, 100, or 1,000 seconds.

The droplet counting process will stop whenever the total selected number of droplets or time limit is reached, whichever happens first. When this occurs, the letter "H" appears in the display, signifying that the system is in hold, awaiting another cycle initiation. The following data is available for readout:

TEMPERATURE of the gas,
VELOCITY of the gas flow,
TIME interval,
TOTAL number of droplets and the
number of droplets in each one of the 14 size INTERVALS.

Handling and Maintenance

A few precautions are necessary in handling the DC-2 to achieve maximum performance and prevent damage to the sensor. The probe should never be treated roughly, nor should the operator attempt to touch the sensing wire. The sensing wire may be broken if the aerosol stream contains large solid particles.

For best operation, the probe should be kept clean. A medium power magnifier may be used to determine the state of cleanliness of the sensor, and liquid cleaners are the best means of removing contaminants.

The electronics of the DC-2 is all solid state and highly reliable. If the unit does not perform, first check the fuse that is located in the bottom of the box near the power ON switch. If the fuse is not open, place the Readout Select Switch in the TEMPERATURE measuring position and press the START button. If the probe is operating properly, the number in the display will count to some finite value and remain there. If the probe is faulty, the number in the display will not reach a fixed value, but will continually cycle from zero to a maximum.

DATA ANALYSIS

The DC-2 Droplet Counter is capable of providing a large amount of data which is usually presented in tables or, more often, on graphs. A volume or mass distribution emphasizes large droplets and de-emphasizes or ignores the small ones. On the other hand, a description of the number of droplets puts the emphasis on the smaller droplets, which are more numerous. A third presentation, seldom used, depicts the surface of the liquid droplets versus its diameter. In this case, the emphasis is a compromise between the other two methods.

In principle, it is possible to convert from one distribution to another, but in practice, care should be exercised to prevent the introduction of large errors due to averages and approximations. An obvious example is the difference between direct average diameter and the diameter of the average volume.

The droplet distribution may be displayed by computing and summarizing the number of droplets or by summarizing the volume of these droplets. The droplet concentration, n_i, corresponding to each droplet size interval is computed by the expression:

$$n_i = \frac{N_i}{v \cdot t \cdot \ell (D_i + d)} \text{ Drop/cm}^3 \qquad (i = 1,14)$$

where

N_i = Droplets counted in the i^{th} channel
v = Flow velocity (cm/sec)
t = Time interval (sec)
ℓ = Sensor length (.1 cm)
D_i = Average droplet diameter for the i^{th} channel (cm)
d = Sensor wire diameter (5×10^{-4} cm).

In plotting the distribution of the number of droplets versus droplet diameter, each of the values of n_i is divided by the width of the droplet size interval, ΔD_i, in microns. This ordinate is then plotted corresponding to values of the related average droplet diameter, D_i. To simplify the computation, all the constants are grouped together by a factor, K_i or K_{iv}, presented in Tables 1, 2, 3 and 4. This allows for the following expression:

$$\hat{n}_i = \frac{n}{\Delta D_i} = \frac{K_i N_i}{v \cdot t}$$

where $\hat{n}_i$ is the number of droplets per unit volume of gas per unit diameter range for the i^{th} size interval.

For the volumetric distributions, V_i, in the i^{th} size interval, the expression becomes

$$V_i = \frac{\pi}{6} D_i^3 n_i .$$

By writing in terms of the constant, K_{iv}, of Tables 1 through 4,

$$\hat{V}_i = \frac{V_i}{\Delta D_i} = \frac{K_{iv} N_i}{v \cdot t} .$$

With the above formulas, the data from the DC-2 can be readily reduced to produce number concentration or volume distribution. Other quantities often encountered in particle sizing, such as mass mean diameter, surface mean diameter, etc., can be derived from the existing data without difficulty. In Section 6, Laboratory Testing, these formulas are applied to make comparisons with the mass measurements from the Brink impactor. Also discussed in Section 6 are the effects of flow conditions on the capture size of the hot wire.

Table 1: Internal Sizing Distribution for Module 1

Size Interval	Droplet Diameter (microns)	D_i (microns)	K_i $\left(\frac{1}{cm^2 micron}\right)$	K_{iv} $\left(\frac{micron^2}{cm^2}\right)$
1	1.0-1.6	1.3	2.6×10^4	3.0×10^4
2	1.6-2.6	2.1	1.4×10^4	6.8×10^4
3	2.6-4.1	3.35	8.0×10^3	1.6×10^5
4	4.1-6.6	5.35	3.9×10^3	3.1×10^5
5	6.6-10	8.3	2.2×10^3	6.6×10^5
6	10 - 17	13.5	7.7×10^2	9.9×10
7	17 - 27	22.0	3.7×10^2	2.1×10^6
8	27 - 43	35.0	1.6×10^2	3.5×10
9	43 - 69	56.0	6.3×10^1	5.8×10^6
10	69 - 110	89.5	2.6×10^1	1.0×10^7
11	110 - 176	143.0	1.0×10^1	1.7×10^7
12	176 - 281	228.5	4.0×10^0	2.8×10^7
13	281 - 450	365.5	1.6×10^0	4.1×10^7
14	> 450	585.0	6.3×10^{-1}	6.6×10^7

Table 2: Internal Sizing Distribution for Module 2

Size Interval	Droplet Diameter (microns)	D_i (microns)	K_i $\left(\frac{1}{cm^2 micron}\right)$	K_{iv} $\left(\frac{micron^2}{cm^2}\right)$
1	1 - 36	18.5	1.2×10^2	4.0×10^5
2	36 - 70	53	5.0×10^1	4.0×10^6
3	70 - 105	87.5	3.0×10^1	1.2×10^7
4	105-139	122.0	2.3×10^1	2.3×10^7
5	139-174	156.5	1.7×10^1	3.6×10^7
6	174-209	191.5	1.5×10^1	5.5×10^7
7	209-243	226.0	1.3×10^1	7.6×10^7
8	243-278	260.5	1.0×10^1	9.6×10^7
9	278-313	295.5	9.5×10^0	1.3×10^8
10	313-347	330.0	8.8×10^0	1.6×10^8
11	347-382	364.5	7.7×10^0	2.0×10^8
12	382-416	399.0	7.3×10^0	2.4×10^8
13	416-450	433.0	6.7×10^0	2.8×10^8
14	> 450	468.0	6.0×10^0	3.3×10^8

Table 3: Internal Sizing Distribution for Module 3

Size Interval	Droplet Diameter (microns)	D_i (microns)	K_i $\frac{1}{cm^2 micron}$	K_{iv} $\frac{micron^2}{cm^2}$
1	1 - 1.4	1.2	4.0×10^4	3.7×10^4
2	1.4-1.8	1.6	3.8×10^4	8.1×10^4
3	1.8-2.5	2.15	2.0×10^4	1.1×10^5
4	2.5-3.3	2.90	1.6×10^4	2.1×10^5
5	3.3-4.5	3.90	9.4×10^3	2.9×10^5
6	4.5-6.1	5.3	6.0×10^3	5.0×10^5
7	6.1-8.2	7.15	4.0×10^3	7.9×10^5
8	8.2-11	9.6	2.4×10^3	1.2×10^6
9	11-15	13	1.4×10^3	1.7×10^6
10	15-20	17.5	8.9×10^2	2.6×10^6
11	20-27	23.5	5.0×10^2	3.6×10^6
12	27-37	32.0	2.7×10^2	4.8×10^6
13	37-50	43.5	1.6×10^2	6.8×10^6
14	> 50	60	7.7×10^1	8.7×10^6

Table 4: Internal Sizing Distribution for Module 4

Size Interval	Droplet Diameter (microns)	D_i (microns)	K_i $\frac{1}{cm^2\ micron}$	K_{iv} $\frac{micron^2}{cm^2}$
1	1 - 3	2	7.1×10^3	3.0×10^4
2	3 - 5	4	5.6×10^3	1.9×10^5
3	5 - 7	6	4.5×10^3	5.2×10^5
4	7 - 9	8	3.8×10^3	1.0×10^6
5	9 - 11	10	3.3×10^3	1.8×10^6
6	11-13	12	2.9×10^3	2.7×10^6
7	13-15	14	2.6×10^3	3.8×10^6
8	15-17	16	2.4×10^3	5.1×10^6
9	17-19	18	2.2×10^3	6.7×10^6
10	19-21	20	2.0×10^3	8.4×10^6
11	21-23	22	1.9×10^3	1.0×10^7
12	23-25	24	1.7×10^3	1.3×10^7
13	25-27	26	1.6×10^3	1.5×10^7
14	> 27	28	1.5×10^3	1.7×10^7

SECTION 5

PRINTER/CONTROLLER

GENERAL DESCRIPTION

The Printer/Controller was designed to work in conjunction with one or two DC-2 Droplet Counters and a Probe Multiplexer. It provides the user with a summary printout of data measured by the Droplet Counters. This eliminates recording the data manually.

The front panel controls make the printer/controller a very versatile instrument. The controls consist of Month and Day thumbwheel switch, Number of Runs switch, Print Mode switch, Time Interval switch, Limit Select switch, Start switch, Paper Feed switch and Clock Control switches. The functions of these switches will be discussed in greater detail later in this section.

At the beginning of each Print Cycle the Serial Number, Date and Time information is printed out. Other information being printed out is Temperature, Total number of droplets counted, Elapsed Time (time required to count droplets), Velocity and Droplet Distribution. When in the MUX Mode, the printer will also print out the number of the probe being monitored.

The Clock Module provides the time information while Month and Day information is set manually with thumbwheel switches. The droplet distribution information is received from the Droplet Counter with respect to the Distribution Module being used. An example of a typical printout is illustrated in Figure 11.

Printing is done by a mosaic printer capable of printing all characters that can be formed within a 7 by 5 dot matrix. The printer is mounted in such a way that access to the paper and ribbon only requires the removal of a cover plate.

FUNCTIONS OF FRONT PANEL SWITCHES

Figure 12 is an illustration of the front panel of the Printer/Controller. The function of the panel switches are as follows:

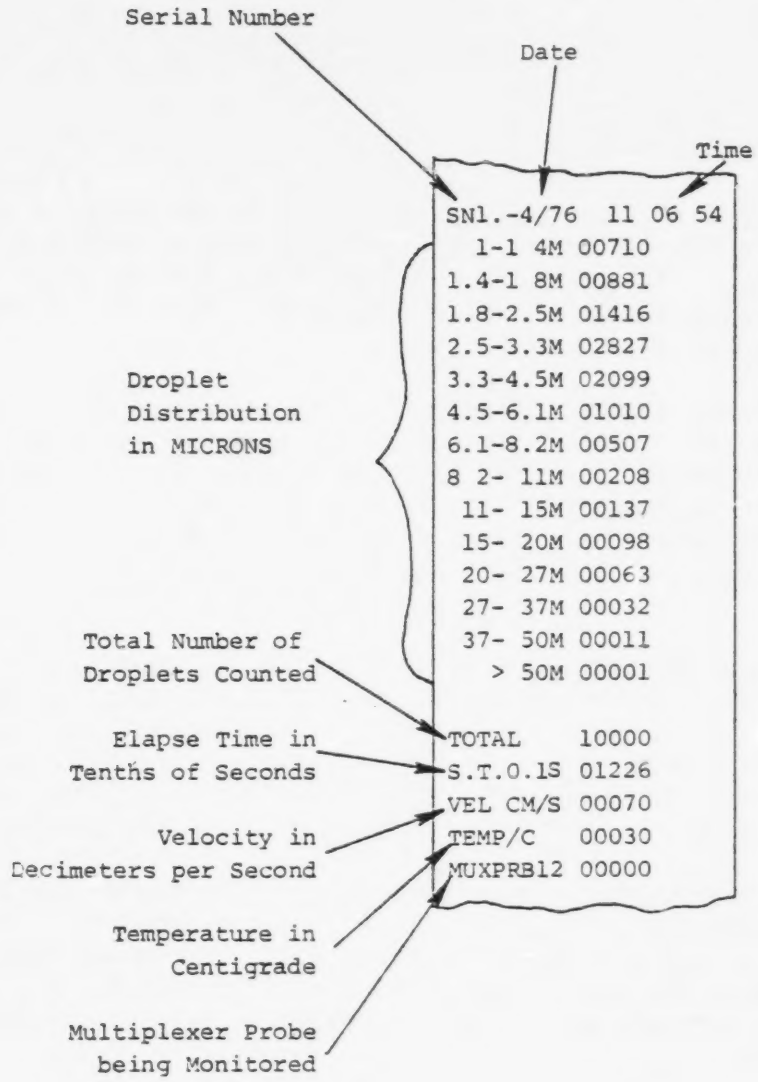

Figure 11: Printout Illustration

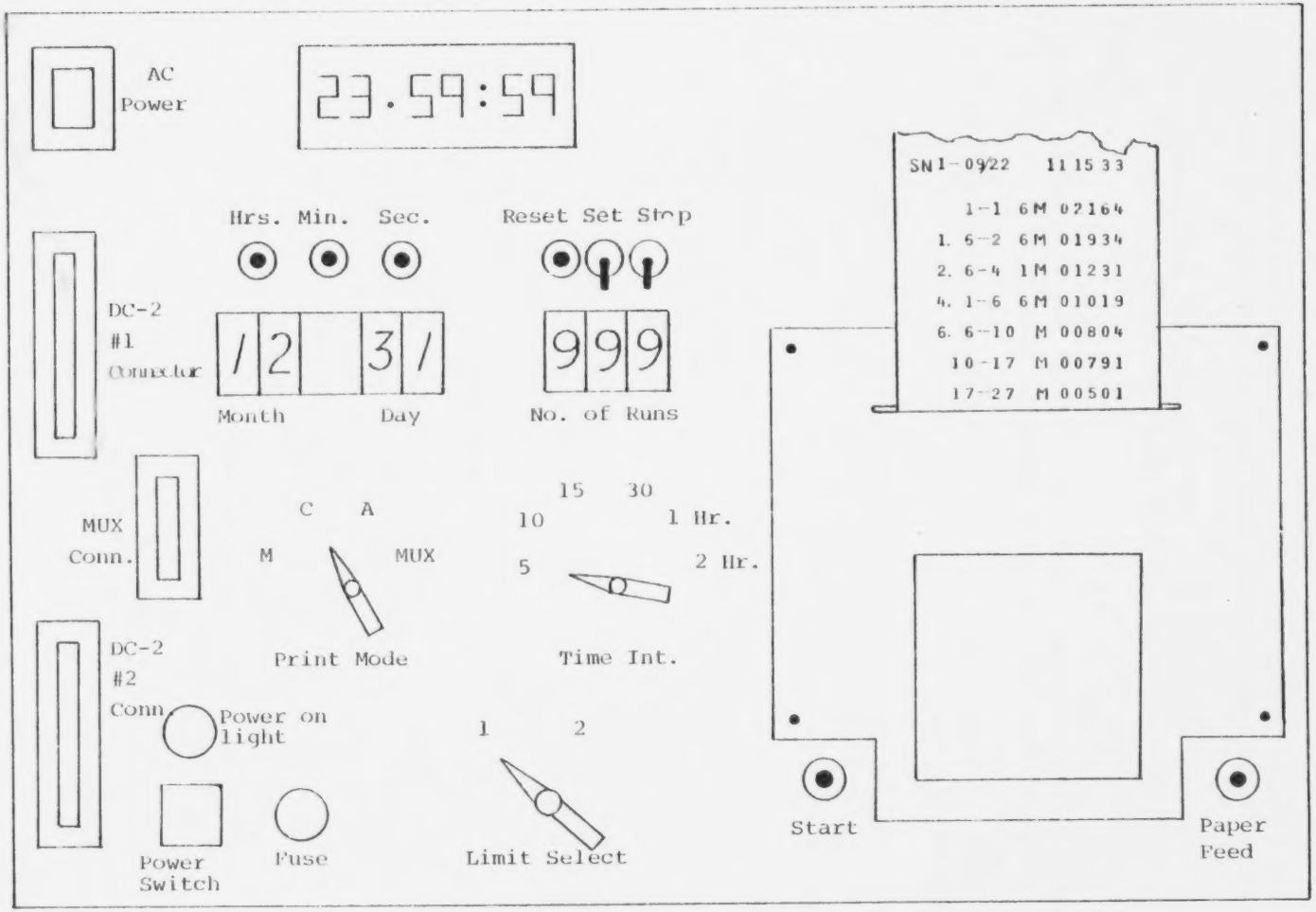

Figure 12. Printer Panel Layout

1. Limit Select switch determines when printer operation begins with respect to the Droplet Counter or Counters.

   a) In the #1 position, the printer is activated whenever either one of the two DC-2's goes into HOLD.

   b) In the #2 position, the printer is activated only when both DC-2's have reached HOLD.

2. Print Mode Switch - This is a four-position switch selecting the following print mode operations:

   a) Manual Mode (M) - Each print cycle has to be initiated by depressing and releasing Start switch.

   b) Continuous Mode (C) - Once the print cycle is initiated, the printer will operate continuously until it is stopped manually or by the Number of Runs switch.

   c) Automatic Mode (A) - This mode of operation is ideal for long-term unmanned testing operations. After initiating the first print cycle, all other print cycles are under the full control of the Number of Runs switch and Time Interval switch.

   d) MUX Mode - Initiation of first print cycle again is required and the remainder is dependent on the setting of the Number of Runs switch. The setting of the Number of Runs switch is dependent on the Number of Probes being monitored by the Multiplexer. Printout of Probe data will be continuous. Each time a set of Data is required, a new print cycle must be initiated.

3. Month and Day Switch - The Month and Day information which is to appear on the printout must be manually set up with these thumbwheel switches.

4. Number of Runs Switch - The setting of this thumbwheel switch determines the number of cycles that will be printed out when the Print Mode Switch is in Continuous, Automatic or MUX.

5. Time Interval Switch - This switch allows the print cycles to be spaced with respect to elapsed time. It is functional only when Print Mode Switch is in Automatic.

6. Start Switch - To initiate printer operation, this switch must be depressed and released. The depressing of the Start switch will put the DC-2's into the count mode and allow them to collect Data.

7. Paper Feed - To advance paper, depress and hold until desired amount of paper has been advanced and then release.

8. Clock Controls - The setting of the Clock Module and Display is accomplished by six Front Panel switches. Their functions are as follows:

   a) Hours Set - The setting of the Hour is done by depressing and releasing the HRS pushbutton until desired hours reading is displayed.

   b) Minutes Set - Minute setting is done by depressing and releasing MIN pushbutton switch until desired Minutes reading is displayed.

   c) Seconds Set - To set the seconds, the SEC push-button must be depressed and released when desired seconds reading is displayed.

   d) Reset - By depressing and releasing switch marked "R," the Clock Module and Display are set to 0 hrs., 0 min. and 0 sec.

   e) Run/Set Switch - This switch prevents the accidental changing of the Time while clock is running. In the RUN Position, Clock Set switches are inhibited.

   f) Run/Stop Switch - Controls operation of Clock Module when Run/Set switch is in the Set position.

INTERFACING WITH TWO DC-2's

The Printer/Controller can be used with one or two DC-2 Droplet Counters. Figure 13 is a schematic of the interface hookup of one and two Droplet Counters with the Printer/Controller. If two counters are connected to the printer, the outputs of each are distinguished by the serial number code on the printout. Each DC-2 functions separately and independently.

PROBE MULTIPLEXER SYSTEM

The Probe Multiplexer, when used with the DC-2 and Printer/Controller, expands the probe monitoring capability from one to 12 probes. Selection of probes to be monitored is done with a 12-position pushbutton Selector Switch. Only one probe will be able to transmit data to the DC-2 at a time. The determination as to which probe will be monitored is controlled by the Selector Switch and the electronics within the Probe Multiplexer. When more than one selector button is depressed, probes are monitored in a descending order, starting with the highest number probe selected.

The data collected by the probe is transmitted to the DC-2 and then printed out by the Printer/Controller in a similar manner as described at the beginning of this section.

The Probe Multiplexer electronics receives its DC power from the Printer/Controller via the Probe Multiplexer Interface cable which is supplied with the Printer Interface. Therefore, any power failure in the Printer/Controller will cause a loss of power in the Probe Multiplexer. Once power has been restored, probe monitoring will again start from the highest number probe selected.

Figure 14 is a schematic of the interface hookup of the DC-2 with the Multiplexer system.

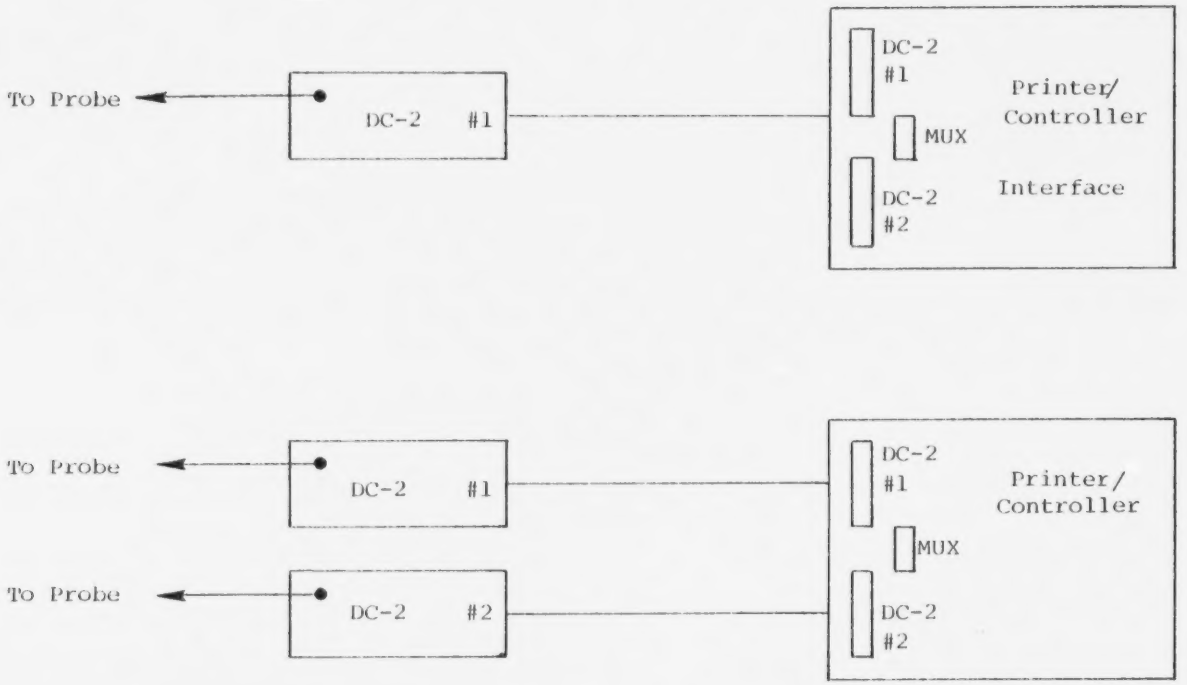

Figure 13 . Schematic of DC-2 Interface with Printer/Controller

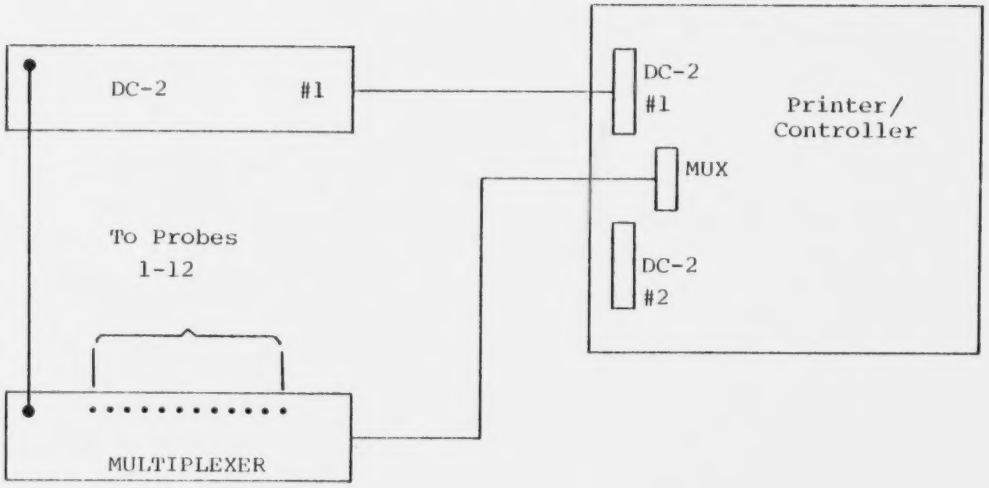

Figure 14: Schematic of DC-2 Interface with Multiplexer System

SECTION 6

LABORATORY INVESTIGATIONS

Extensive laboratory investigations were performed using the DC-2 and the hot wire probe. The laboratory studies concentrated on two main topics:

- Calibration Tests
  The objective of this effort was to calibrate the DC-2 for a range of operating conditions using laboratory equipment. The procedures and apparatus used for these tests are described in this section. In addition, several analytical studies were performed in support of the calibration effort. The most important result from the analytical studies was the analysis of the capture size of the wire.

- Laboratory Tests with the Impactor
  The objective of these tests was to accumulate laboratory data using a Brink impactor and to then make comparisons with the measurements from the DC-2. Extensive tests were performed to achieve this objective and these tests are tabulated in Appendix A along with the test purpose and configuration of the experimental apparatus. Again, certain analytical studies were performed in support of the experimental work. Both the experimental and analytical results are discussed in the following section.

CALIBRATION TESTS

A special apparatus was designed and built by KLD to perform the calibration of the DC-2. The approach adopted for calibration is optical. As an interacting droplet makes contact with the hot wire sensor, it is observed under a microscope. A photographic camera records the image of both the sensor and the droplet. By adopting this technique, a permanent record is obtained to study the attachment mechanism and to provide the calibration data. Since the interaction

time is short, an electronic flash is used to stop the motion at the instant of droplet-sensor contact. Thus, no appreciable shrinkage due to evaporation takes place and accurate calibration data is obtained. The duration of the flash is approximately one microsecond, which is compatible with the time a droplet, with a diameter range of interest, moves and shrinks. The electronic flash provides a bright background for the hot wire. Both wire and droplet appear dark with sharp boundaries, making a clear contrasting photograph. Figure 15 shows the arrangement of the main components. The camera is a Polaroid with Type 107 film. Optics capable of magnifying the subject up to 100 times its actual size were used. Magnification limits were set by the length of the wire (~1 mm) and the diagonal dimension (10 cm) in the photographic plane. A standard Leitz compound microscope was used, and the microscope specimen holder was adapted for the support of the probe. The micrometric positioning setup was used to position the sensor in the microscope field.

Simultaneously, as the photograph of the interacting droplet was taken, an oscilloscope picture of the electrical signal was also recorded. Measurements from each pair of pictures were recorded, obtaining droplet diameter size in microns and corresponding peak electrical signal in volts.

An important aspect of this calibration is the generation of water droplets. A variety of devices were investigated to create water droplets within the diameter range of interest. The ideal droplet generator should provide a monodisperse aerosol of adjustable droplet sizes. Instruments with these characteristics are available, but their cost and complexity do not always justify their use. Therefore, KLD designed and constructed a cost-effective device capable of generating droplets using a compressed air-driven spray. Droplet diameter sizes were controlled by adjusting the pressure; low air pressure emphasizes large droplets while high pressure creates a fine mist or small droplets. In order to measure the electrical signal peak amplitude over the wide random range of droplet sizes, a two-beam scope was used with a different gain for each trace.

The sensor was mounted away from the apparatus creating the spray (within 1 foot) so that one interaction every few seconds was obtained. This period between droplets allowed time for setting the calibration apparatus and avoided multiple droplet interactions.

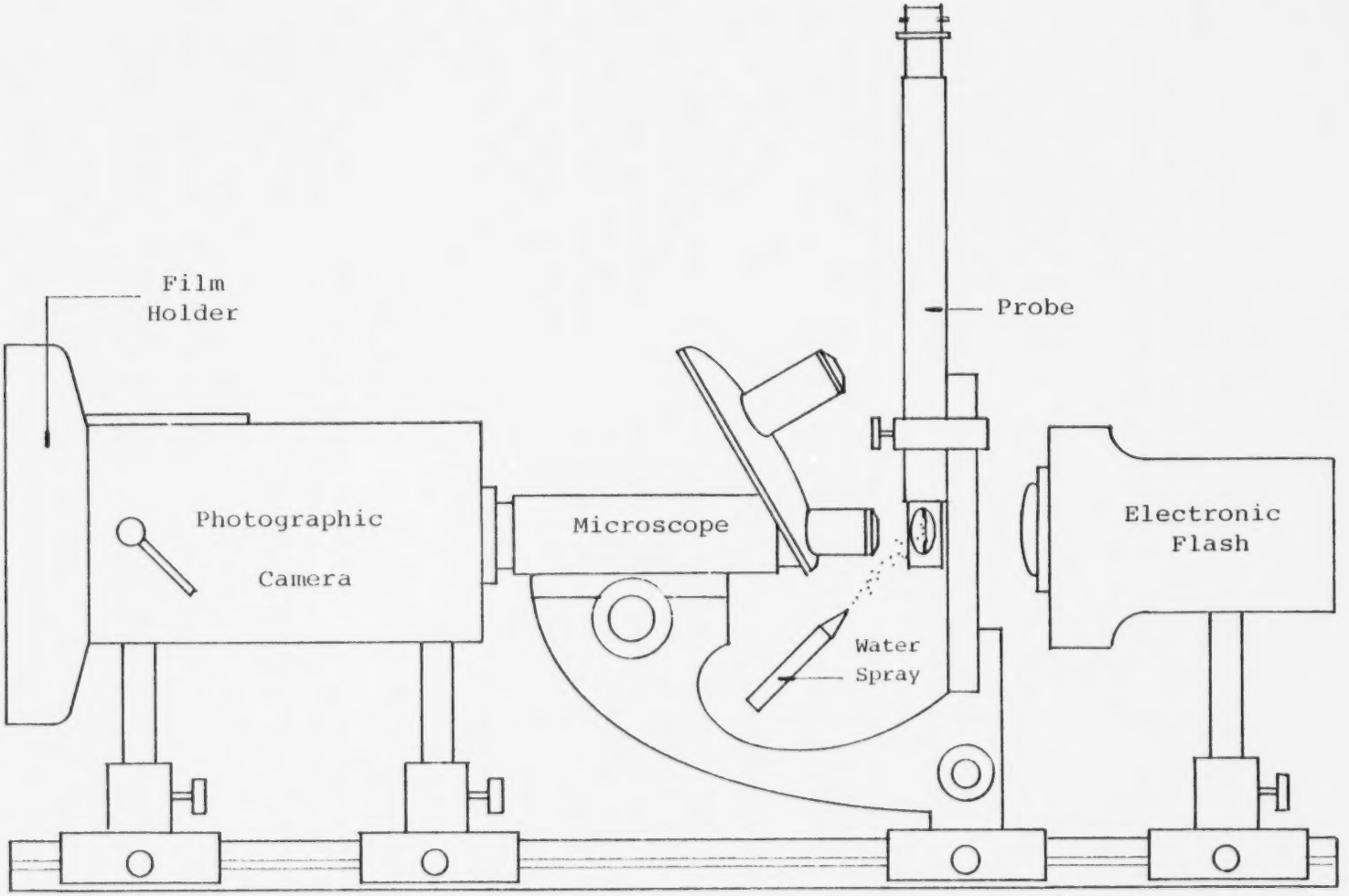

Figure 15: Droplet Calibration Apparatus

Temperature Calibration

The temperature calibration was performed by immersing the sensor in water with temperatures ranging from melting ice to boiling water. A precision mercury column thermometer was used as a control. Temperature readings were displayed on the front panel of the DC-2.

An important condition to be satisfied when using the sensor as a thermometer is that the electrical current should only heat the sensor negligibly. On the other hand, such current is necessary to operate the Wheatstone bridge which measures the temperature. (A large current improves the signal-to-noise ratio of the electronic circuit.) The effect of sensor self-heating was investigated by repeated measurements with several gas velocities. The temperature reading should remain independent of gas velocity.

Gas Velocity Calibration

The calibration of the DC-2 operating as a hot wire anemometer was performed with the use of a Thermo System Calibrator Model No. 1125. This instrument generates a turbulence-free flow whose velocity may be controlled to 1%. Additional equipment required for this measurement consisted of a micromanometer for the measurement of the decrease in pressure across the calibrated orifice, a mercury thermometer to correct the flow for temperature difference, and finally a supply of compressed air.

Analysis of Capture Area

As presented in the Data Analysis of Section 5, the droplet concentration, n_i, corresponding to the i^{th} interval can be computed with the expression:

$$n_i = \frac{N_i}{v \cdot t \cdot \ell (D_i + d)} \qquad (i = 1,14).$$

The denominator in the equation represents the volume sampled and is based on the assumption that all sizes of droplets have sufficient inertia to maintain a linear trajectory. This assumption, however, may not be accurate for particles smaller than the diameter of the wire. Flow problems of this type have been investigated in aerosol filtration (Ref. 2 and 3) using a two-dimensional analysis for the

flow past an infinite cylinder. Although an exact description of the stream lines and droplet trajectories is not possible, the interception mechanism can be evaluated for limiting cases. As a convenience in the analysis, the non-dimensionalized capture size function, f, is defined as

$$\text{Sampled Volume} = vt\ell d \cdot f(D_i d).$$

Then, with the streamlines characterized by the Reynold Number based on the wire diameter (i.e., vd/ν), the capture size of the fiber can be determined. Inertial impaction occurs because the droplet deviated from the fluid motion in accordance with Stokes' Law for a sphere in an unbounded fluid; namely,

$$\text{Stk} \frac{dU_p}{dt} = v - U_p$$

where

$$\text{Stk} = \frac{\rho_w v}{9\mu d} D_i^2$$

v = flow velocity
t = dimensionless time = time multiplied by $\frac{d}{2v}$
U_p = particle velocity.

Some limiting solutions of the foregoing equation are tabulated below and provide insight into the capture size function, $f(D_i d)$, when normalized by $(1+D_i/d)$.

Flow Condition	$f(D_i,d)/(1+D_i/d)$
1) Stk → ∞ Particles follow a straight trajectory	1
2) Stk = 0; no particle inertia	
a) Potential flow	$1 - \frac{1}{(1+D_i/d)^2}$
b) Oseen flow	$\frac{\ln(1+\frac{D_i}{d}) - \frac{D_i}{d}\frac{(2+\frac{D_i}{d})}{2(1+D_i/d)^2}}{2.002 - \ln(Re)}$

In Figure 16, the capture size function is plotted as a function of the dimensionless droplet size. For the case of Oseen flow, the Reynold Number is assumed to be 0.3. For small droplets ($D_i/d<1$), the capture size, f, is significantly influenced by the flow field. Hence, for the DC-2 (d=5μm), the capture size can be represented by $1+D_i/d$ if $D_i>10\mu m$. For small droplets between 1 to 10 μm, the more complicated expressions for $f(D_i,d)$ should be used.

For the experimental studies performed in the laboratory, the number of droplets below 10 μm was large and KLD applied the modified values of the capture size function to the measured data. The effect of the capture size function on the final experimental results is discussed in the next section.

LABORATORY TESTS WITH THE IMPACTOR

As reported in Appendix A, a large number of experiments were performed in the laboratory during the period from June to December 1977. The objective of this work was to accumulate data and to compare measurements made with the Brink impactor and the DC-2. Once the experiments were initiated, a secondary objective emerged; namely, to better understand the flow behavior in the impactor and its effect on the measured data. Several qualitative experiments were performed to accomplish the secondary objective.

To minimize measurement error, a closed system with a steady flow was used in the laboratory (Figure 17). The droplets were generated using a rotating disc, and the speed of the disc was carefully controlled with an optical tachometer. Several designs of this droplet generator were developed and refined to achieve the required stable droplet distribution. The final design utilized a small volumetric pump with a controlled motor speed to continuously pump the liquid to the center of the rotating disc. As shown in Figure 17, the rotating disc was enclosed in a plastic box. This approach provides a reliable and repeatable source of entrained droplets.

The droplets were entrained in the flow and drawn through the impactor using a peristaltic pump with a stable but adjustable speed. The flow was monitored using a calibrated orifice and manometer. Most of the experiments were performed with a flow rate of .03 cfm (.85 liter/min) for which a substantial amount of calibration data is available for the

Figure 16: Capture Size vs. D_i/d

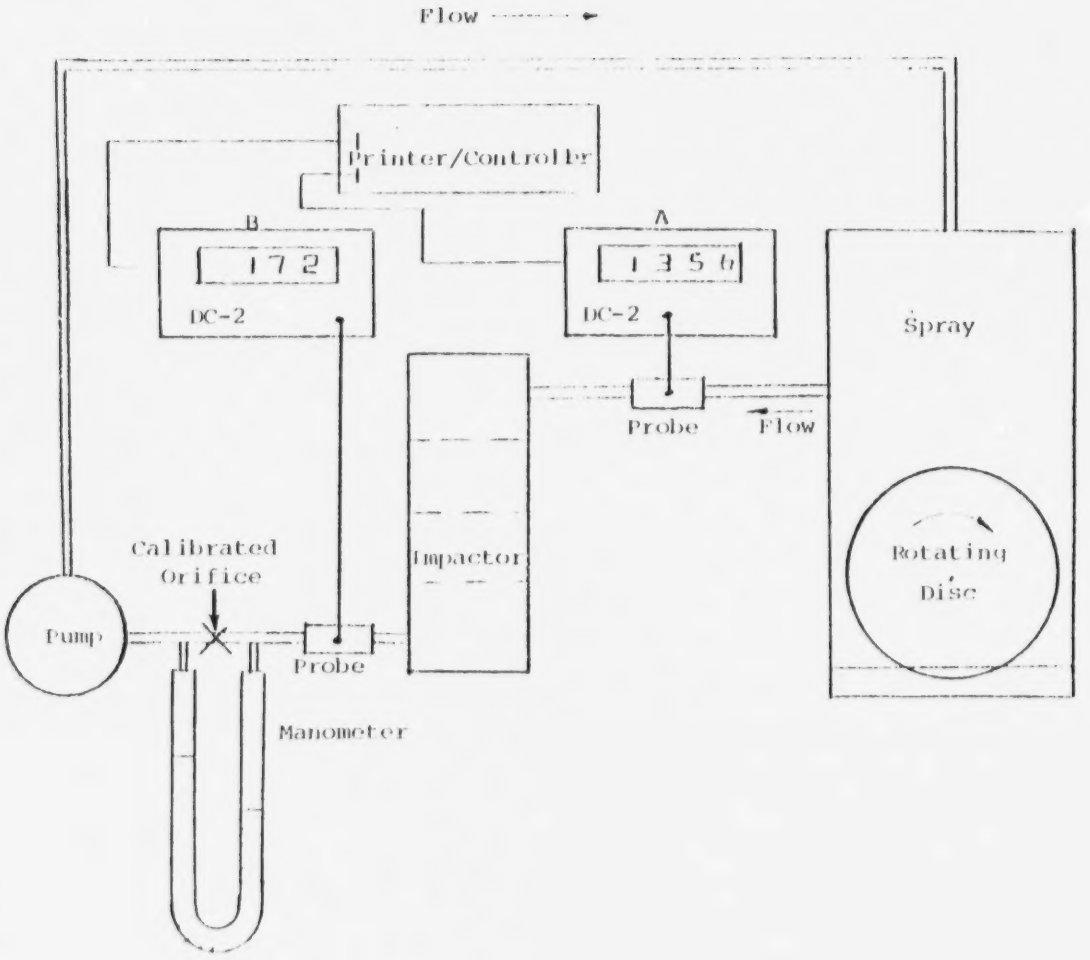

Figure 17: Laboratory Set-up

impactor. Other flow rates were used to investigate the effect of flow velocity on the measurements.

The impactor was operated with a cyclone and one to five stages, depending upon the type of experiment. Instead of using the stainless steel targets of the standard impactor, aluminum foil cups were used as targets. This approach simplified the procedure and increased the accuracy of the measurement. The aluminum foil cups were especially useful for the fourth and fifth stages of the impactor when the operating time was less than 20 minutes.

Depending upon the type of test, measurements with the DC-2 were performed upstream (A) and/or downstream (B) of the impactor (Figure17). The DC-2 data was automatically recorded using the Printer/Controller described in Section 5. For this application, a special hot wire probe was designed and built as an integral part of the 4.8 mm diameter glass tube, which was placed in the flow line. The hot wire was mounted perpendicular to the longitudinal axis of the tube to achieve a well defined flow condition about the wire. For the prescribed flow conditions (.85 liter/min), the air velocity at the probe was .78 m/sec.

Experimental Procedure

To obtain the desired accuracy in the data, careful laboratory procedures had to be established early in the test program. The sources of data scatter had to be identified and, where possible, techniques used to minimize the errors. For example, the system was operated with pure water or a 10% NaCl solution. The tests with pure water identified some sources of measurement errors in the impactor. For example, the DC-2 at location A indicated a stable droplet distribution, but the impactor results were erratic. The length of the sampling time has a pronounced influence on the measurements with the impactor, and the scatter of data was found to be unacceptable. These problems were attributed to evaporation and/or condensation taking place at various points in the impactor. Because of these problems with the impactor, the quantitative studies with pure water were discontinued early in the research.

The impactor measurements with a salt solution were more dependable, but still exhibited scatter (see Discussion of Results). To control the scatter in the data, carefully

controlled techniques for measuring the samples at each stage were used. As mentioned above, small aluminum foil cups provided better accuracy and convenience when weighing the samples at each stage. As a check upon the data, periodic measurements of the accumulated liquid were made and the evaporation history in the ambient environment was plotted. This procedure supplied data with respect to the total amount of liquid collected per stage when the test was completed but before the samples were dried and weighted. Such measurements were used to verify the data obtained from the dried sample of the NaCl residue.

Depending upon the number of impactor stages, a "time delay" was observed as the impactor achieved steady-state conditions. After the initial period of approximately 45 minutes, the measured droplet distribution became stable within ±10%. Numerous tests were performed to understand this phenomenon and develop acceptable experimental procedures. The "time delay" effect is attributed to the condensation/evaporation phenomenon occurring inside the impactor.

Also, a procedure had to be established with respect to the total sample period for a generic experiment. Again, a series of tests were performed to establish this methodology, and a sample period of 20 to 40 minutes was used for the majority of the experiments.

The performance and data analysis with the Brink impactor was based upon the best information available. Efficiency curves, which accounted for wall losses at different stages, are given in Table 8 of Reference 4, and the cyclone efficiency curve appears as Figure 24 of Reference 5. These two reports are based upon a particle density of 1.35 gm/cm^3 and 1.0 gm/cm^3, respectively. For the present study, the 10% NaCl solution has a density of 1.05 gm/cm^3 approximately. The values of D_{50} used in this study have been properly adjusted for any differences in density. Moreover, the diameter of each impactor nozzle was measured carefully to be sure that it was within the tolerance of the published value. The D_{50} for the present study is given below in Table 5.

Table 5: D_{50} for Brink Impactor at .85 liter/min Flow Rate, 22°C, 751.84 mm Hg and Particle Density 1.05 gm/cm^3

Stage	D_{50}
Cyclone	17.00 µm
1	5.27 µm
2	3.61 µm
3	2.29 µm
4	1.07 µm
5	0.74 µm

The DC-2 was operated in the standard manner. As expected, salt accumulated on the hot wire, and after several minutes of continuous operation, the response of the instrument would degrade. To define a convenient sampling time, the instrument was operated for various periods. Based on these tests, a sampling time of approximately 100 seconds was adopted for the DC-2. With this procedure, the effect of the salt accumulation was negligible. It was also observed that by leaving a contaminated sensor in the flow, a self-cleaning action occurred when the sensor was cold. With a time delay of five minutes between sample periods of 100 seconds, the response of the sensor was unaffected and the probe was seldom replaced.

Discussion of Results

The results from the laboratory tests permit a direct comparison of droplet number and volume distributions as obtained with the Brink impactor and the DC-2. In addition, extensive data was accumulated with respect to the operating characteristics of the impactor. In this subsection both these topics are discussed.

The experimental data consistently shows that the measurements with the DC-2 were lower than the impactor measurements in the region from 1 to 10 µm. Some of the difference in the measurements can be attributed to the aerodynamic influence on the capture size of the wire as discussed under the Calibration Procedures. In addition, tests were indicative of condensation occuring in the impactor.

However, it is not possible to quantify completely all the effects which contribute to the differences in the measurements, nor was such a quantification within the scope of the present research.

To achieve a meaningful comparison of the data from the many tests, KLD examined approximately four similar experiments with the impactor and averaged the results for each impactor stage. The simultaneous measurements with the DC-2 for each experiment were average for each of the 14 size intervals. All of this data in the form of a number concentration, $\hat{n}$, was plotted as a function of droplet diameter. Then an equivalent factor, K, was defined as

$$K = \frac{\hat{n}_i \text{ for Impactor}}{\hat{n}_i \text{ for DC-2}} \qquad i = 1,....$$

The computed values of K are tabulated below:

Interval No.	Size Range	K Ratio of Impactor to DC-2	K_{aero} Aerodynamic factor	$\Delta K = K - K_{aero}$
1	1 - 1.6	5.0	2.5	2.5
2	1.6 - 2.6	2.8	1.8	1.0
3	2.6 - 4.1	2.0	1.2	0.8
4	4.1 - 6	1.6	1.0	0.6
5	6 - 10	1.2	1.0	0.2
6	10 - 17	1.0	1.0	0
:	:	:	:	:
:	:	:	:	:

As shown, the values of K approach one after the fifth size interval. The factor, K, includes the aerodynamic effect on the capture area. The aerodynamic effect can be computed and is represented by the column labelled K_{aero} in the above table. The difference $\Delta K = K - K_{aero}$ has also been tabulated.

The tabulated values of K were applied to various sets of experimental data to demonstrate the consistency of results. In Figures 18 and 19, the results from two experiments are compared. The dashed curve represents the measured number concentration with the impactor whereas the solid curve is for the DC-2 data after the factor K is applied. A similar comparison is shown in Figures 20 and 21 for the results in terms of the accumulated volume concentration.

The foregoing curves are in acceptable agreement and the results from the two techniques of measurement can be related using an equivalence coefficient, K. It should be emphasized that the agreement emerged only after very careful laboratory work to minimize data scatter and by averaging results from several tests.

During the experimental work, the operational characteristics of the impactor became evident and it is worthwhile to document some of the observations for the benefit of other researchers. Although the Brink impactor has been evaluated on a theoretical basis by others and can be calibrated using known solid particles, its use for entrained liquid droplets is based upon assumptions which may not be justified. The complex flow at various stages can result in condensation or evaporation depending upon the operating environment. During many tests, the collection of significant amounts of liquid on the walls of the impactor was observed. These problems can cause scatter in the data and control of the scatter is a difficult task in the laboratory and certainly more difficult in the field. If the liquid is without trace elements, the measurements with the impactor are significantly less reliable and of little quantitative value.

A typical example of the scatter in the laboratory data is shown in Figures 22 and 23 for stages 1 and 3. In each diagram, the weight of the dried NaCl residue is plotted as a function of sampling time. In theory, the accumulated salt should be a linear function of the sampling time. For stages 1 and 3, there is an obvious increase in the accumulated salt with time, but the slope of this curve cannot be accurately defined. Several attempts were made to provide better insight into the data. For example, all the tests on a particular day with known environmental conditions were grouped and studied. Unfortunately, this grouping tended to reduce the scatter at some stages but not at all stages.

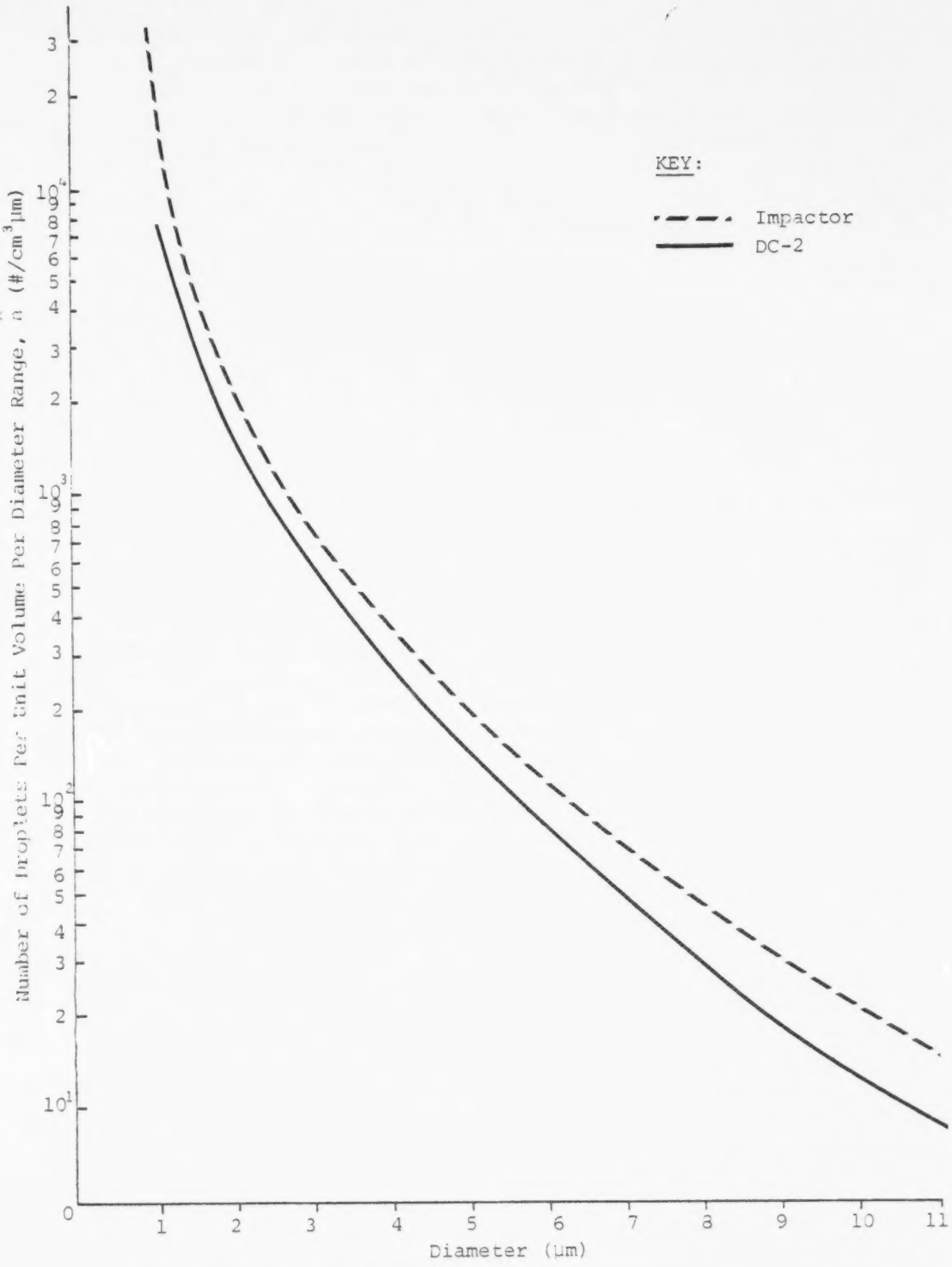

Figure 18 : Average Number Concentration for Impactor and the DC-2 Data (Test No. 216)

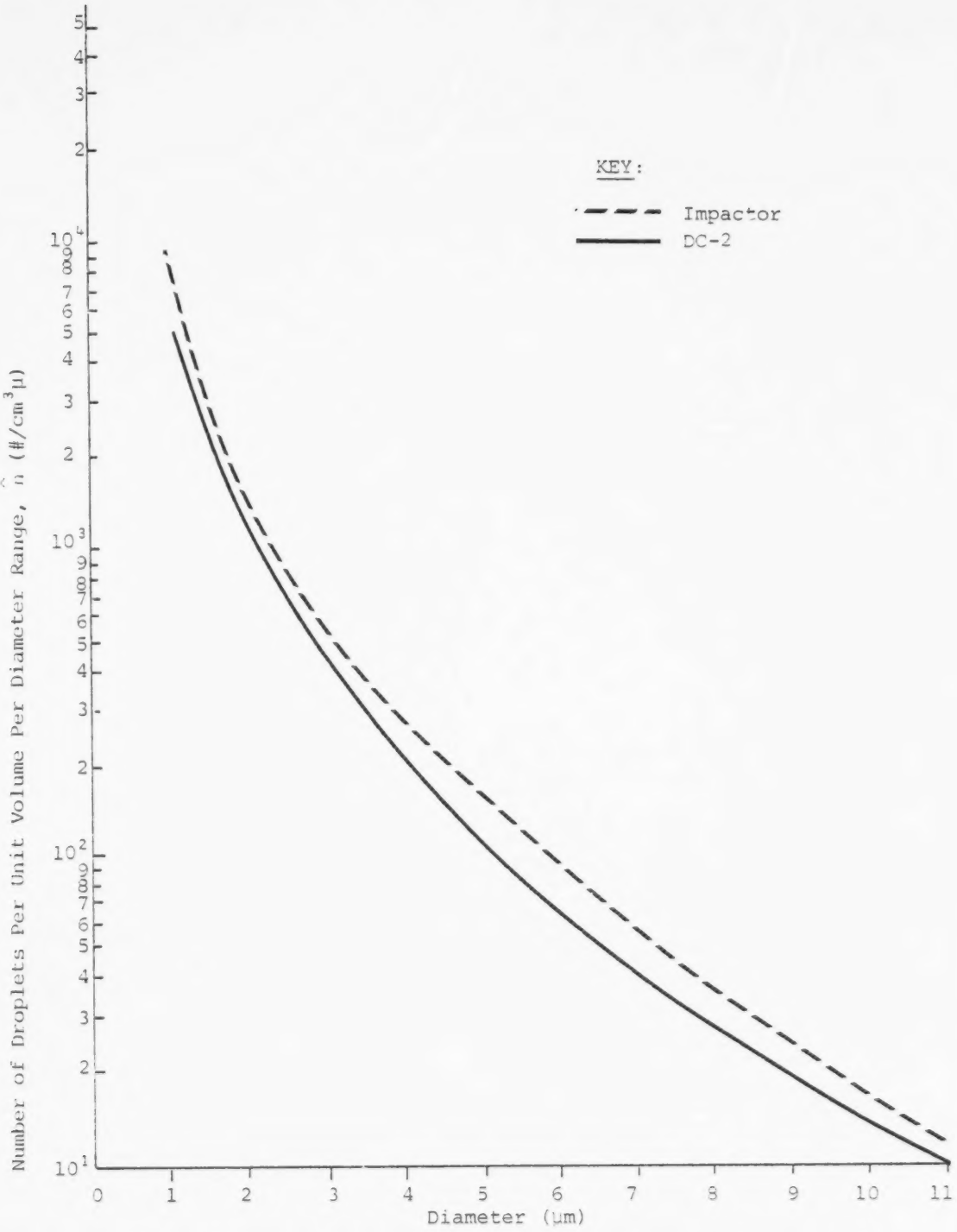

Figure 19: Average Number Concentration for Impactor and the DC-2 (Test No. 212)

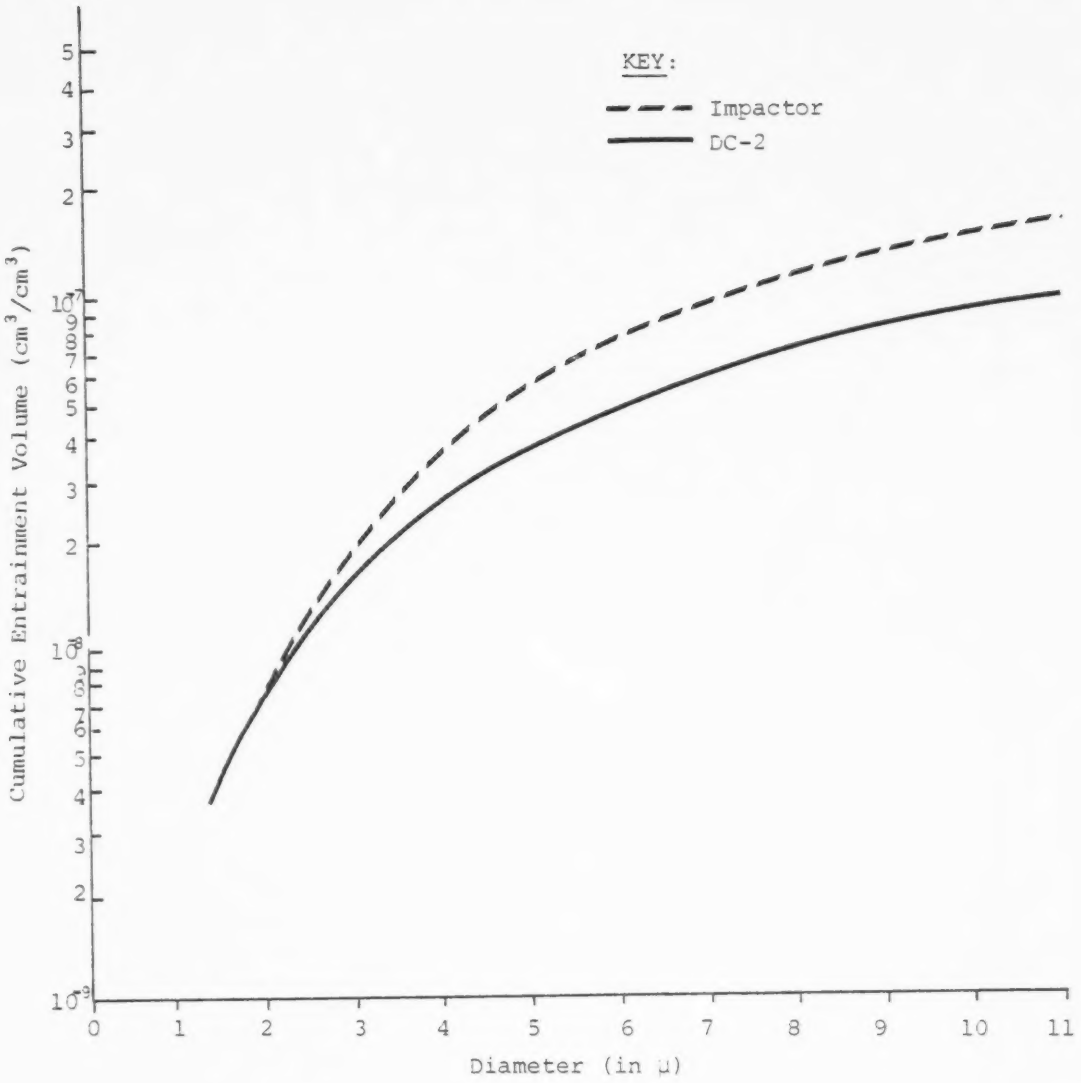

Figure 20 : Cumulative Entrainment Volume for Impactor and the DC-2 Data (Test No. 212)

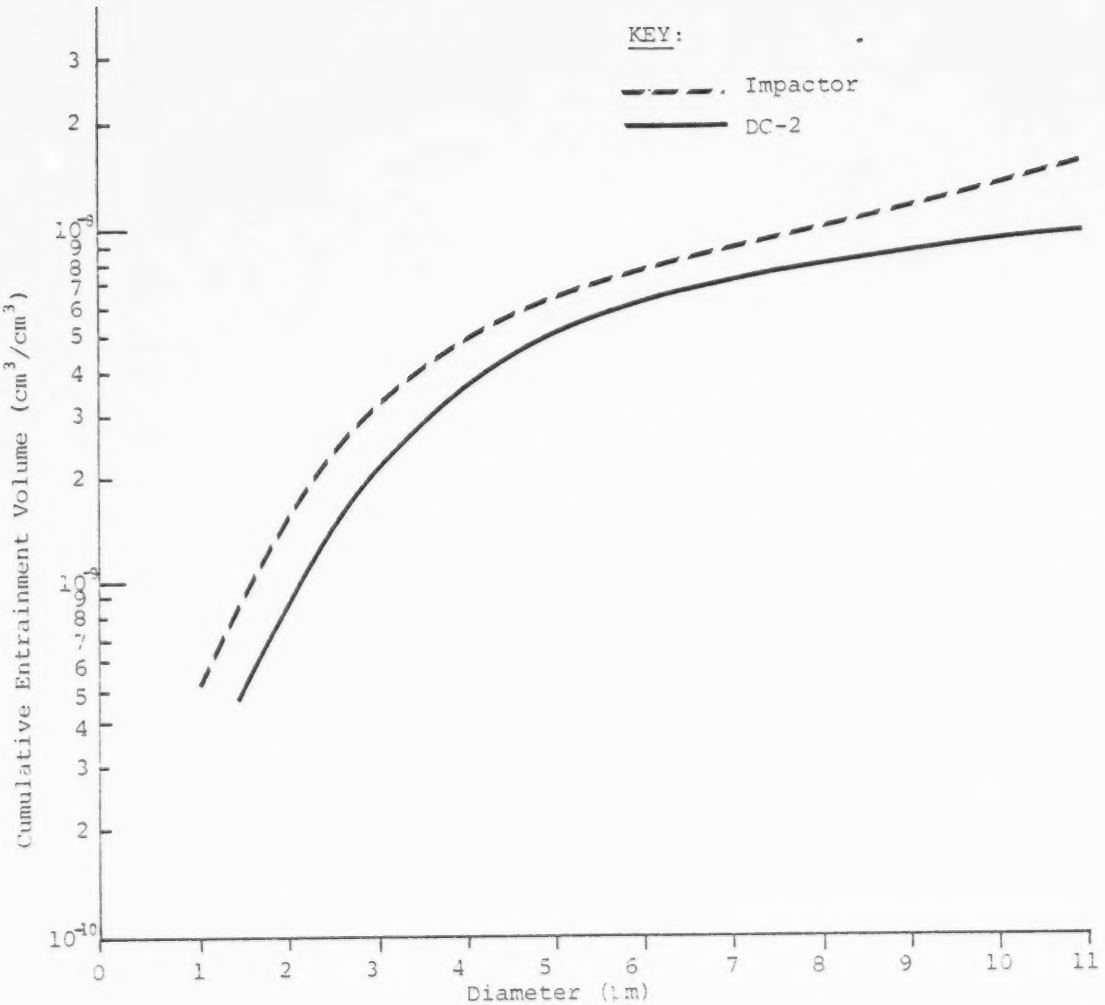

Figure 21: Cumulative Entrainment Volume for Impactor and the DC-2 Data (Test No. 210)

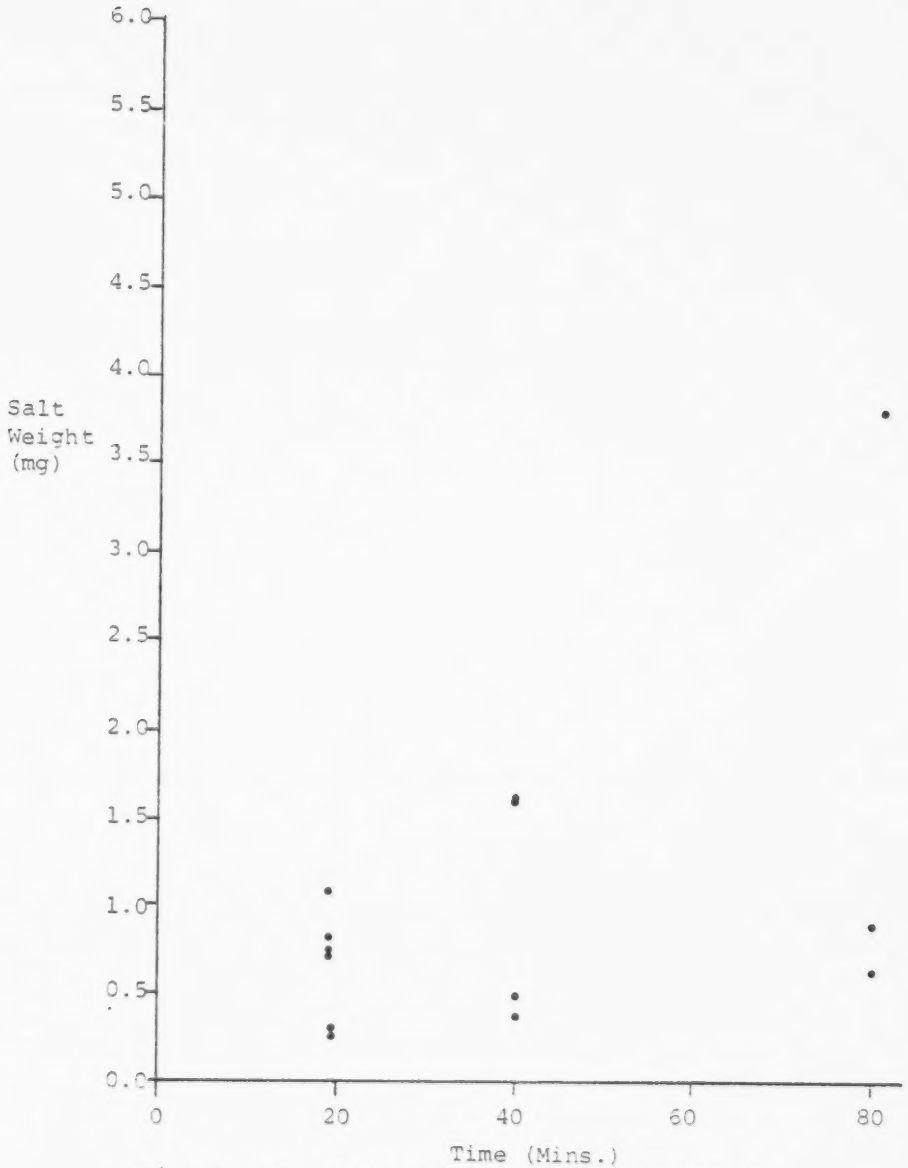

Figure 22: Salt Collected on Stage 1

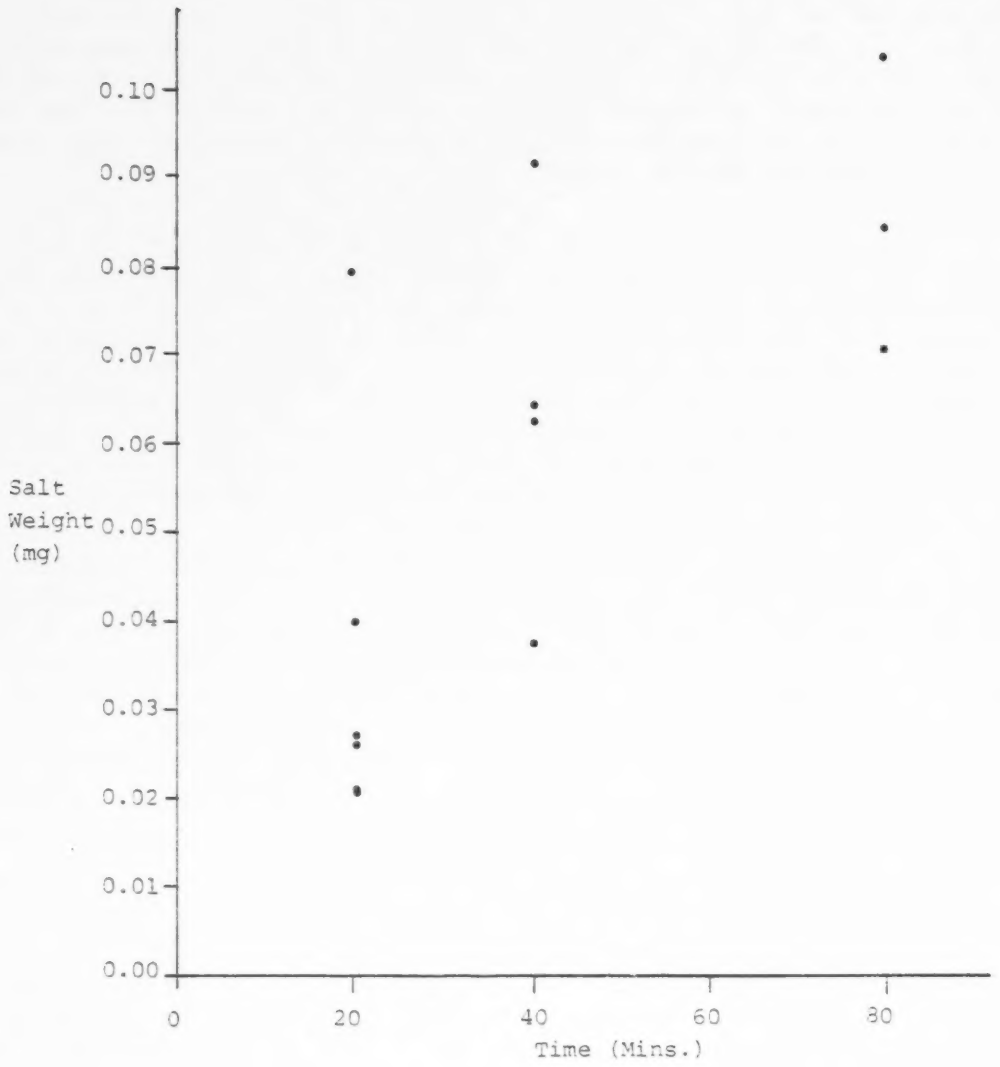

Figure 23: Salt Collected on Stage 3

Several experiments were performed with the Brink impactor inside the box where the droplets are generated. This approach was adopted with the assumption that scatter would be minimized if the impactor is in equilibrium with the sample flow. It should be emphasized that the procedure was equivalent to the field practice of placing the sample train in the flow for long "soaking" periods. The results from these experiments were disappointing since no appreciable reduction in the scatter was observed.

KLD performed several experiments to gain better insight into the phenomenon causing data scatter. A glass tube was constructed to resemble the impactor, and by visually monitoring the flow inside the tube, varying conditions of evaporation and/or condensation were observed. When the two-phase flow was introduced into the tube, wall condensation was very evident. The condensation on the wall could be correlated with the droplet distribution at the outlet of the tube. The distribution at the outlet did not stabilize until the condensation on the walls achieved a stable condition. If a light source is placed near the tube (causing an undetectably small temperature difference), the condensation phenomenon was greatly altered with evaporation on the side exposed to the light and condensation on the diametrically opposite side. These qualitative experiments demonstrated the sensitivity of the internal flow to extremely small changes in wall conditions. Further study to quantify this effect is of interest and possible, but such an effort is beyond the scope of this project.

Analytical Considerations

Several analytical studies were undertaken in support of the experimental effort. The objective of the studies was to provide additional insight into the thermodynamic and aerodynamic conditions in the impactor. The procedures used for the studies are briefly reviewed in this subsection.

An idealized pressure and temperature distribution in the impactor can be determined using a one-dimensional flow theory for a compressible, isentropic flow. The temperature and pressure ratios at a cross section with velocity, v, are given by

$$\frac{T}{T_o} = \left(1 + \frac{\lambda-1}{2} M^2\right)^{-1}$$

$$\frac{P}{P_o} = \left(1 + \frac{\lambda-1}{2} M^2\right)^{-\frac{\lambda}{\lambda-1}}$$

where λ is ratio of specific heat ($\lambda \approx 1.4$)
M is the Mach number
T_o is the stagnation temperature
P_o is the stagnation pressure.

These equations are used to obtain the idealized pressure and temperature conditions in the impactor for a given set of nozzle geometries. The nozzle dimensions, the jet velocity at each nozzle exit, as well as the pressure drop are presented in References 4 and 6. For the Brink impactor, these parameters are given in Table 6 for stages 0 through 6.

The resulting temperature and pressure distributions are given in Figures 24 and 25. The first three stages, which have a jet velocity less than 10 m/sec, show negligible temperature and pressure drop. Temperature difference of 0.5°C to 1.5°C and pressure drop of 3 to 17 mmHg are found in stages 4, 5 and 6.

A second analysis was used to qualitatively describe the growth or reduction in droplet size. It is well known that aerosol particles, when in supersaturated atmosphere, may act as nuclei, enhance condensation and growth. A droplet passing through an impactor undergoes a similar process. In theory, droplets may grow or shrink inside an impactor.

A complete analysis on the history of a droplet passing through an impactor could be achieved numerically. However, such a complete study was not undertaken during this contract. Rather, an idealized and simplified model was used for the condensation/evaporation rate of droplets in the impactor environment.

For a spherical motionless droplet, assuming stationary condensation/evaporation and ideal behavior of the vapor, the rate of change of the droplet radius can be described by Maxwell's equation:

TABLE

Cascade Impactor Stage Parameters

Modified Brink Model B Cascade Impactor

Stage No.	No. of Jets	D_j-Jet Diameter (cm)	S-Jet to Plate Distance (cm)	$\frac{S}{D_j}$	Reynolds Number	Jet Velocity (m/sec)	Cumulative Fraction of Impactor Pressure Drop at each stage
0	1	.3598	1.016	2.82	326	1.4	0.0
1	1	.2439	0.749	3.07	481	3.0	0.0
2	1	.1755	0.544	3.10	669	6.0	0.0
3	1	.1375	0.424	3.08	853	9.7	0.0
4	1	.0930	0.277	2.98	1263	21.2	0.065
5	1	.0726	0.213	2.93	1617	35.3	0.255
6	1	.0573	0.191	3.33	2049	58.8	1.000

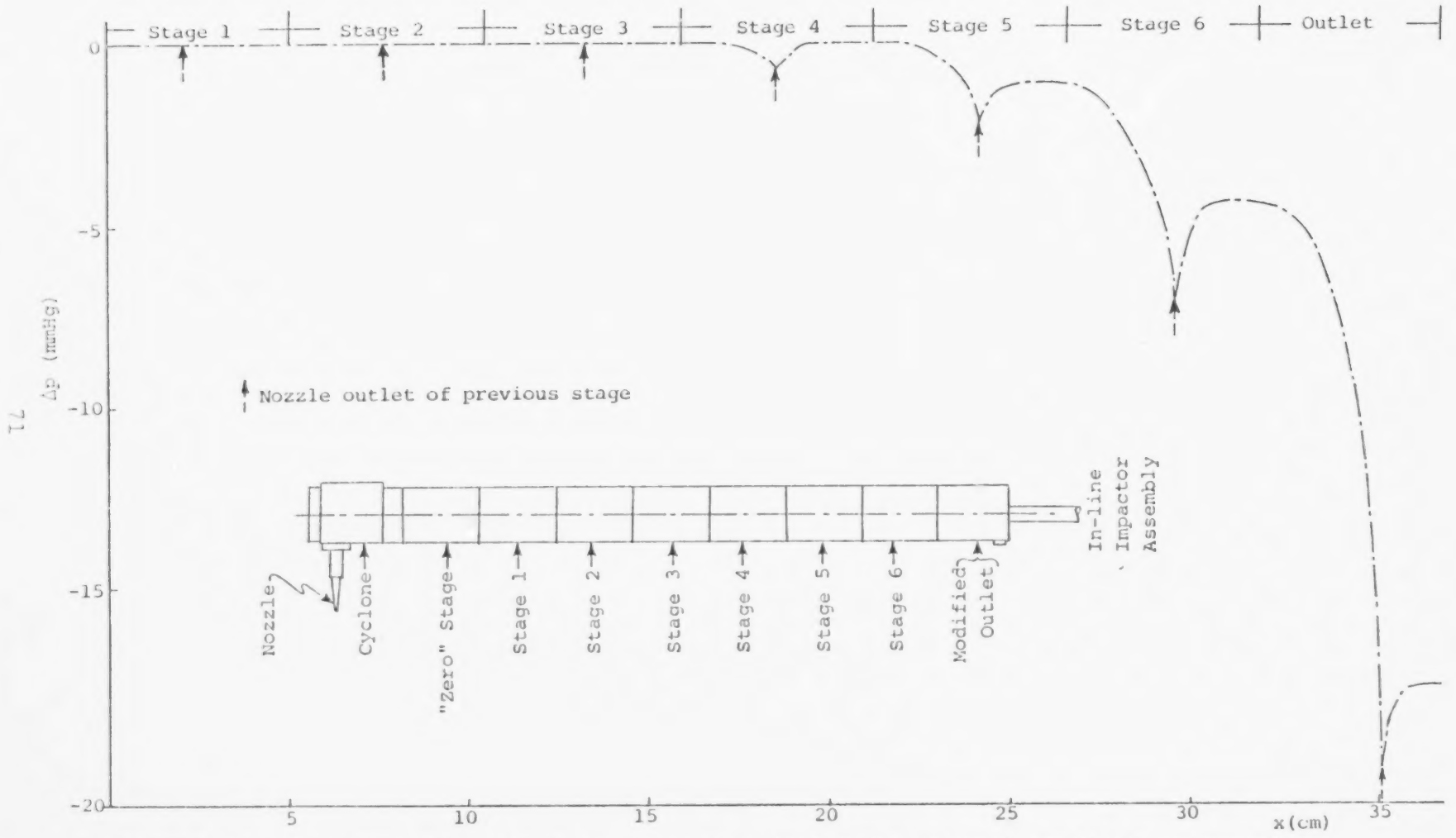

Figure 24: Pressure drop along the impactor (760 mmHg is used as inlet pressure)

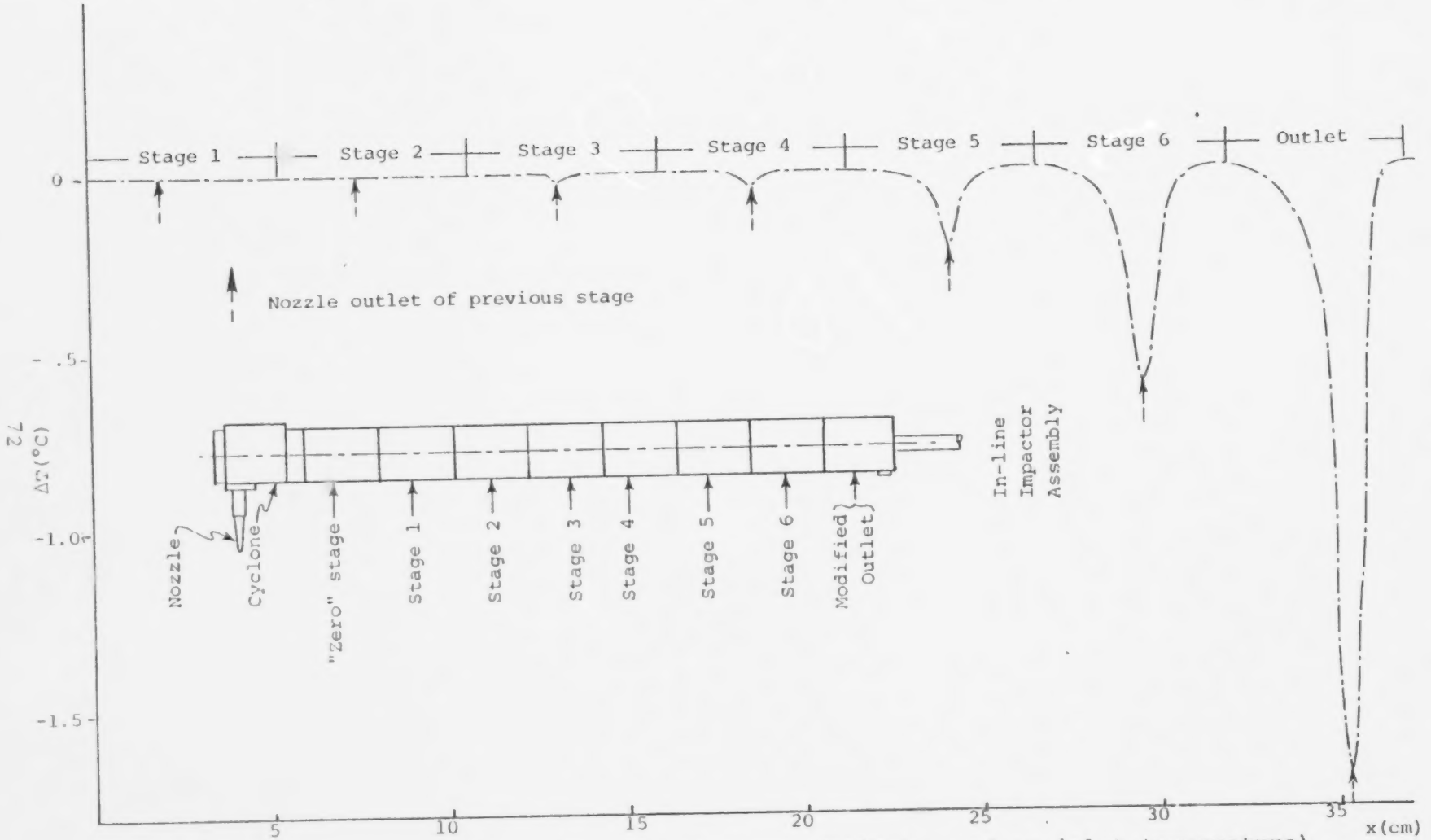

Figure 25. Temperature drop along the impactor. (20°C is used as inlet temperature)

$$r \frac{dr}{dt} = \frac{DM}{\rho_L RT} (P_\infty - P_o)$$

where r = radius of the droplet
t = time
D = vapor diffusivity
M = molecular weight of the vapor
ρ_L = density of the droplet
R = ideal gas constant
P_o = vapor pressure at the drop surface calculated from the drop temperature
P_∞ = vapor pressure in the air stream.

By assuming $P_\infty - P_o$ = 0.1 mmHg, the rate of change of the droplet radius, dr/dt, for typical conditions is given in the following table. As shown, dr/dt is most significant for small droplets.

Table 1: Rate of Change in Radius for Water Droplets at 293°K and $P_\infty - P_o$ = 0.1 mmHg

r(μm)	$\frac{dr}{dt}$ (μm/sec)
0.25	11.40
0.50	5.72
1.0	2.86
2.5	1.14
5.0	0.56
10.0	0.28

The evaporation of small droplets in a saturated atmosphere was also investigated. The vapor pressure on the surface of a droplet of radius, r, is given by Kelvin's equation:

$$\frac{P_r}{P_\infty} = \exp \left(\frac{2\sigma M}{RT\rho_L r}\right)$$

where σ = surface tension.

The evaporation effect on dr/dt can be calculated accordingly. The supersaturation ratio, P_r/P_∞, for various values of r is given in Table 7 and dr/dt at 293°K is presented in Table 8. Again, the small droplets have the most significant rates of change.

Table 8: Supersaturation Ratio, P_r/P_∞, for Water Droplet at 293°K

r(μm)	P_r/P_∞
0.25	1.0044
0.50	1.0022
1.0	1.0011
2.5	1.00044
5.0	1.00022
10.0	1.00011

Table 9: Rate of Change in Radius for Water Droplet at 293°K

r(μm)	$-\frac{dr}{dt}$ (μm/sec)
0.25	9.40
0.50	2.36
1.0	0.59
2.5	0.094
5.0	0.0236
10.0	0.0059

The above calculations are based on the assumption that the droplet is pure water and Maxwell's equation applies. Theoretical consideration on the concentration change at the surface of the droplet as well as the evaporation/condensation constant lead to

$$r \frac{dr}{dt} = \frac{MD}{\rho_L RT} (P_\infty - P_O) \left[\frac{1}{\frac{D}{r\nu\alpha} + 1} \right]$$

where α = evaporation/condensation constant for a liquid

$\nu = \sqrt{\frac{RT}{2\pi M}}$ = 1/4 of the mean absolute velocity of the vapor molecules.

For pure water, $\alpha = 0.034$, and the above equation gives a smaller value of dr/dt than obtained from Maxwell's equation.

Hence, the evaporation or growth of droplets in the impactor appears possible for the small droplet sizes (D<10um) and may account for the sensitivity of the impactor data to environmental conditions. These studies did not include the influence of the walls as condensation surfaces nor the effect of re-entrainment of droplets from wet surfaces.

SECTION 7

FIELD TESTING

An important objective of the research effort was to demonstrate the use and suitability of the DC-2 under field conditions. In all, four different sites were used in the demonstration. At the Shippingport Power Plant, which has a limestone scrubber, data was obtained with the DC-2 and was to be compared with impactor data measured by an independent source. Unfortunately, the impactor data is not available and the comparison cannot be reported.

For each site, a test report was prepared and submitted to the EPA Contract Monitor. In this section, the results from each site are summarized.

COLBERT PILOT PLANT

A schematic of the demister scrubber at the Colbert Pilot Plant in Muscle Shoals, Alabama is shown in Figure 26. It consists basically of a duct where the flow carrying SO_2 interacts with water within a prescrubber-demister. The scrubber injects saturated ammonia and the resulting droplets are recovered in a demister. This flow is created by means of a centrifugal pump installed in the stack.

A total of 1260 measurements were performed at the four available ports shown in Figure 26. The ports and the corresponding number of measurements taken are:

Port	No. of Measurements
A. Prescrubber-Demister Inlet	315
B. Prescrubber-Demister Outlet	314
C. Exit Demister-Inlet	316
D. Exit Demister-Outlet	315

Each measurement includes gas temperature, flow velocity and droplet size distribution.

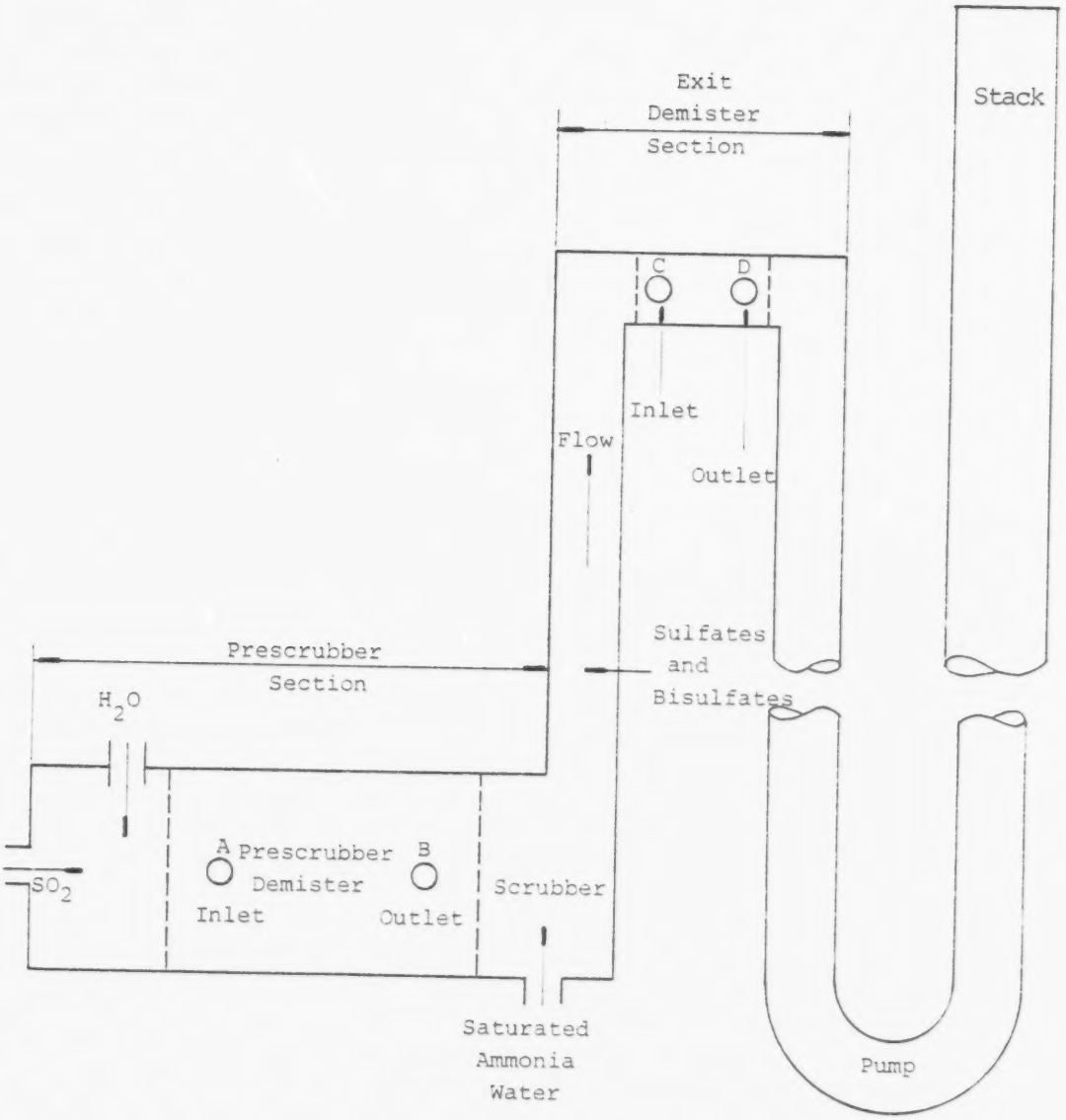

Figure 26 : Schematic of the Demister Scrubber at the Colbert Facility

Most of the measurements were performed with one probe so as to monitor any degradation of its performance due to the accumulation of contaminants. The only detected accumulation was crystals of ammonia sulphate. A periodic cleaning of the probe after 15 minutes of operation was required for proper measurement. Crystals of ammonia sulphate are highly soluble in water, so that the sensor was cleaned simply by immersing in tap water for a few seconds.

For the performance of a single measurement (a total of 1000 droplets) the time limit was below 100 seconds, assuring negligible deterioration of the sensor during a single measurement. The measured droplet distributions are presented in Figures 27, 28, 29 and 30.

WATER TREATMENT PLANT IN NEW YORK

Field testing at the New York site was made within a demister located at the exhaust of diesel engines operating with either fuel oil or methane. At the site, a scrubber was used to clean the exhaust gas of odors and carbon particles. The function of the demister was to capture water droplets after the scrubbing action took place.

A cross-section of the demister is shown in Figure 31. Several thousand measurements were performed at this facility. The main emphasis was to test the DC-2 performance under field conditions rather than to evaluate the facility. It was observed that conditions at the facility changed with time. Furthermore, the spinner caused localized conditions in the flow.

The measurements with the various instruments, i.e. one prototype unit and two deliverable units were performed simultaneously by locating their respective probes as close together as possible. Measurements were taken over the cross sections at various vertical locations with the sensor placed perpendicular to the flow. The three instruments produced results which are all rather similar. Differences, when present, may be traced to either spatial or time fluctuations.

SHIPPINGPORT POWER PLANT

Field tests at Shippingport, Pennsylvania were made in the demisters which are located at the exhaust of the coal-fired power plant. The droplets were generated by venturi

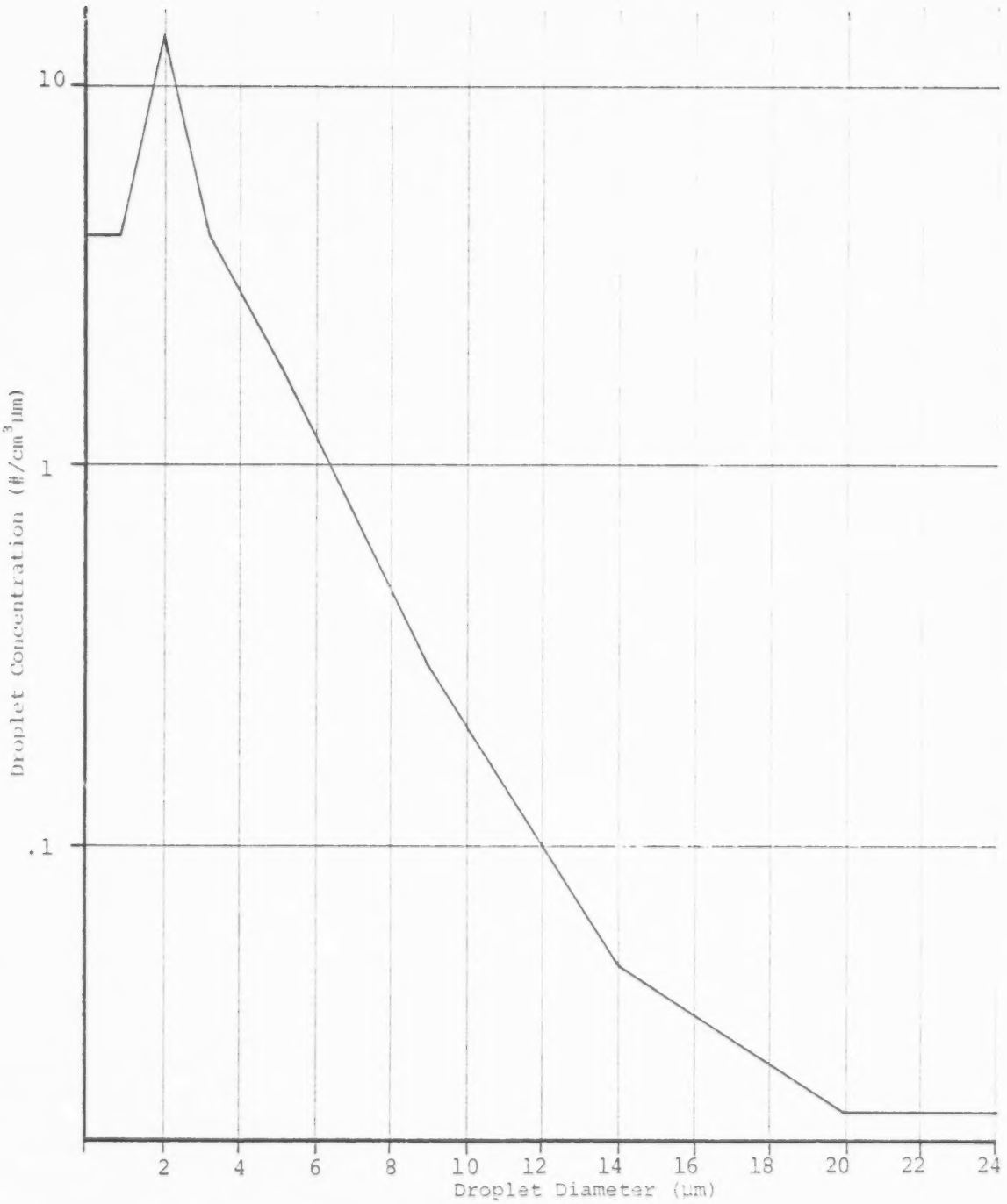

Figure 27: Distribution at the Prescrubber Demister Inlet Colbert Plant

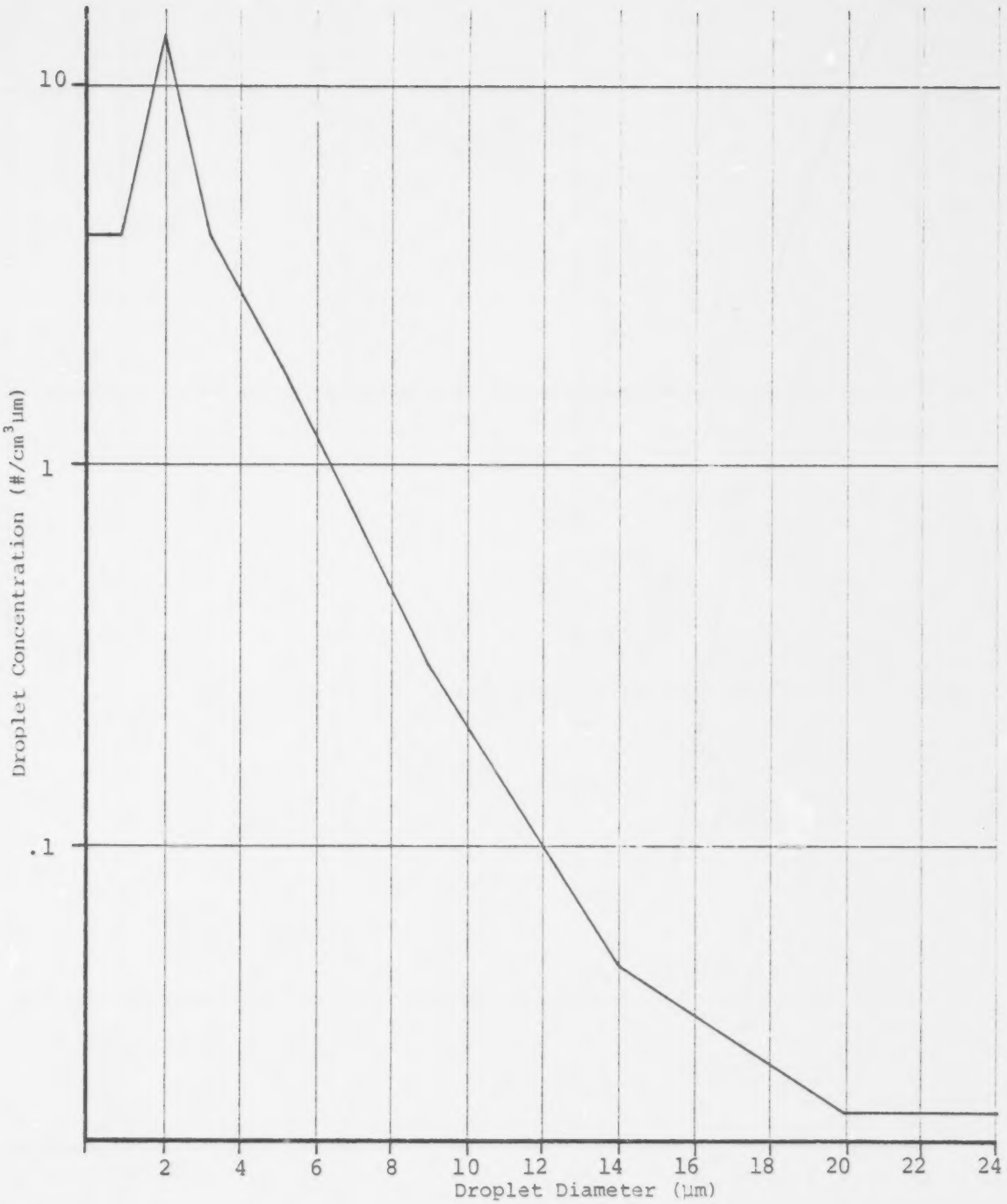

Figure 27: Distribution at the Prescrubber Demister Inlet Colbert Plant

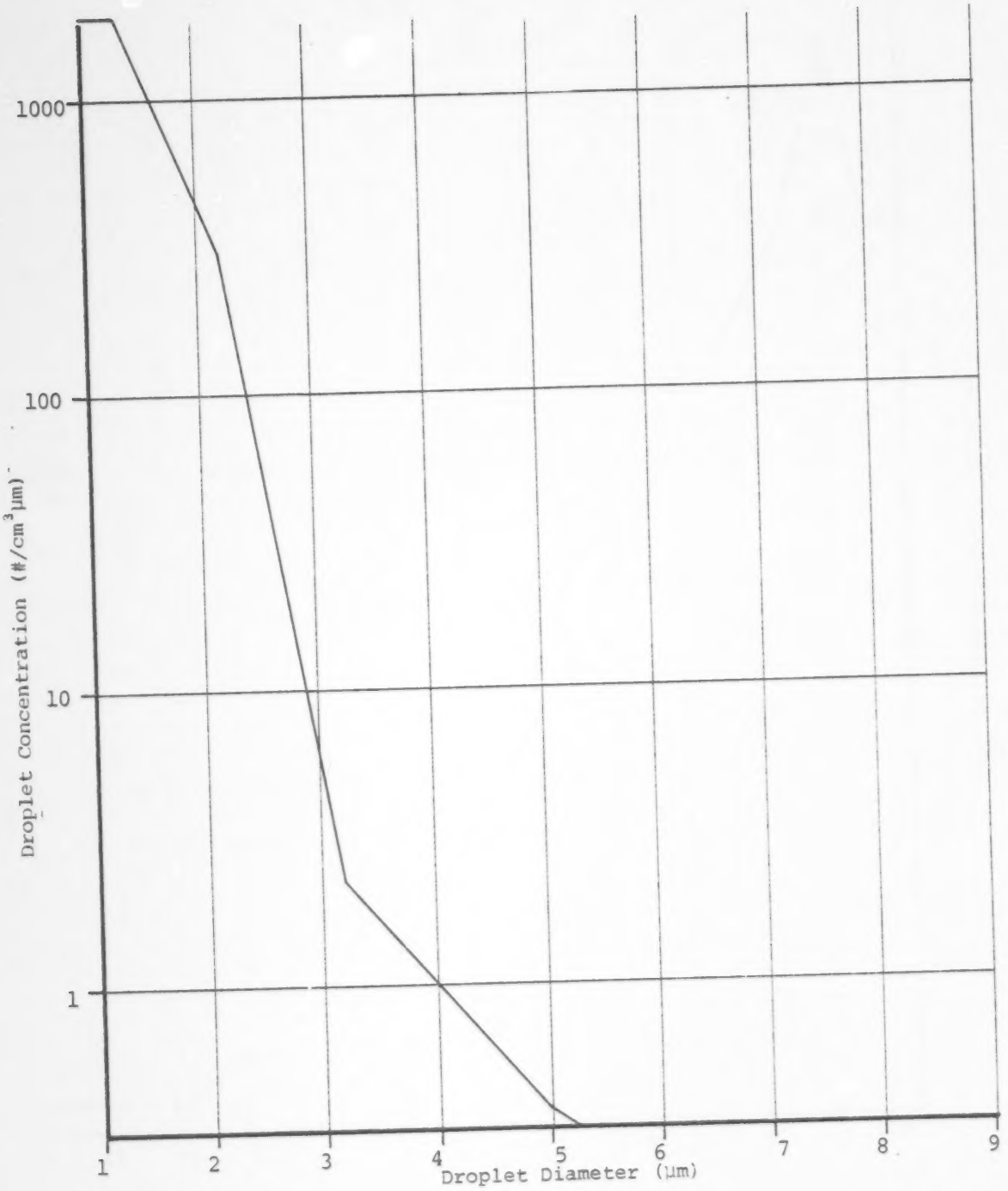

Figure 28 : Distribution at the Prescrubber Demister Outlet, Colbert Plant

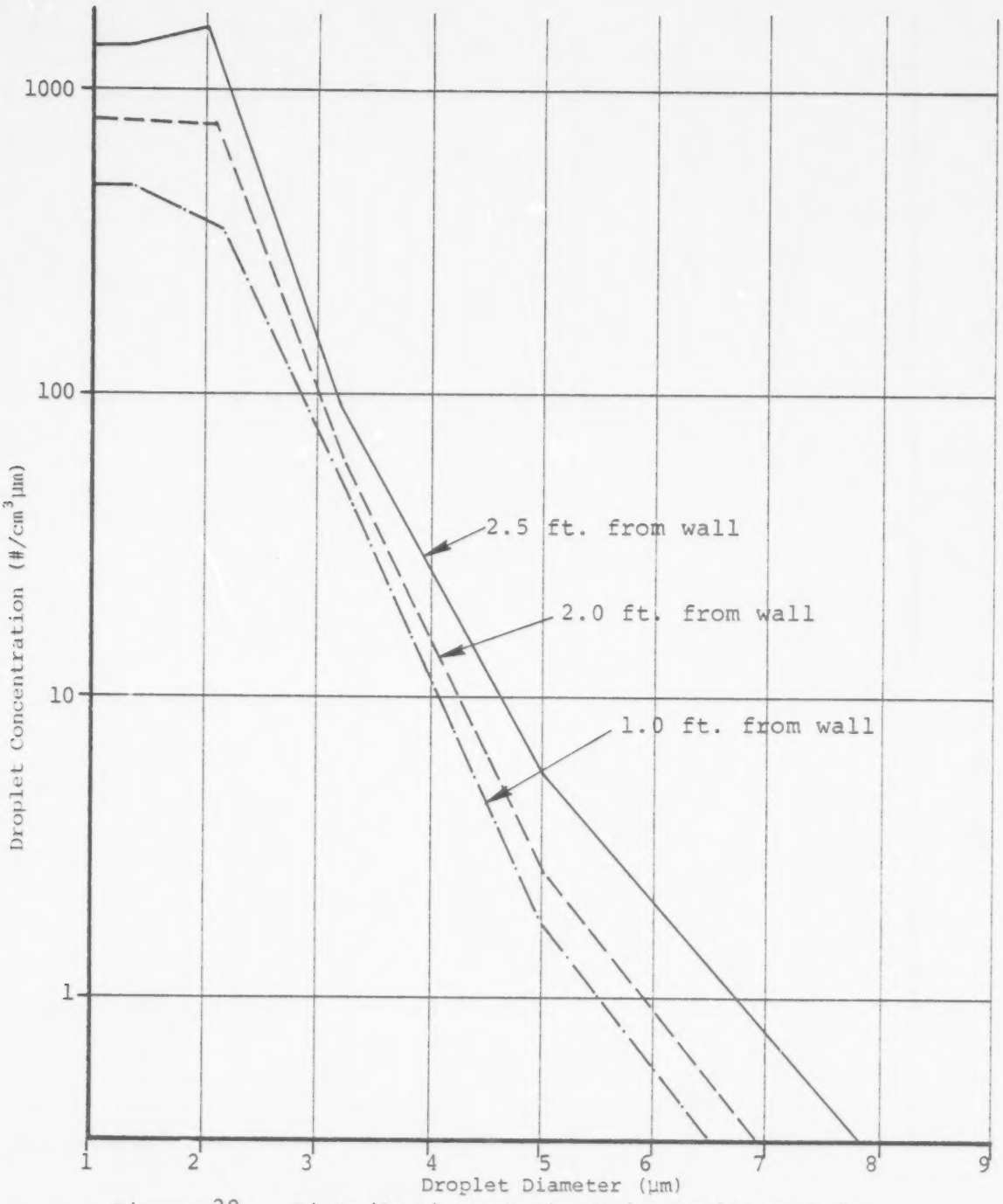

Figure 29 : Distribution at the Exit Demister Inlet Colbert Plant

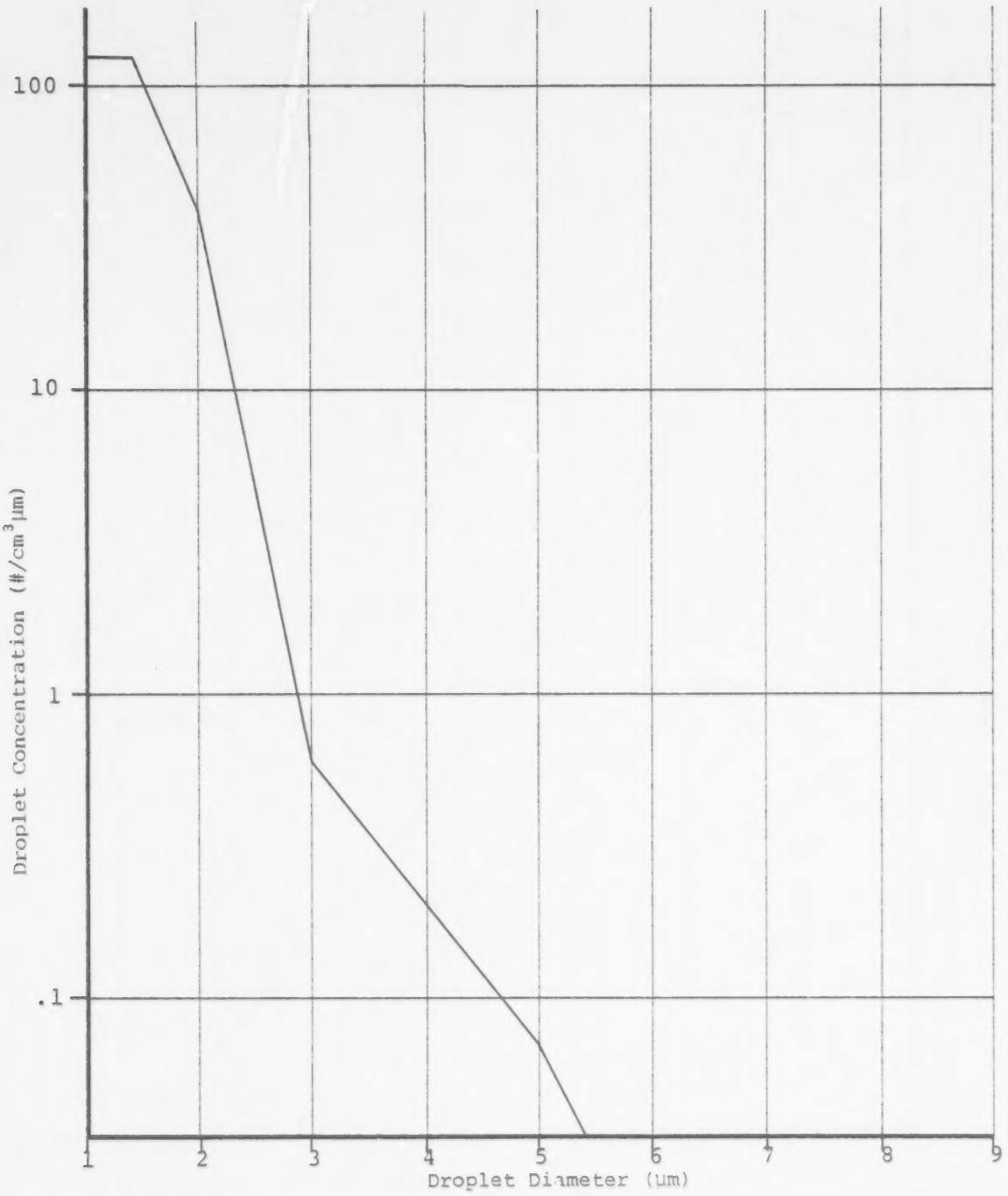

Figure 30: Distribution at the Demister Outlet
Colbert Plant

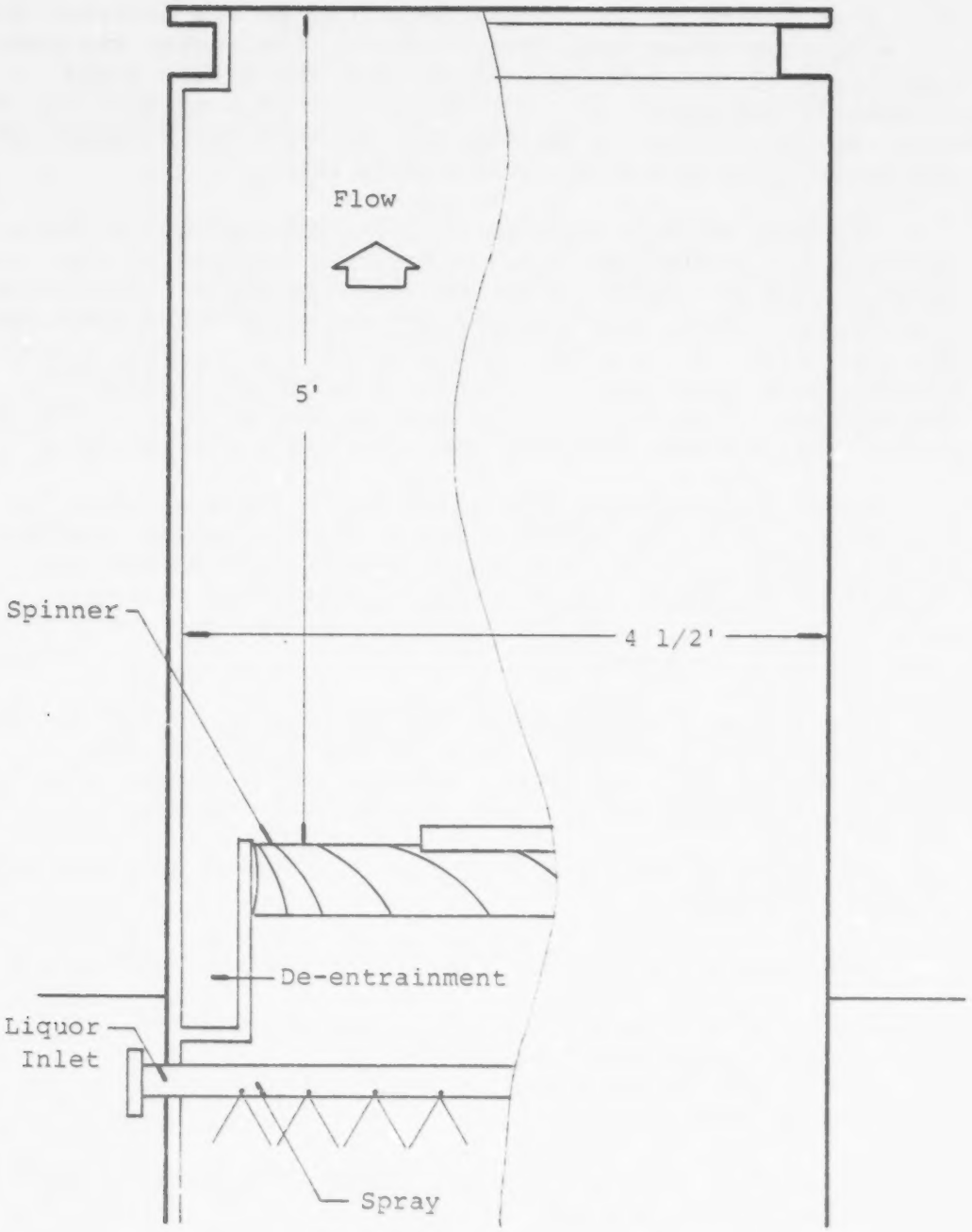

Figure 31: Demister Cross Section at the Treatment Plant in Wantagh, New York

scrubbers and the liquor contained limestone in suspension to remove the major pollutant, SO_2. One double demister and one single demister were investigated. The survey was made downstream of the demister and covered the entire cross section of the duct. Six access ports were available for the measurement. The cross section of the duct and location of the survey points are shown in Figure 32.

The most serious problem encountered during the field work was the contamination of the sensor because of the accumulation of limestone on the hot-wire probe. This contamination problem was overcome by inserting the probe into the duct only when the DC-2 was actively taking data and by choosing the measuring time to be as short as 10 seconds. Temperature, flow velocity and droplet concentration were within the expected range of operation at the facility.

Large fluctuations were observed in the operating conditions of the demisters. The fluctuations are inherent to the operation of this type of demister and extend for periods of minutes. Based on this observation, average values of the various measurements were used for the computation of the results.

The average number and volume concentration for the single demister and double demister are presented in Figure 33 and 34. The single demister has a larger droplet concentration than the double demister, as expected.

COOLING TOWER OF THE HIGH FLUX BEAM REACTOR AT BROOKHAVEN NATIONAL LABORATORY

The objectives of this field test were to demonstrate:

- the DC-2 Droplet Counter connected with the Multiplexer and Printer/Controller. Four multiplexer probes were used in these experiments;

- two DC-2 Droplet Counters interconnected with the Printer/Controller.

For both types of experiments, all of the data was recorded using the automatic mode of the Printer/Controller. The equipment arrangements for the two configurations are shown in Section 5 of this report.

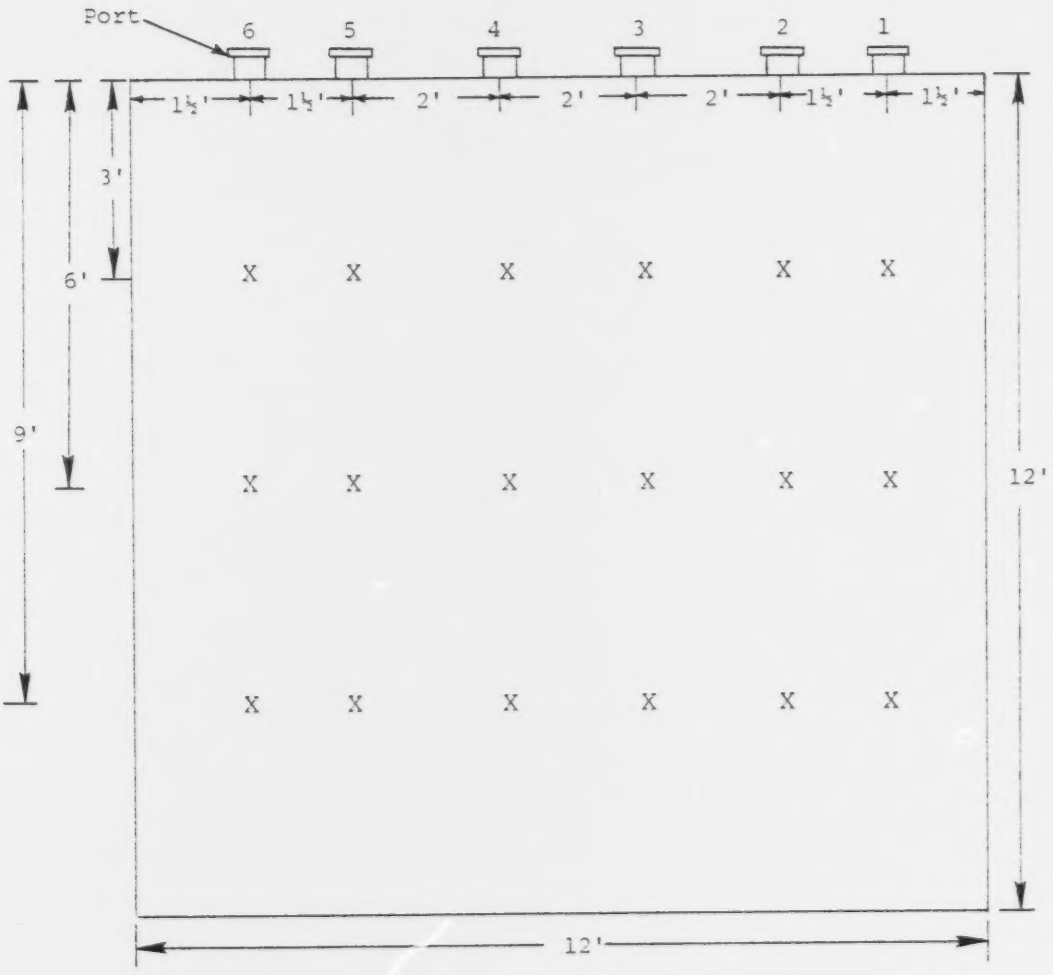

Figure 32 : Test Section of a Duct at Shippingport, Pennsylvania

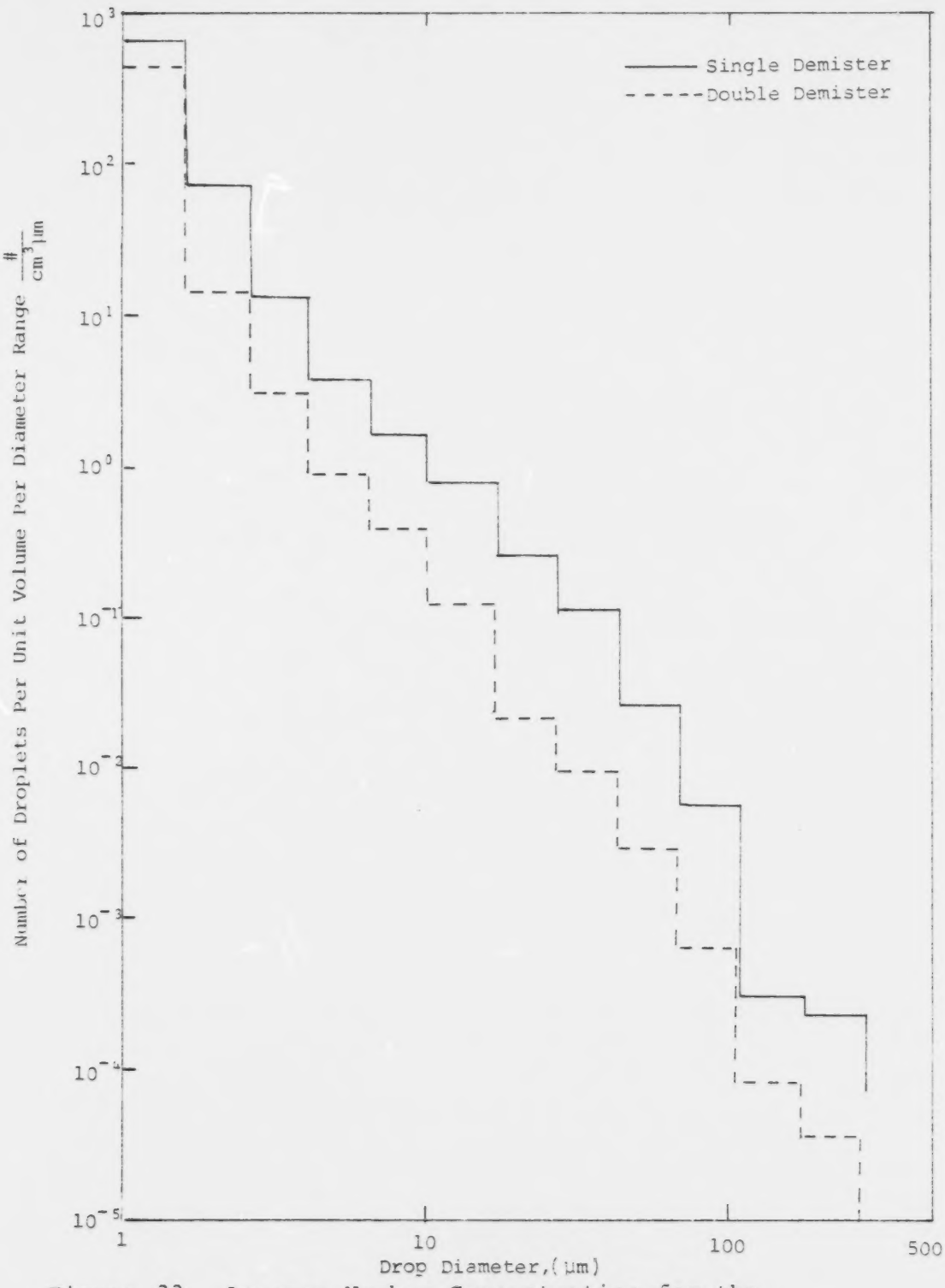

Figure 33: Average Number Concentration for the Demister Sections at Shippingport, Pennsylvania

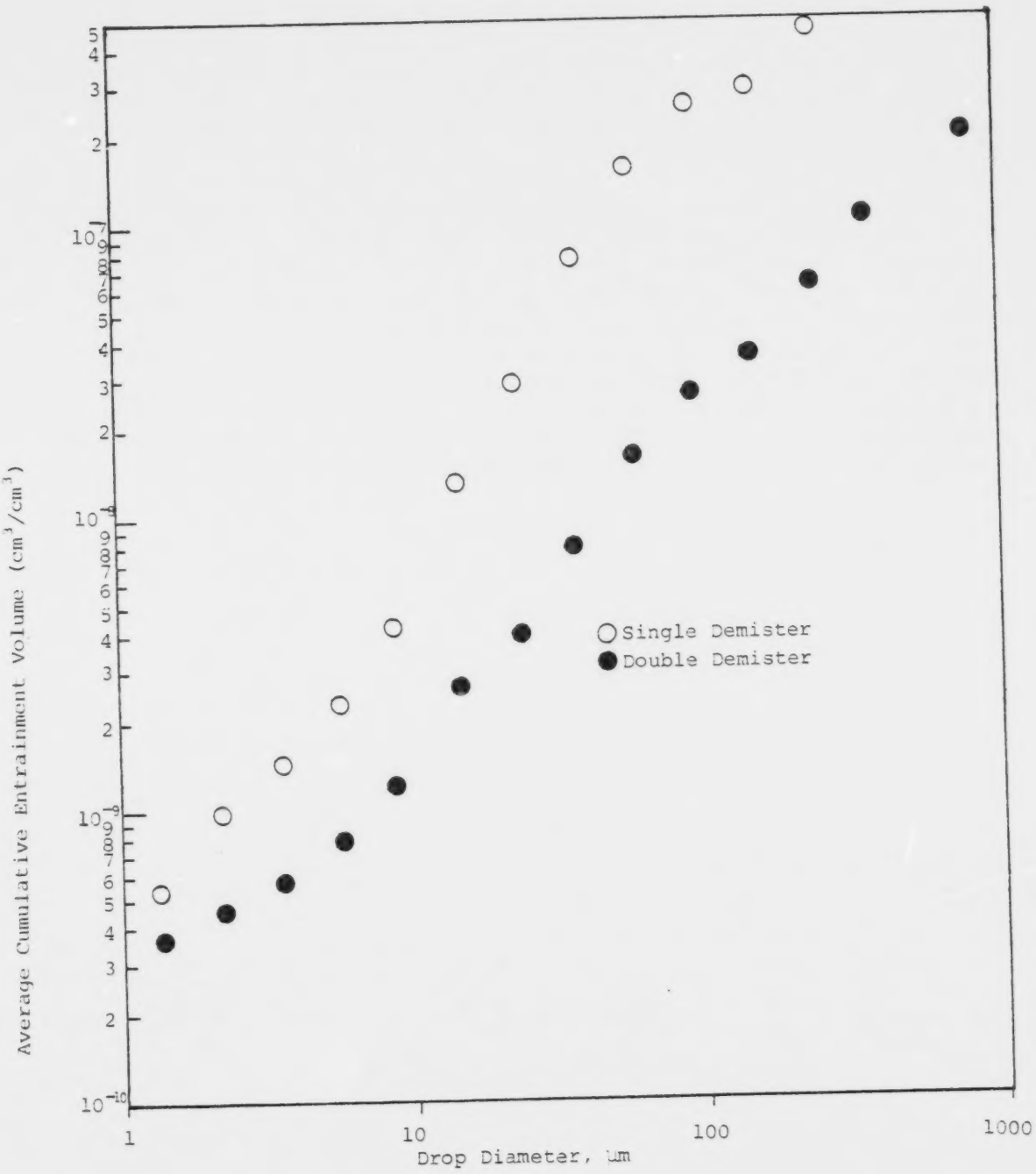

Figure 34: Average Cumulative Entrainment Volume as a Function of Diameter for the Demister Sections at Shippingport, Pennsylvania.

The droplets were generated from domestic water with a maximum of 1 PPM chloride chemical added for maintenance purposes inside the cooling tower. The survey covered several radial cross sections in two of the five exhaust cell units. The investigation included measurements with the exhaust fan on and off during the test.

The entire test program required approximately two hours, but had to be scheduled over two days because of weather conditions. Measurements were taken automatically every five minutes and were printed out by the Printer/Controller. Throughout the testing, all equipment operated properly. No probe breakage occurred and no contamination was detected either by the operation of the instrument or by observing the sensors under a microscope. Typical results are given in Figure 35 and 36. It is found that both number and volume concentration are dominated by drops smaller than 30 μm.

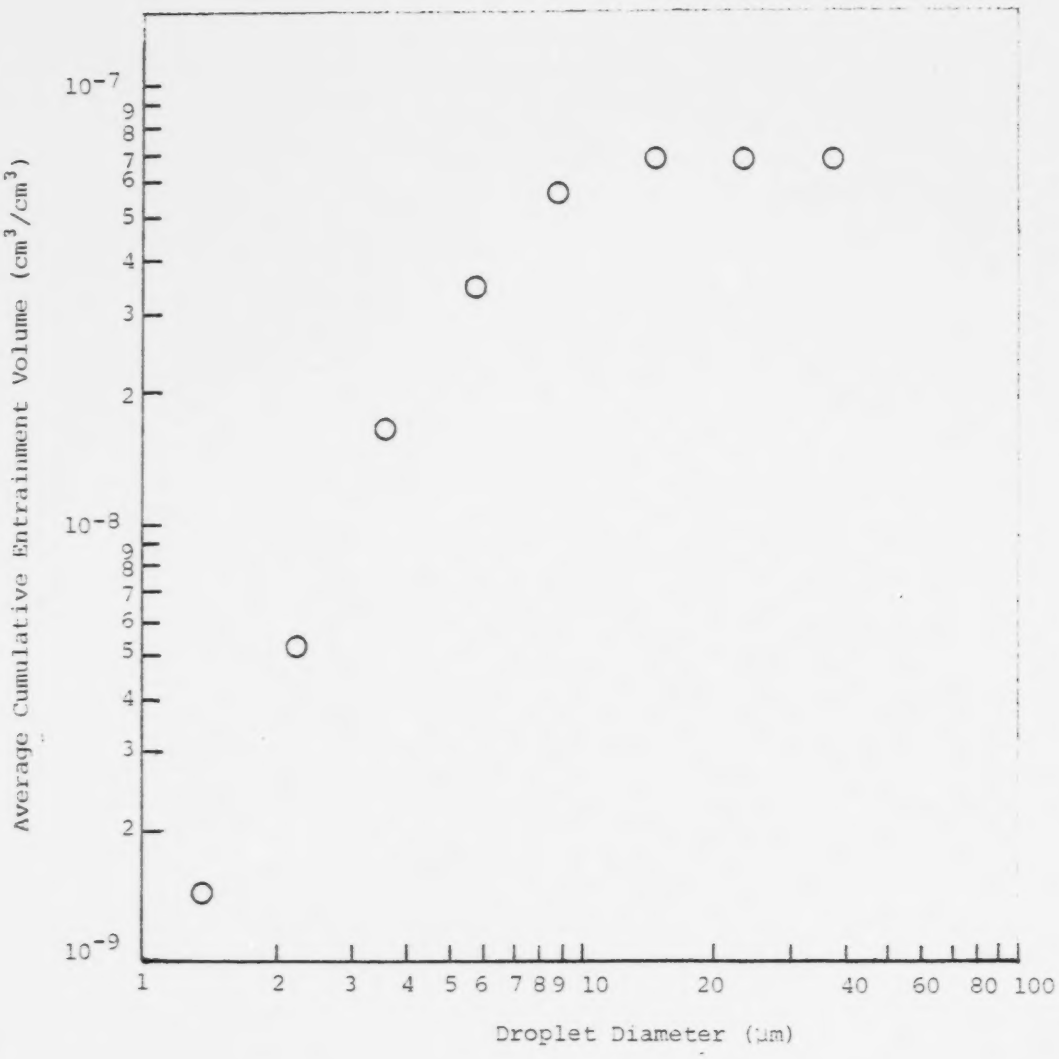

Figure 35: Average Cumulative Entrainment Volume as a Function of Droplet Size in the Exhaust of the Cooling Tower at Brookhaven National Laboratory

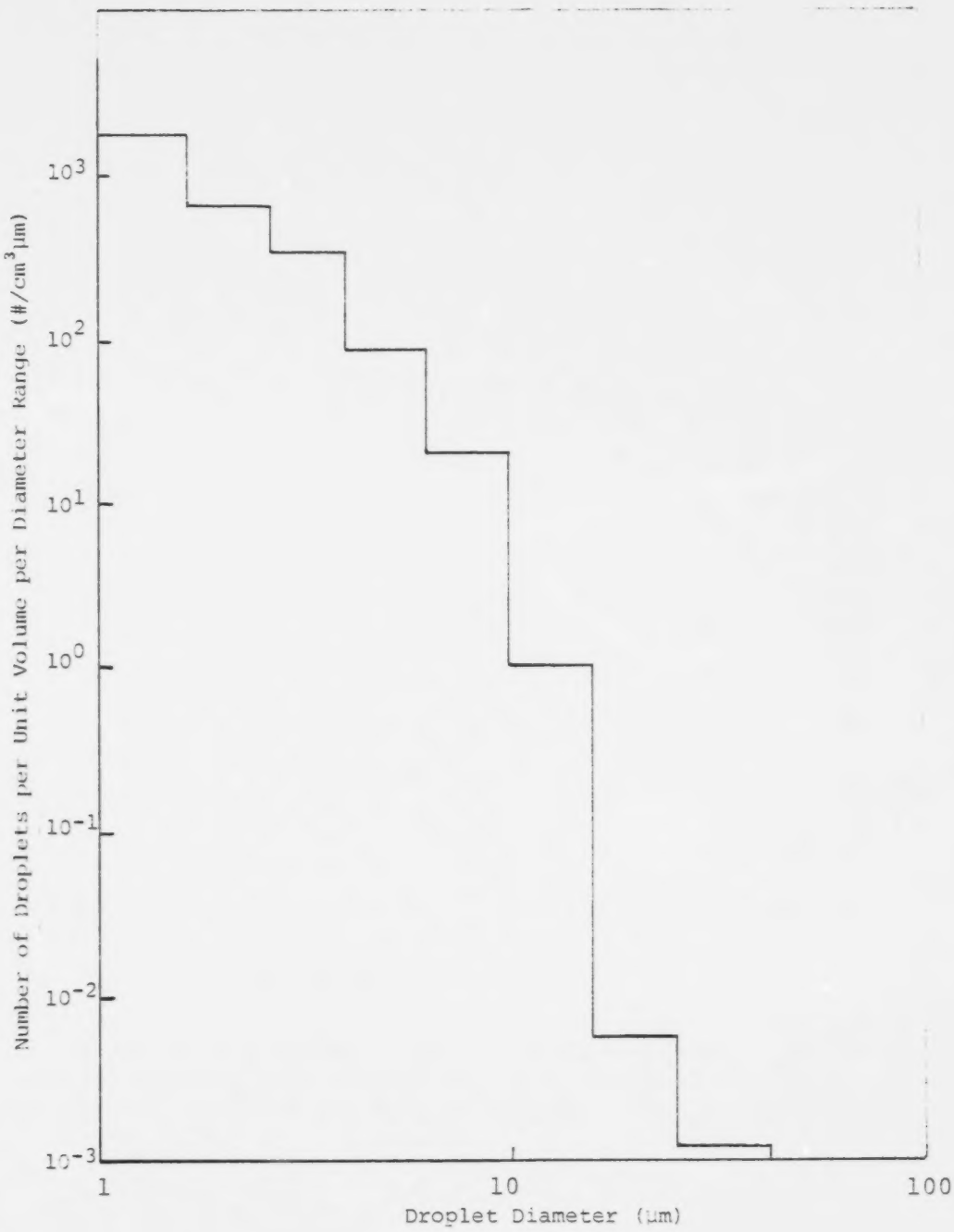

Figure 36: Droplet Number Concentration Measured in the Exhaust of the Cooling tower at Brookhaven National Laboratory

REFERENCES

1. Medecki, H., Kaufman, M., and Magnus, D., "Design, Development, and Field Test of a Droplet Measuring Device," EPA-650/2-75-018, U.S. Environmental Protection Agency, Research Triangle Park, N. C., 1976.

2. Fuchs, N. A., "The Mechanics of Aerosol," MacMillan Company, 1964.

3. Davies, C. N., "Aerosol Science," Academic Press, New York, N. Y., 1966.

4. Cushing, K. M., Lacey, G. E., McCain, J. D. and Smith, W. B., "Particulate Sizing Techniques for Control Device Evaluation: Cascade Impactor Calibrations," EPA-600/2-76-280, U.S. Environmental Protection Agency, Research Triangle Park, N. C., 1976.

5. Smith, W. B., Cushing, K. M. and McCain, J. D., "Particulare Sizing Techniques for Control Device Evaluation," EPA-650/2-74-102, U. S. Environmental Protection Agency, Research Triangle Park, N. C., 1974.

6. Harris, D. B., "Procedures for Cascade Impactor Calibration and Operation in Process Streams," EPA-600/2-77-004, U. S. Environmental Protection Agency, Research Triangle Park, N. C., 1977.

APPENDIX A

TABULATION OF LABORATORY TESTS

Over the period from June 30 to December 28, 1977, approximately 160 experiments were performed in the KLD laboratory using the Brink impactor and the DC-2 to measure droplet concentration. In Appendix A, these tests are summarized in tabular form.

For each test, a purpose number is assigned in the table. The definition of each purpose number (P.1...P.21) is presented in tabular form at the end of this section. Each test is further described by referring to a configuration (C.1...C.29) which is defined by the sketches appearing in this Appendix. For example, configuration C.5 consists of a Brink impactor with a cyclone and three stages and a DC-2 probe located at the exit from the impactor.

The only other tabulated parameter requiring explanation is the flow rate, which is given in inches of water. This pressure drop is across a calibrated orifice and the flow rate is obtained from the following equation:

$$\Delta P = CQ^2$$

where ΔP = pressure drop

Q = flow rate

$$C = 7.03 \frac{(\text{cm of } H_2O)}{(\text{liter/min})^2} = 2222 \frac{(\text{inch of } H_2O)}{(\text{ft}^3/\text{min})^2}$$

No. of Test	Date	Config.	Droplet Counter	Liquid Type	Flow Rate (inch of H_2O)	No. D.C. Samples	Total Test Period (sec.)	Purpose No.
101	6/30/77	C.1	DC-2 SN-1	Pure Water	7/8"	6	520	P.1
102	6/30/77	C.1	DC-2 SN-1	Pure Water	1"	9	180	P.1
103	6/30/77	C.1	DC-2 SN-1	Pure Water	1 1/2"	7	100	P.1
104	6/30/77	C.1	DC-2 SN-1	Pure Water	2"	6	60	P.1
105	6/30/77	C.1	DC-2 SN-1	Pure Water	2 1/2"	5	40	P.1
106	6/30/77	C.1	DC-2 SN-1	Pure Water	3"	4	280	P.1
107	6/30/77	C.1	DC-2 SN-1	Pure Water	3 1/2"	3	185	P.1
108	6/30/77	C.1	DC-2 SN-1	Pure Water	4"	4	235	P.1
109	6/30/77	C.1	DC-2 SN-1	Pure Water	4 3/4"	5	235	P.1
110	6/30/77	C.1	DC-2 SN-1	Pure Water	1 5/8"	4	400	P.1
111	6/30/77	C.1	DC-2 SN-1	Pure Water	1 1/8"	4	690	P.1
112	6/30/77	C.1	DC-2 SN-1	Pure Water	7/8"	5	1480	P.1
113	6/30/77	C.1	DC-2 SN-1	Pure Water	3/4"	3	1270	P.1
114	7/1/77	C.1	DC-2	Pure Water	2"	3	340	P.2
115	7/1/77	C.1	DC-1	Pure Water	2"	5	500	P.2
116	7/1/77	C.1	DC-2	Pure Water	3/4"	2	300	P.2
117	7/1/77	C.1	DC-1	Pure Water	3/4"	2	440	P.2
118	7/1/77	C.1	DC-2	Pure Water	2 5/8"	3	300	P.2
119	7/1/77	C.1	DC-1	Pure Water	2 5/8"	2	160	P.2

No. of Test	Date	Config.	Droplet Counter	Liquid Type	Flow Rate (inch of H_2O)	No. D.C. Samples	Total Test Period (sec.)	Purpose No.
120	7/5/77	C.1	DC-2	Pure Water	2"	1	40	P.3
121	7/5/77	C.2	DC-2	Pure Water	2"	2	60	P.3
122	7/5/77	C.3	DC-2	Pure Water	2"	2	90	P.3
123	7/5/77	C.4	DC-2	Pure Water	2"	3	200	P.3
124	7/5/77	C.5	DC-2	Pure Water	2"	3	240	P.3
125	7/5/77	C.6	DC-2	Pure Water	2"	3	270	P.3
126	7/5/77	C.7	DC-2	Pure Water	2"	2	140	P.3
127	7/6/77	N.A.	N.A.	Pure Water	2"	N.A.	N.A.	P.4
128	7/11/77	C.1	DC-2 SN-2	Pure Water	2"	6	180	P.3
129	7/11/77	C.2	DC-2 SN-2	Pure Water	2"	6	1200	P.3
130	7/11/77	C.3	DC-2 SN-2	Pure Water	2"	6	2000	P.3
131	7/11/77	C.4	DC-2 SN-2	Pure Water	2"	1		P.3
132	7/12/77	C.8	DC-2 SN-2	Pure Water	2"	5	340	P.5
133	7/12/77	C.8	DC-2 SN-2	Pure Water	2"	5	920	P.5
134	7/12/77	C.8	DC-2 SN-2	Pure Water	2"	4	1200	P.5
135	7/12/77	C.8	DC-2 SN-2	Pure Water	2"	3	430	P.5
136	7/12/77	C.8	DC-2 SN-2	Pure Water	2"	4	550	P.5
137	7/12/77	C.8	DC-2 SN-2	Pure Water	2"	4	580	P.5
138	7/12/77	C.8	DC-2 SN-2	Pure Water	2"	4	800	P.5
139	7/12/77	C.8	DC-2 SN-2	Pure Water	2"	4	700	P.5
140	7/12/77	C.8	DC-2 SN-2	Pure Water	1"	4	900	P.5

No. of Test	Date	Config.	Droplet Counter	Liquid Type	Flow Rate (inch of H_2O)	No. D.C. Samples	Total Test Period (sec.)	Purpose No.
141	7/12/77	C.8	DC-2 SN-2	Pure Water	1"	4	1050	P.5
142	7/12/77	C.8	DC-2 SN-2	Pure Water	1"	4	950	P.5
143	7/12/77	C.8	DC-2 SN-2	Pure Water	1"	4	1300	P.5
144	7/13/77	C.9	DC-2 SN-2	Pure Water	3/4"	5	260	P.6
145	7/13/77	C.8	DC-2 SN-2	Pure Water	3/4"	5	110	P.6
146	7/13/77	C.8	DC-2 SN-2	Pure Water	3/4"	7	310	P.6
147	7/13/77	C.8	DC-2 SN-2	Pure Water	3/4"	5	120	P.6
148	7/13/77	C.10	DC-2 SN-2	Pure Water	3/4"	4	1300	P.6
149	7/13/77	C.10	DC-2 SN-2	Pure Water	3/4"	4	1300	P.6
150	7/13/77	C.10	DC-2 SN-2	Pure Water	1 1/2"	3	320	P.6
151	7/13/77	C.10	DC-2 SN-2	Pure Water	1 1/2"	6	60	P.6
152	7/14/77	C.11	DC-2 SN-2	Pure Water	2"	4	2800	P.6
153	7/14/77	C.11	DC-2 SN-2	Pure Water	2"	5	65	P.6
154	7/14/77	C.12	DC-2 SN-2	Pure Water	2"	5	60	P.6
155	7/14/78	C.12	DC-2 SN-2	Pure Water	2"	5	1050	P.6
156	7/19/77	N.A.	N.A.	Pure Water	N.A.	N.A.	1200	P.7
157	7/19/77	N.A.	N.A.	Pure Water	N.A.	N.A.	1300	P.8
158	7/19/77	N.A.	N.A.	Pure Water	N.A.	N.A.	840	P.8
159	7/20/77	C.3	N.A.	Pure Water	2"	N.A.	1800	P.8
160	7/20/77	C.3	N.A.	Pure Water	2"	N.A.	900	P.9

No. of Test	Date	Config.	Droplet Counter	Liquid Type	Flow Rate (inch of H_2O)	No. D.C. Samples	Total Test Period (sec.)	Purpose No.
161	7/20/77	C.3	N.A.	Pure Water	2"	N.A.	900	P.9
162	7/20/77	C.3	N.A.	10% Saline Solution	2"	N.A.	1800	P.10
163	7/20/77	C.3	DC-1	10% Saline Solution	2"	6	3600	P.11
164	7/21/77	C.3	DC-1	10% Saline Solution	2"	9	7200	P.11
165	7/21/77	C.3	DC-1	10% Saline Solution	2"	21	3600	P.11
166	7/22/77	C.4	DC-1	10% Saline Solution	2"	17	7200	P.11
167	7/22/77	C.4	DC-1	10% Saline Solution	2"	19	3600	P.11
168	7/22/77	N.A.	N.A.	10% Saline Solution	N.A.	N.A.	450	P.12
169	7/25/77	C.14	DC-1	10% Saline Solution	2"	13	2700	P.13
170	7/25/77	C.14	DC-1	10% Saline Solution	2"	12	1300	P.13
171	7/25/77	C.13	DC-1	10% Saline Solution	2"	17	2700	P.13

No. of Test	Date	Config.	Droplet Counter	Liquid Type	Flow Rate (inch of H_2O)	No. D.C. Samples	Total Test Period (sec.)	Purpose No.
172	7/25/77	C.14	DC-1	10% Saline Solution	2"	8	1300	P.13
173	7/27/77	C.14	DC-1 DC-2	10% Saline Solution	2"	8	600	P.13
174	7/27/77	C.14	DC-1	10% Saline Solution	2"	2	300	P.13
175	7/27/77	C.14	DC-1	10% Saline Solution	2"	5	600	P.13
176	7/27/77	C.14	DC-1	10% Saline Solution	2"	4	600	P.13
177	7/28/77	C.14	N.A.	10% Saline Solution	2"	N.A.	300	P.14
178	7/28/77	C.14	DC-1	10% Saline Solution	2"	14	1200	P.13
179	7/28/77	C.14	DC-2 SN-2	10% Saline Solution	2"	6	300	P.13
180	7/29/77	C.14	DC-1	10% Saline Solution	2"	4	600	P.13
181	7/29/77	C.14	DC-1	10% Saline Solution	2"	14	2400	P.13
182	7/29/77	C.14	DC-1	10% Saline Solution	2"	12	1200	P.13

No. of Test	Date	Config.	Droplet Counter	Liquid Type	Flow Rate (inch of H_2O)	No. D.C. Samples	Total Test Period (sec.)	Purpose No.
201	8/1/77	C.15	DC-2 SN-1 DC-2 SN-2	10% Saline Solution	2"	4	300	P.13
202	8/1/77	C.15	DC-2 SN-1 DC-2 SN-2	10% Saline Solution	2"	12	300	P.13
203	8/1/77	C.15	DC-2 SN-1 DC-2 SN-2	10% Saline Solution	2"	3	600	P.13
204	8/1/77	C.15	DC-2 SN-1 DC-2 SN-2	10% Saline Solution	2"	6	1200	P.13
205	8/2/77	C.15	DC-2 SN-1 DC-2 SN-2	10% Saline Solution	2"	10	2400	P.13
206	8/2/77	C.12	DC-2 SN-2	10% Saline Solution	2"	7	1300	P.6
207	8/2/77	C.15	DC-2 SN-1 DC-2 SN-2	10% Saline Solution	2"	10	3600	P.13
208	8/3/77	C.15	DC-2 SN-1 DC-2 SN-2	10% Saline Solution	2"	6	3600	P.13
209	8/3/77	C.16	DC-2 SN-1 DC-2 SN-2	10% Saline Solution	2"	8	2400	P.13
210	8/5/77	C.17	DC-2 SN-1 DC-2 SN-2	10% Saline Solution	2"	12	140	P.15

No. of Test	Date	Config.	Droplet Counter	Liquid Type	Flow Rate (inch of H_2O)	No. D.C. Samples	Total Test Period (sec.)	Purpose No.
211	8/10/77	C.17	DC-2 SN-1 DC-2 SN-2	10% Saline Solu-tion	2"	8	2400	P.13
212	8/10/77	C.17	DC-2 SN-1 DC-2 SN-2	10% Saline Solu-tion	2"	8	2400	P.13
213	8/10/77	C.17	DC-2 SN-1 DC-2 SN-2	10% Saline Solu-tion	2"	16	4800	P.13
214	8/11/77	C.18	DC-2 SN-1 DC-2 SN-2	10% Saline Solu-tion	2"	16	4800	P.13
215	8/11/77	C.18	DC-2 SN-1 DC-2 SN-2	10% Saline Solu-tion	2"	5	1200	P.13
216	8/11/77	C.18	DC-2 SN-1 DC-2 SN-2	10% Saline Solu-tion	2"	2	1200	P.13
217	8/12/77	C.18	DC-2 SN-1 DC-2 SN-2	10% Saline Solu-tion	~2"	16	2400	P.13
218	8/12/77	C.18	DC-2 SN-1 DC-2 SN-2	10% Saline Solu-tion	2"	6	600	P.13
219	8/16/77	C.18	DC-2 SN-1 DC-2 SN-2	10% Saline Solu-tion	2"	4	1200	P.13
220	8/16/77	C.18	DC-2 SN-1 DC-2 SN-2	10% Saline Solu-tion	2"	5	1200	P.13

No. of Test	Date	Config.	Droplet Counter	Liquid Type	Flow Rate (inch of H_2O)	No. D.C. Samples	Total Test Period (sec.)	Purpose No.
221	8/16/77	C.18	DC-2 SN-1 DC-2 SN-2	10% Saline Solu-tion	2"	4	1200	P.13
222	8/16/77	C.18	DC-2 SN-1 DC-2 SN-2	10% Saline Solu-tion	2"	3	1200	P.13
223	8/17/77	C.18	DC-2 SN-1 DC-2 SN-2	10% Saline Solu-tion	2"	4	2400	P.13
224	8/17/77	C.18	DC-2 SN-1 DC-2 SN-2	10% Saline Solu-tion	2"	4	2400	P.13
225	8/17/77	C.18	DC-2 SN-1 DC-2 SN-2	10% Saline Solu-tion	2"	8	4800	P.13
226	8/18/77	C.19	DC-2 SN-1 DC-2 SN-2	10% Saline Solu-tion	2"	2	2400	P.16
227	8/18/77	C.19	DC-2 SN-1 DC-2 SN-2	10% Saline Solu-tion	2"	2	2400	P.16
228	8/18/77	C.19	DC-2 SN-1 DC-2 SN-2	10% Saline Solu-tion	2"	8	2400	P.16
229	8/19/77	C.20	DC-2 SN-1 DC-2 SN-2	10% Saline Solu-tion	2"	8	3600	P.17

No. of Test	Date	Config.	Droplet Counter	Liquid Type	Flow Rate (inch of H_2O)	No. D.C. Samples	Total Test Period (sec.)	Purpose No.
301	8/2/77	C.21	DC-2 SN-1 DC-2 SN-2	10% Saline Solution	2"	8	2100	P.18
302	8/2/77	C.21	DC-2 SN-1 DC-2 SN-2	5% Saline Solution	2"	8	2100	P.18
303	8/2/77	C.21	DC-2 SN-1 DC-2 SN-2	Pure Water	2"	8	2100	P.18
304	8/2/77	C.22	DC-2 SN-1 DC-2 SN-2	10% Saline Solution	2"	8	2100	P.18
305	8/2/77	C.22	DC-2 SN-1 DC-2 SN-2	5% Saline Solution	2"	8	2100	P.18
306	8/2/77	C.22	DC-2 SN-1 DC-2 SN-2	Pure Water	2"	8	2100	P.18
307	8/3/77	C.23	DC-2 SN-1 DC-2 SN-2	10% Saline Solution	2"	8	2100	P.18
308	8/3/77	C.23	DC-2 SN-1 DC-2 SN-2	5% Saline Solution	2"	21	~2 hrs.	P.18
309	8/3/77	C.23	DC-2 SN-1 DC-2 SN-2	Pure Water	2"	8	2100	P.18
310	8/4/77	C.12	DC-2 SN-1 DC-2 SN-2	10% Saline Solution	2"	10	~1 hr.	P.18

No. of Test	Date	Config.	Droplet Counter	Liquid Type	Flow Rate (inch of H_2O)	No. D.C. Samples	Total Test Period (sec.)	Purpose No.
311	8/4/77	C.12	DC-2 SN-1 DC-2 SN-2	5% Saline Solution	2"	10	~1 hr.	P.18
312	8/4/77	C.12	DC-2 SN-1 DC-2 SN-2	Pure Water	2"	26	~2 hrs.	P.18
313	8/2/77	N.A.	DC-1	10% Saline Solution	3 1/2"	2	2.1	P.19
314	8/2/77	N.A.	DC-1	10% Saline Solution	3 1/4"	2	2.8	P.19
315	8/2/77	N.A.	DC-1	10% Saline Solution	3"	3	4.6	P.19
316	8/2/77	N.A.	DC-1	10% Saline Solution	2 3/4"	2	3.3	P.19
317	8/2/77	N.A.	DC-1	10% Saline Solution	2 1/2"	2	2.5	P.19
318	8/2/77	N.A.	DC-1	10% Saline Solution	2 1/4"	2	3.6	P.19
319	8/2/77	N.A.	DC-1	10% Saline Solution	2"	3	7.4	P.19
320	8/2/77	N.A.	DC-1	10% Saline Solution	1 3/4"	2	9	P.19

No. of Test	Date	Config.	Droplet Counter	Liquid Type	Flow Rate (inch of H_2O)	No. D.C. Samples	Total Test Period (sec.)	Purpose No.
321	8/2/77	N.A.	DC-1	10% Saline Solution	1 1/2"	3	6.7	P.19
322	8/2/77	N.A.	DC-1	10% Saline Solution	1"	2	6.8	P.19
323	8/2/77	N.A.	DC-1	10% Saline Solution	3/4"	2	9	P.19
324	8/2/77	N.A.	DC-1	10% Saline Solution	1/2"	2	11.4	P.19
325	8/2/77	N.A.	DC-1	10% Saline Solution	1/4"	2	11.2	P.19
326	8/2/77	N.A.	DC-2 SN-2	10% Saline Solution	3 1/2"	1	3.9	P.19
327	8/2/77	N.A.	DC-2 SN-2	10% Saline Solution	3 1/4"	1	5.2	P.19
328	8/2/77	N.A.	DC-2 SN-2	10% Saline Solution	3"	1	5.8	P.19
329	8/2/77	N.A.	DC-2 SN-2	10% Saline Solution	2 3/4"	1	5.5	P.19
330	8/2/77	N.A.	DC-2 SN-2	10% Saline Solution	2 1/2"	1	5.2	P.19

No. of Test	Date	Config.	Droplet Counter	Liquid Type	Flow Rate (inch of H_2O)	No. D.C. Samples	Total Test Period (sec.)	Purpose No.
331	8/2/77	N.A.	DC-2 SN-2	10% Saline Solu-tion	2 1/4"	1	4.8	P.19
332	8/2/77	N.A.	DC-2 SN-2	10% Saline Solu-tion	2"	1	4.7	P.19
333	8/2/77	N.A.	DC-2 SN-2	10% Saline Solu-tion	1 3/4"	1	4.3	P.19
334	8/2/77	N.A.	DC-2 SN-2	10% Saline Solu-tion	1 1/2"	1	5.3	P.19
335	8/2/77	N.A.	DC-2 SN-2	10% Saline Solu-tion	1 1/4"	1	6.0	P.19
336	8/2/77	N.A.	DC-2 SN-2	10% Saline Solu-tion	1"	1	7.2	P.19
337	8/2/77	N.A.	DC-2 SN-2	10% Saline Solu-tion	3/4"	1	8.8	P.19
338	8/2/77	N.A.	DC-2 SN-2	10% Saline Solu-tion	1/2"	1	11.6	P.19
339	8/2/77	N.A.	DC-2 SN-2	10% Saline Solu-tion	1/4"	1	13.4	P.19

No. of Test	Date	Config.	Droplet Counter	Liquid Type	Flow Rate (inch of H_2O)	No. D.C. Samples	Total Test Period (sec.)	Purpose No.
401	8/24/77	C.21	DC-2 SN-1 DC-2 SN-2	10% Saline Solu-tion	2"	5	2400	P.18
402	8/24/77	C.22	DC-2 SN-1 DC-2 SN-2	10% Saline Solu-tion	2"	5	2400	P.18
403	8/25/77	C.23	DC-2 SN-1 DC-2 SN-2	10% Saline Solu-tion	2"	14	3000	P.18
404	8/26/77	C.15	DC-2 SN-1 DC-2 SN-2	10% Saline Solu-tion	2"	9	4800	P.18
405	9/16/77	C.17	DC-2 & Multi-plexer	10% Saline Solu-tion	2"	16		P.20
406	9/19/77	C.17	DC-2 & Multi-plexer	10% Saline Solu-tion	2"	7		P.20
407	9/19/77	C.24	DC-2 & Multi-plexer	10% Saline Solu-tion	2"	15	3600	P.18
408	9/20/77	C.25	DC-2 & Multi-plexer	10% Saline Solu-tion	2"	10	3600	P.18
409	9/20/77	C.25	DC-2 & Multi-plexer	10% Saline Solu-tion	2"	15	4200	P.18
410	11/23/77	C.26	DC-2 SN-1 2 probes	10% Saline Solu-tion	2"	5	1800	P.21

No. of Test	Date	Config.	Droplet Counter	Liquid Type	Flow Rate (inch of H_2O)	No. D.C. Samples	Total Test Period (sec.)	Purpose No.
411	11/23/77	C.26	DC-2 SN-1 2 probes	10% Saline Solu-tion	2"	8	2400	P.21

Definition of Purpose Number

No.	Purpose
P.1	Investigate the response of instrument for different flow rates
P.2	Compare results given by DC-1 and that of DC-2 under the same operating condition
P.3	Investigate the output response of impactor by using DC-2
P.4	Measure the pressure and temperature drop after the cyclone--cyclone + 1 state, cyclone + 2 stages and cyclone + 3 stages individually
P.5	Obtain the droplet distribution curves at the inlet and outlet of a vertical brass tube
P.6	Investigate the distribution curves at the inlet and outlet of a vertical glass tube for the study of condensation/evaporization and delay effect
P.7	Obtain the evaporation rate of pure water on foil target using the Cahn Balance
P.8	Investigate the evaporation rate of pure water on paper target using the Cahn Balance
P.9	Use paper as absorbing material to investigate the condensation effect behind the target
P.10	Investigate the evaporation rate and/or concentration change for drops collected on stage 1 of an impactor
P.11	Exercise the combined operation of impactor and DC-1
P.12	Obtain the evaporation rate for a drop of saline solution using the Cahn Balance
P.13	Perform experiment for comparison of DC-2 against the Brink impactor

No.	Purpose
P.14	Perform experiment for comparison of the DC-2 against the Brink impactor with the impactor connected to the spray box overnight to establish an equilibrium initial condition
P.15	Compare the time required for measuring 100 drops by DC-2 SN-1 and DC-2 SN-2
P.16	Perform experiment for comparison of DC-2 against impactor by leaving the impactor inside the spray box
P.17	Investigate the distribution curve at the inlet and outlet of an impactor with no targets inside the impactor
P.18	Obtain distribution curves at the inlet and outlet of the designed configuration for investigation of collection efficiency and delay phenomena
P.19	Investigate droplet size distribution and rate of counting for different flow velocities
P.20	Check the validity of measurement for two probes
P.21	Compare the mass of droplets collected by stage 1 of impactor with the mass difference indicated by the DC-2 measurements at the inlet and outlet

Test Configurations of Equipment

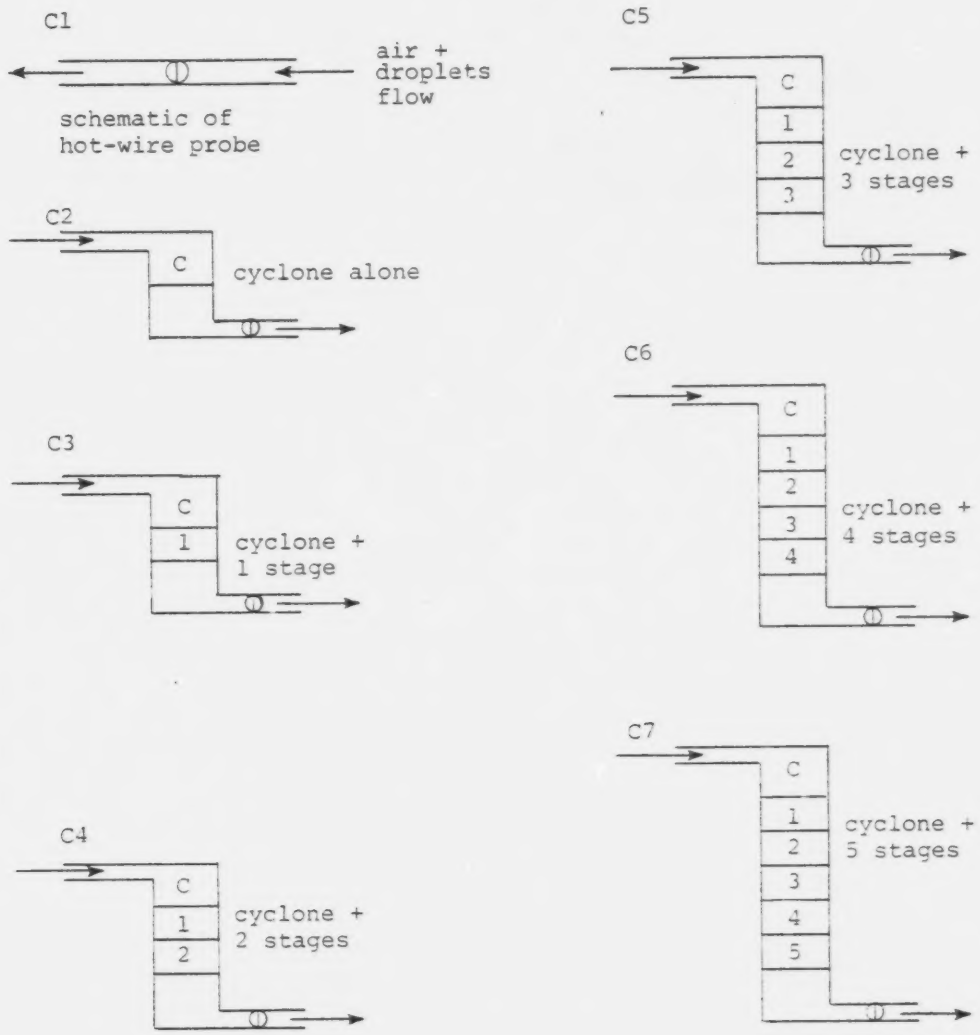

C8

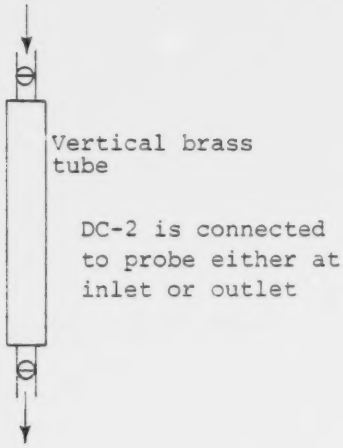

C9

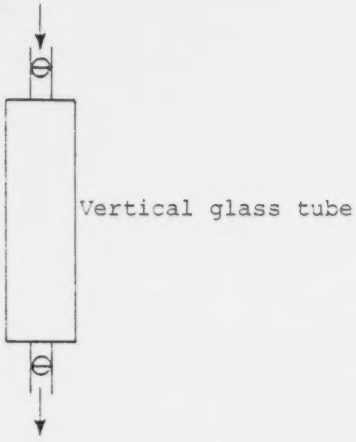

C10

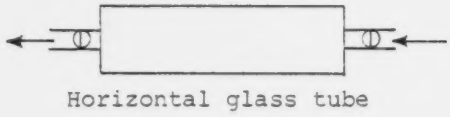

C11

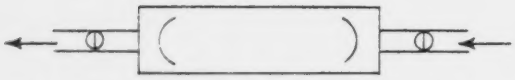

C12

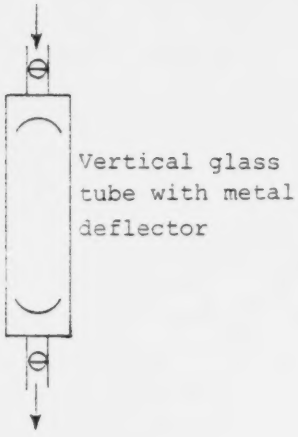

C13

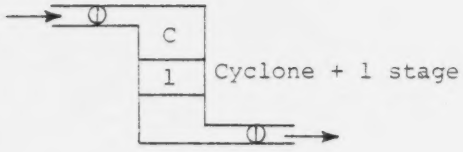

C14

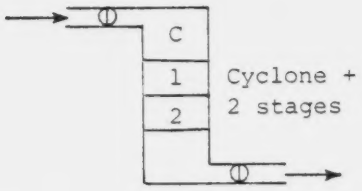

C15

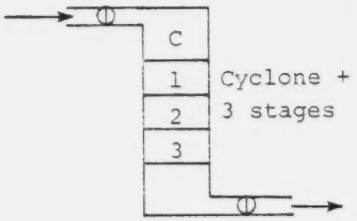

C16

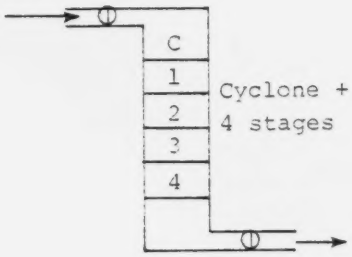

C17

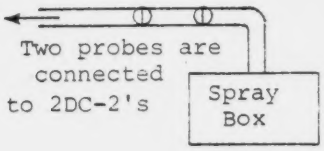

C18

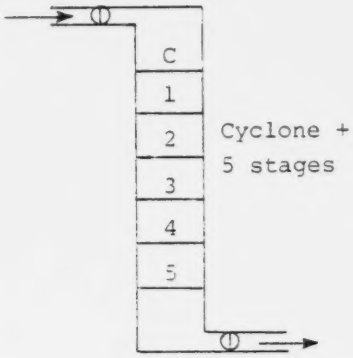

C19

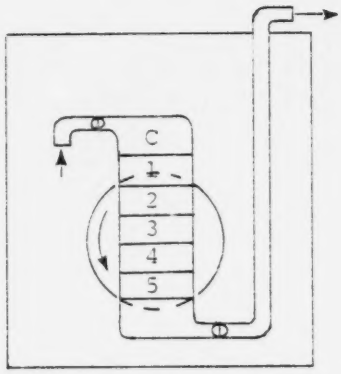

C20

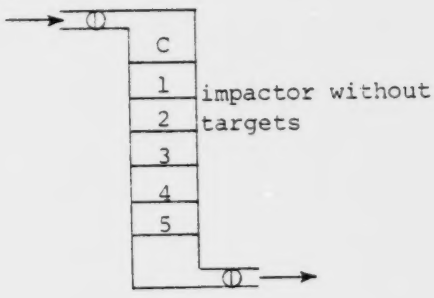

C21

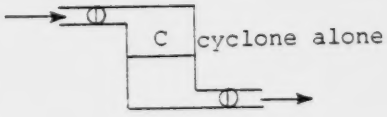

C22

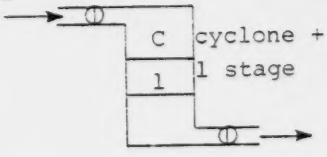

C23

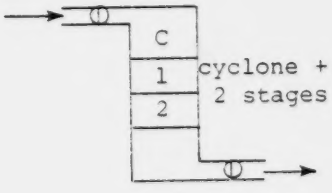

C24

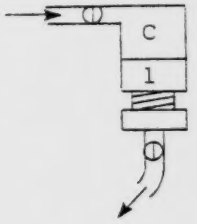

C25

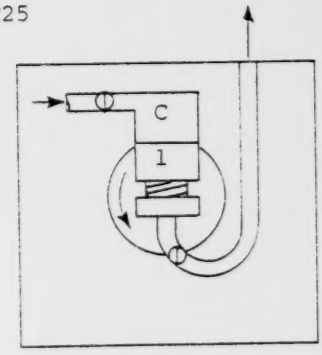

C26

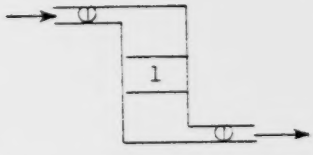

Stage 1 only (no cyclone in front of it